

A MASTERS OF APPLIED SCIENCE THESIS IN THE GRADUATE PROGRAM OF  
BUILDING SCIENCE / BUILDING ENGINEERING

# Assessment of Natural Ventilation Design and Efficacy in a Net-Zero Energy House

---

## A Case Study of the Harmony House

James Ellis

May 2016

**British Columbia Institute of Technology**  
**Building Science Graduate Program**

This is to certify that the thesis prepared by:

James Ellis,

entitled:

Assessment of Natural Ventilation Design and Efficacy in a Net-Zero Energy House: A Case Study of the Harmony House

and submitted in partial fulfillment of the requirements for the degree of:

**Master of Applied Science in Building Science/Building Engineering**

complies with the regulations of the Institute and meets the accepted standards with originality and quality.

Signed by the final Examining Committee:

\_\_\_\_\_  
Dr. Rodrigo Mora, Supervisor

\_\_\_\_\_  
Dr. Panagiota Karava, Examiner

\_\_\_\_\_  
Dr. Alejandra Menchaca, Examiner

\_\_\_\_\_  
Dr. Fitsum Tariku, Chair

Approved by:

\_\_\_\_\_  
Graduate Program Director

## **Acknowledgements**

Most importantly, I would like to thank my supervisor Dr. Rodrigo Mora for his support, direction, and help throughout obstacles overcome during the completion of my thesis and time at the British Columbia Institute of Technology (BCIT). I would like to also thank The School of Construction and the Environment at BCIT for allowing me to conduct this research by providing funding to access various softwares and purchasing measurement equipment and supplies. I would also like to thank Julien Schwartz for his contributions towards papers we have authored and help he has offered throughout this project. In addition, I would like to extend my sincere gratitude to the home owners of the Harmony House who allowed their home to be instrumented and monitored for educational purposes, as well as the architect who offered his vast knowledge on the intent and construction decisions of the house, as well as provided documentation that helped with this research. I would also like to thank the rest of the staff and faculty in the Building Science department at BCIT for their knowledge and assistance that immensely helped me to complete this research.

## **Abstract**

Achieving acceptable indoor environmental quality and thermal comfort in buildings can be difficult without relying on energy intensive mechanical equipment. When the climate conditions permit, natural ventilation could potentially help minimize the reliance on mechanically conditioned air; however, natural ventilation is rarely engineered. Houses are typically designed as fully enclosed climate systems in which the connection with the outdoor environment is rarely planned. Unlike in commercial or specialized buildings, houses are not designed with many energy conservation measures in mind. Reconnecting them with the outdoors has a great potential to increase thermal comfort and reduce reliance on mechanical systems. With such a connection to the dynamic weather conditions of the outdoors, it is difficult for architects to choose beneficial design elements to be included in the construction of their houses. Knowing which elements work and to what extent under particular conditions can potentially achieve increased thermal comfort using little or no energy. This research aims to offer a thorough assessment of a case study house and determine the effects of the design choices made by the architect of the house. This research may help architects know the risk factors affecting natural ventilation design in a systematic manner; and in doing so, enable quantifying the benefits of natural ventilation to meet the design goals of maintaining satisfactory indoor conditions without the use of air conditioning, particularly in the summer. A constructed net-zero case study house located in the Pacific marine climate of Canada was used to develop the proposed research. The house had been designed by an architect to rely solely on natural ventilation for cooling during the summer and much of the spring and fall. The house was instrumented and its indoor environment was monitored for a period of several months in 2014 to collect data to evaluate the effectiveness of design choices made, including the effect of a large atrium and the air flow characteristics of the windows intended by the architect to deliver most of the ventilation. Recorded data showed the house performed commendably and this was confirmed through evidence from the home owners. To aid in the understanding of the dynamics of the Harmony House, whole-building, multizone air flow network modeling and computational fluid dynamics (CFD) modeling of the house was developed and calibrated with monitored data and testing. The models were used to assess the indoor air quality and further quantify the natural ventilation of the house, as well as test hypothetical situations that were once considered for the house. Simulations revealed some additional insight into the design choices that were implemented in the house and showed that further technologies intended to increase ventilation were unnecessary and some instead, reduced ventilation through the house.

## Table of Contents

Acknowledgements .....	iii
Abstract .....	iv
Table of Contents .....	v
List of Tables .....	viii
List of Figures .....	ix
1. INTRODUCTION .....	1
1.1. Potential of natural ventilation and motivation .....	2
1.1.1. Potential of the climate .....	6
1.1.2. Adaptive thermal comfort .....	11
1.2. The use of passive technologies for cooling .....	14
1.3. Significance of window characterization .....	16
1.4. Objectives and scope .....	17
1.5. Thesis arrangement .....	20
2. HARMONY HOUSE .....	22
2.1. Introduction .....	22
2.2. Air behavior within the atrium .....	23
2.2.1. Zone 1: Potential core region .....	24
2.2.2. Zone 2: Flow decay region .....	25
2.2.3. Zone 3: Terminal region .....	25
2.2.4. Zone 4: Extraction region .....	26
2.3. Features and operation .....	26
3. LITERATURE REVIEW .....	29
3.1. Natural ventilation and related mechanisms .....	29
3.1.1. Wind, buoyancy and their interactions .....	30
3.1.2. Contributions of thermal mass .....	35
3.2. Effects of openings and pressure differentials across the envelope .....	36
3.2.1. The orifice equation and the discharge coefficient .....	37
3.2.2. Factors affecting the discharge coefficient .....	38
3.2.3. Previous studies on window types .....	43

3.3.	Previous studies on natural ventilation assessment .....	47
3.3.1.	Field monitoring .....	47
3.3.2.	Field measurements.....	48
3.3.3.	Small and full-scale models.....	49
3.3.4.	The benefits of computational simulations for assessment .....	50
3.3.4.1.	Empirical and analytical models .....	51
3.3.4.2.	Dynamic thermal models .....	52
3.3.4.3.	Computational fluid dynamics .....	55
3.3.4.3.1.	Turbulence modeling .....	56
3.3.4.3.2.	Boundary conditions .....	60
4.	PROBLEM STATEMENT .....	63
5.	METHODOLOGY .....	65
5.1.	Monitoring during occupancy .....	65
5.1.1.	Instrumentation and placement within the case study house.....	66
5.1.2.	Calibration of equipment.....	68
5.1.3.	Timeline of data acquisition .....	69
5.2.	Testing the window discharge coefficients.....	70
5.2.1.	On-site window testing .....	70
5.2.2.	Off-site window testing.....	74
5.3.	Model development .....	75
5.3.1.	Dynamic thermal model .....	76
5.3.2.	CFD model .....	76
5.3.3.	Validation process of the computer models .....	77
5.3.4.	Determination of discharge coefficients .....	79
5.3.5.	CFD cell resolution testing.....	80
5.4.	Prediction of adaptive thermal comfort of occupants.....	81
5.5.	Chimney-cap technology integration .....	82
6.	RESULTS AND DISCUSSION.....	84
6.1.	Occupant behavior and comfort conditions .....	84
6.2.	Results of off-site window testing.....	86
6.2.1.	Summary of the compiled data .....	86

6.2.2.	Trends observed in recorded data .....	87
6.3.	Results of on-site window testing .....	92
6.4.	Dynamic thermal model of the Harmony House .....	92
6.5.	CFD model of the Harmony House .....	94
6.5.1.	Optimal size of CFD cell resolution .....	96
6.5.2.	Coefficient of discharge for windows and skylights.....	98
6.6.	Validation of computer models .....	102
6.7.	Assessment of adaptive thermal comfort.....	109
6.8.	Evaluation of chimney-cap technologies.....	111
6.9.	Comfort conditions in the bedroom.....	113
7.	CONCLUSIONS .....	117
8.	LIMITATIONS AND FURTHER WORK .....	120
	REFERENCES .....	123
	APPENDIX A – Floor plan and sensor location .....	132
	APPENDIX B – Compiled data.....	134
	APPENDIX C – Results from the validation of the dynamic thermal model .....	137
	APPENDIX D – Results of the CFD model.....	142
	APPENDIX E – Results of questionnaire .....	145

## List of Tables

Table 1: Natural ventilation design relies on many aspects and they often directly interact with each other.....	2
Table 2: International Climate Zone definitions (ASHRAE, 2013) .....	7
Table 3: Climate normals 1981 – 2010 (Environment Canada, 2015). .....	8
Table 4: The values of $C_v$ for a top-hung window (Integrated Environmental Solutions Limited, 2007).....	45
Table 5: Comparison of capabilities of multizone and CFD to model natural ventilation. Adapted from Menchaca Brandan (2012). .....	51
Table 6: Constants used in the standard and RNG $k - \varepsilon$ models.....	58
Table 7: Summary of the performance of the $k - \varepsilon$ models for predicting indoor air flow. A=excellent, B=good, C=fair, D=poor, E=unacceptable (Chen Q. , 1995).....	59
Table 8: List of equipment used in the instrumentation of the Harmony House.....	68
Table 9: A list of instruments used in the test. Calibration was achieved where necessary according to operation manuals. ....	74
Table 10: Coefficients of pressure for venturi-shaped roofs (van Hooff, Blocken, Aanen, & Bronsema, 2011). .....	83
Table 11: The simulations resulted in pressure differentials across the wall. The results for various opening angles and grid resolutions reveal coefficients of discharge for each opening. ...	99
Table 12: Matched days peak temperatures ( $^{\circ}\text{C}$ ) between dynamic and recorded results for <b>1m/s</b> wind.....	103
Table 13: Surface temperatures ( $^{\circ}\text{C}$ ) obtained from dynamic results for 1 m/s wind on a cool, average, and warm day. ....	105
Table 14: Temperatures ( $^{\circ}\text{C}$ ) compared for 1m/s wind typical day. * marks operative temperature readings. ....	106
Table 15: Volumetric Air flow [ $\text{m}^3/\text{s}$ ] results compared for 1 m/s wind on a typical day. ....	109

## List of Figures

Figure 1: U.S. Residential sector delivered energy intensity for selected end uses, 2013 and 2040 (million Btu per household per year) (U.S. Energy Information Administration, 2015).....	6
Figure 2: Outdoor daily average monthly temperature for 2013 at a local weather station.....	9
Figure 3: Daily air temperature profile at a local weather station in August of 2013. ....	9
Figure 4: Wind-rose from local weather station from May to August, 2013 (top left). Daily average wind speed and direction from May to September, 2013 (top right). Probability distribution of air speeds from the local weather station from May to August, 2013 (bottom). ...	10
Figure 5: Comfort conditions in which 80% and 90% of occupants are comfortable. Buildings with centralized HVAC (left) are much narrower than those in naturally ventilated buildings (right) (de Dear & Brager, 1998).....	13
Figure 6: A solar chimney absorbs solar radiation, heating air and causing it to rise out of the chimney while extracting air from the space, promoting ventilation (Bansal, Mathur, & Bhandari, 1994).....	16
Figure 7: Evaluation of different window opening types and some of their properties under typical use. Description of symbols: - poor; O medium; + good (Roetzel, Tsangrassoulis, Dietrich, & Busching, 2010).....	17
Figure 8: Design Concepts by the architect on the natural ventilation of the house during summer months. ....	23
Figure 9: The four main regions of air within the Harmony House’s main atrium. The behaviour of air is different at each location. ....	24
Figure 10: The stratification of a ventilated space with sources of buoyancy (Cooper & Linden, 1992).....	31
Figure 11: Interface heights as a function of fluid strength ratio. Experimental results (left) show good agreement with mathematical model (right). ....	32
Figure 12: Pythagorean Addition of speeds induced by wind and buoyancy (Hunt & Linden, 1999).....	34
Figure 13: A visual representation of the sealed body assumption(True, Sandberg, Heiselberg, & Nielsen, 2003).....	40
Figure 14: The pressure differential across a window is typically constant at pressures above 10 Pa (Heiselberg, Svidt, & Nielsen, Characteristics of airflow from open windows, 2001).....	41
Figure 15: The discharge coefficient as a function of k. k represents the ratio of the average air speed in the opening to the ambient outside wind speed (Sawachi, et al., 2004).....	43
Figure 16: The method to obtain the geometrical opening area of an awning, side-hung, or casement window (Heiselberg, Svidt, & Nielsen, 2001). ....	45
Figure 17: Values of $Ck$ , adapted from (Prestandard prEN 15242, 2005).....	46
Figure 18: A solution to vertical spaces in multizone models is to divide one zone into multiple, as seen with zone 4 (left) split into multiple zones 4, 5, 6, and 7 (Tan & Glicksman, 2005). ....	54

Figure 19: A shape divided into many elements (left). A CFD simulation of a simple space (right). (CRADLE-CFD).	56
Figure 20: Location of many of the sensors installed in the Harmony House.	67
Figure 21: The temperature deviations of the HOBO sensors. Variation among the sensors was at most 0.5°C	69
Figure 22: A flow chart of methodology used to assess the thermal comfort of the Harmony House.	79
Figure 23: The completed “Aerocap” planned to be place atop the Harmony House(Sustainability Television).	83
Figure 24: Several months of recorded data. The data is difficult to interpret in such a large scale so smaller segments must be investigated to make any conclusions.	84
Figure 25: Status of the sensors used. Shaded regions represent time when the sensors were online. Non-shaded regions represent holes in data due to sensor malfunction or delayed installation.	86
Figure 26: July 12, 2014 from the compiled data.	88
Figure 27: A two week segment featuring full use of the skylights and the cooling effect they provide. Note that some of the data seen in the legend is not shown as this data was recorded during the shutdown of some equipment.	89
Figure 28: The interior climate data and the outdoor temperature for July 9, 2014 (left) and July 17, 2014 (right).	90
Figure 29: The outdoor and indoor relative humidity recorded, plotted with the outdoor and indoor temperatures.	91
Figure 30: Visualization of the dynamic thermal model of the Harmony House.	93
Figure 31: The three separated zones of the dynamic thermal model: the first floor, the second floor, and the skylight.	94
Figure 32: Photograph of the Harmony House (left). Meshed CFD model of the Harmony House (right).	95
Figure 33: An overhead view of the computational domain used.	96
Figure 34: The determination of the optimal mesh cell size. Uniform refers to a constant cell size throughout the computational domain. Nonuniform refers to a refined mesh cell size around the opening, of a different cell resolution than the rest of the computational domain.	97
Figure 35: Comparison of simple window discharge coefficient results by Hult et al. (2012) and work done in scSTREAM CFD for model validation.	100
Figure 36: Comparison of detailed window discharge coefficient results by Hult et al. (2012) and work done by scSTREAM CFD for model validation.	100
Figure 37: Discharge coefficients for the windows at various opening angles.	101
Figure 38: Comparison of simulated (dotted) and measured (solid) results in temperature for July 13 (recorded) and July 22 (simulated).	104

Figure 39: Inputting a fixed temperature on all surfaces on the first floor (red). Second floor and skylight temperature were also set as fixed, according to the results of the dynamic thermal model. ....	105
Figure 40: CFD profile of the house for a cool day, showing clear temperature stratification within the main atrium. The level of stratification and mixing varies depending on the wind speed. ....	106
Figure 41: CFD representation of air flow through the house in a cross section showing the increased air flows at the inlet and outlet with low air speeds in most areas of the house. ....	107
Figure 42: Comparison of simulated (triangle) and measured air speeds (square) near the skylights, location 1 (Figure 20, sensor a), beam, location 2 (Figure 20, sensor b), and central area, location 3 (Figure 20, sensor c). Error bars represent one standard deviation from the mean. ....	108
Figure 43: Integrating the air velocity across the openings results in the volumetric air flow. ..	109
Figure 44: The operative temperatures of the first floor for each measurement's respective prevailing mean outdoor temperature. Recorded data shown in blue, dynamic thermal model results are shown in black. ....	110
Figure 45: A comfort chart of operative temperatures under typical conditions (blue) and with a venture-shaped cap on the chimney (black). ....	112
Figure 46: Operative temperatures of the bedroom (top, a) and the first floor of the atrium (bottom, b). Note that there is no data for the outdoor temperature in the graph on the bottom. ....	115
Figure 47: Adaptive thermal comfort of the bedroom (left, a) and the first floor of the atrium (right, b). ....	116
Figure 48: Main floor of the Harmony House. This area consists of six temperature sensors, two air-speed sensors, and three state sensors. Numbers beside sensor symbols indicate their approximate height, in feet, above the floor level. ....	132
Figure 49: Upper floor of the Harmony House. This area consists of five temperature sensors, one air-speed sensor, and one state sensor. ....	133
Figure 50: Roof of the Harmony House. This area consists of two state sensors, one on each skylight. ....	133

## 1. INTRODUCTION

The need to decrease worldwide energy consumption is evident within all energy sectors: transportation, commercial, residential, and industrial. Residential energy subsectors include domestic hot water, lighting, food preparation, appliances, and others, but heating, ventilation, and air conditioning take up substantially more energy than any other subsector (Perez-Lombard, Ortiz, & Pout, 2008). This presents a sizable opportunity to reduce energy use by substituting HVAC systems with alternatives that use substantially less, if any, energy. The integration of natural ventilation into homes is one approach that has a large potential of reducing the residential energy demand. The problem with doing so becomes apparent when considering the number of aspects affecting natural ventilation. Natural ventilation is highly dependent on many of the factors seen in Table 1, and as a result, engineering systems for natural ventilation is challenging and to work towards a solution to this problem, one must thoroughly understand the problem and these factors relating to it. While many beneficial design guidelines have already been developed based on previous experiments, the guidelines rarely include full characterizations of indoor and outdoor air movement. Some reasoning behind this limitation is outlined by Ernest, Bauman, and Arens (1991).

1. Effects of external building geometry and wind characteristics are not accounted for.
2. Wind tunnel tests are often compromised by model sizes too large for a given wind tunnel.
3. Upwind obstructions are rarely considered.
4. Interior space configurations are simple and have little variability.
5. Interior air turbulence is not measured.

6. Air speeds measured inside could not be related to local climate data.

**Table 1: Natural ventilation design relies on many aspects and they often directly interact with each other.**

<p>4. <b>Terrain:</b></p> <ul style="list-style-type: none"> <li>• Topography</li> <li>• Hills, mountains</li> <li>• Surrounding obstacles</li> <li>• Neighboring Buildings</li> </ul>	<p>1. <b>Climate:</b></p> <ul style="list-style-type: none"> <li>• Prevailing winds</li> <li>• Solar radiation</li> <li>• Temperature</li> <li>• Relative humidity</li> </ul>	<p>5. <b>Surroundings:</b></p> <ul style="list-style-type: none"> <li>• Air pollution</li> <li>• Noise</li> <li>• Heat island effect</li> </ul>
<p>6. <b>Operation Strategies:</b></p> <ul style="list-style-type: none"> <li>• Control strategy</li> <li>• Natural/Hybrid</li> <li>• Day/Night</li> <li>• Season, Weather</li> <li>• Daily Peaks</li> <li>• Passive: lag, damping</li> </ul>	<p>2. <b>Building:</b></p> <ul style="list-style-type: none"> <li>• Type</li> <li>• Architecture</li> <li>• Windows</li> <li>• Orientation</li> <li>• Internal partitions</li> <li>• Construction</li> </ul>	<p>7. <b>Passive strategies:</b></p> <ul style="list-style-type: none"> <li>• Aperture</li> <li>• Control (e.g. solar)</li> <li>• Absorber</li> <li>• Thermal mass</li> <li>• Distribution</li> </ul>
<p>8. <b>Technologies: (efficiency)</b></p> <ul style="list-style-type: none"> <li>• Location, position, exposure</li> <li>• Driving forces: <math>\Delta t</math>, <math>\Delta C_p</math>, <math>\Delta P</math></li> <li>• Resistance to flow <math>C_D</math></li> <li>• Geometry</li> <li>• Design specs</li> <li>• Velocity, flow</li> <li>• Air tempering efficiency</li> <li>• Distribution</li> </ul>	<p>3. <b>Occupancy:</b></p> <ul style="list-style-type: none"> <li>• Behaviors, Schedules</li> <li>• Processes</li> <li>• Operations</li> </ul>	<p>9. <b>Risk Factors:</b></p> <ul style="list-style-type: none"> <li>• Control</li> <li>• Rain penetration</li> <li>• Fire &amp; Smoke control</li> <li>• Safety</li> <li>• Security, Privacy</li> <li>• Pollution</li> <li>• Noise</li> <li>• Drafts</li> <li>• Acceptable air distribution</li> <li>• Under/Over-ventilation</li> </ul>

The reminder of this introduction presents some background information on the local climate, indoor thermal comfort requirements, and natural ventilation technologies. This information is fundamental to support the methodology laid out for this research. The last two sections of the introduction include the objectives of this research, and the thesis organization.

### **1.1. Potential of natural ventilation and motivation**

Achieving acceptable indoor environmental quality without a dependence on mechanical systems has historically been unsuccessful. Santamouris (2007) observed that among residential constructions, the architectural styles used today are often poorly designed and

do not use the local climate conditions to their advantage, such as solar gains, thermal controls, and inventive window placement. A proper design considers the many aspects that are affected by natural ventilation, most notably the climate, which can require an accurate knowledge of typical wind speeds and directions (Santamouris, 2013). As a result, these homes' potential to benefit from natural ventilation is seriously limited and mechanical systems are relied on to meet cooling and ventilation needs, which are usually precisely defined and enforced. In general, homes today typically are not built with much attention given to allowing them to efficiently ventilate. Sherman and Matson (2002) noted that they are built tighter and more disconnected from the outdoor environment in an attempt to keep the heat out during the warmer seasons and in during the colder ones. Typically, homes built in the past were leakier and breathed significantly more which beneficially allowed warm air to escape in the summer, but this had the side effect of significant heat loss in the winter. Now, especially in industrialized countries, they are enclosed, independent, and static environments (Tzikopoulos, Karatza, & Paravantis, 2005). With the decrease of air infiltration and exfiltration, the occupants of these tighter homes are becoming too accustomed to the narrow environmental conditions and any slight variations from these strict conditions cause a sense of discomfort (Nicol, Humphreys, & Roaf, Adaptive Thermal Comfort: Principles and Practice, 2012).

Because of the complex and often opposing interactions between aspects affecting natural ventilation, the processes of natural ventilation are difficult to optimize. Building designers and architects must be able to design with special consideration to the internal gains of the space. The natural ventilation process relies almost entirely on free solar energy to operate, which includes direct solar radiation and indirectly, the wind. To a lesser extent, internal electrical loads and people can account for some energy added to the indoor environment as well.

Storing solar energy within interior thermal mass is an effective method to control thermal energy to the interior for later use. It also helps keep temperatures stable, which is another important aspect of acceptable thermal comfort (Gregory, Moghtaderi, Sugo, & Page, 2007). The occupants have plenty of control over this process through opening windows and closing blinds and shades.

Outdoor air is required to maintain healthy indoor environmental conditions indoors; homes must be ventilated, whether mechanically or naturally. Usually architects do not design houses to utilize natural ventilation as the primary source of ventilation; however, some houses are now being built with that goal. The problem architects face with incorporating natural ventilation into homes is that the application of natural ventilation is incredibly case-specific and the dynamic interactions between the building structure, occupants, weather conditions, and HVAC systems are dynamic and difficult to predict (Loonen, Hoes, & Hensen, 2014). A single methodology cannot be applied to every new or existing construction since one house may differ from any other in a multitude of ways and there can be an infinite combination of factors that affect the indoor air flows. Spengler et al. (2000) make note of several factors that affect differences between buildings with respect to natural ventilation potential. Weather conditions can be significantly different within a climate or microclimate region, and wind speeds and directions can be highly variable. Some areas lie within or induce their own heat islands so incoming air is less desirable, and some areas are sheltered from the sun which limits the solar radiation entering the house. Natural ventilation depends heavily on these factors and thus, these aspects must be well defined and quantified in order to effectively apply and tune them to residential homes.

The motivation for this problem is the need to reduce global energy consumption, especially under the threat of climate change, by reducing or eliminating the use of HVAC systems while achieving acceptable indoor environmental conditions. The vast majority of the industrialized world's energy use is on the climatization of buildings in order to control the indoor environment for acceptable environmental conditions (Awbi, 2003). These energy-dependent buildings are largely unsustainable, and some reports claim that heating, ventilation, and air conditioning take up half of all residential building energy use, as reported by the U.S. Energy Information Administration (2015) and seen in Figure 1. Others state this number could be as high as 70% and 30 – 50% of this is from ventilation and infiltration, alone (Khan, Su, & Riffat, 2008). Energy used on mechanical systems is often wasted since natural ventilation design into buildings could potentially achieve similar results of cooling and ventilation using just the local climate and the physical properties of air. The cost of implementing energy-saving features is typically only 3-5% extra on the cost of the construction of a house and it is usually returned through energy bill savings within only a few years (Pimentel, et al., 1994); however, some claim purely naturally ventilated buildings can cost 10% – 15% less than its mechanically ventilated counterparts (The Department of the Environment, Transport, and the Regions, 1998), due to the lack of mechanical engineering services and equipment required during construction. Another issue arises because people tend to be concerned with their own well-being; energy-conserving actions that are deemed inconvenient to someone's daily life are less likely to be taken (Kollmuss & Agyeman, 2002). Exposing this notion as untrue and showing the value and ease of conserving energy could motivate and inspire more people to taking the necessary actions to conserve energy. This would ultimately reduce the energy use of buildings would be a

promising opportunity to significantly reduce global energy consumption, as well as  $CO_2$  emissions.

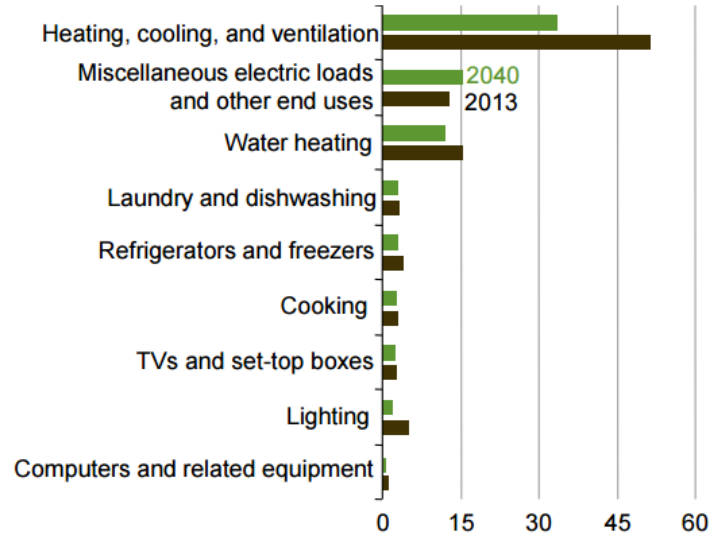


Figure 1: U.S. Residential sector delivered energy intensity for selected end uses, 2013 and 2040 (million Btu per household per year) (U.S. Energy Information Administration, 2015).

### 1.1.1. Potential of the climate

The climate of any location is by far the most critical factor in natural ventilation design and many studies have investigated it with regards to the potential to use natural ventilation. ASHRAE Standard 90.1 (2013) classified the mild climate of Vancouver British Columbia to fall under the marine climate zone. This classification follows several criteria, first involving categorizing many major cities with a zone number based on a thermal criteria (Table 2) including the location's associated number of cooling and heating degree days. Vancouver and its surrounding suburbs fall under zone 5.

**Table 2: International Climate Zone definitions (ASHRAE, 2013)**

Zone Number	Name	Thermal Criteria
1	Very Hot-Humid (1A), Dry (1B)	$9000 < CDD50^{\circ}\text{F}$
2	Hot-Humid (2A), Dry (2B)	$6300 < CDD50^{\circ}\text{F} \leq 9000$
3A and 3B	Warm-Humid (3A), Dry (3B)	$4500 < CDD50^{\circ}\text{F} \leq 6300$
3C	Warm-Marine	$CDD50^{\circ}\text{F} \leq 4500$ and $HDD65^{\circ}\text{F} \leq 3600$
4A and 4B	Mixed-Humid (4A), Dry (4B)	$CDD50^{\circ}\text{F} \leq 4500$ and $3600 < HDD65^{\circ}\text{F} \leq 5400$
4C	Mixed-Marine	$3600 < HDD65^{\circ}\text{F} \leq 5400$
5A, 5B and 5C	Cool-Humid (5A), Dry (5B), Marine (5C)	$5400 < HDD65^{\circ}\text{F} \leq 7200$
6A and 6B	Cool-Humid (6A), Dry (6B)	$7200 < HDD65^{\circ}\text{F} \leq 9000$
7	Very Cold	$9000 < HDD65^{\circ}\text{F} \leq 12600$
8	Subarctic	$12600 < HDD65^{\circ}\text{F}$

Zone 5 contains the sub-zones, 5A (cool-humid), 5B (dry), and 5C (marine). The requirements for a location to be labeled within Zone 5C include the following:

- The mean temperature of the coldest month falls between 27°F (-3°C) and 65°F (18°C).
- The warmest month has a mean temperature of < 72°F (22°C).
- At least four months with mean temperatures over 50°F (10°C).
- Dry season in summer. The month with the heaviest precipitation in the cold season has at least three times as much precipitation as the month with the least precipitation in the rest of the year. The cold season is October through March in the Northern Hemisphere.

Vancouver satisfies these requirements, and thus is classified as zone 5C: marine, much due to warm moist air carried over the Pacific Ocean by the Westerlies. The local Coast

Mountains also impact the local climate significantly, serving as a barrier to the arctic air as well as cause cool air to rise and condense, resulting in widespread rain over the area. The resultant warm climate normals can be seen in Table 3 with more warming and changes in climate expected to cause temperatures to rise higher than the global average (IPCC, Intergovernmental Panel on Climate Change, 2013).

**Table 3: Climate normals 1981 – 2010 (Environment Canada, 2015).**

<b>Air Temperature</b>	<b>Jan</b>	<b>Feb</b>	<b>Mar</b>	<b>Apr</b>	<b>May</b>	<b>Jun</b>	<b>Jul</b>	<b>Aug</b>	<b>Sep</b>	<b>Oct</b>	<b>Nov</b>	<b>Dec</b>
Daily Average (°C)	3.9	4.6	6.8	9.1	12.5	15.2	17.6	18.1	15.0	10.4	6.0	3.3
Daily Maximum (°C)	6.3	7.5	10.2	12.9	16.7	19.3	22.2	22.7	19.1	13.6	8.3	5.6
Daily Minimum (°C)	1.4	1.6	3.4	5.3	8.3	11.0	13.0	13.4	10.8	7.2	3.6	0.9
Extreme Maximum (°C)	16.5	19.0	24.0	28.0	34.5	33.5	33.5	34.0	32.5	28.0	19.0	15.5
Date (yy/dd)	81/ 20	86/ 27	04/ 29	87/ 27	83/ 29	89/ 03	94/ 20	81/ 08	96/ 02	87/ 01	81/ 02	96/ 02
Extreme Minimum (°C)	-14.0	-13.0	-7.8	-1.0	-1.0	4.4	-2.5	7.2	1.0	-7.0	-15.5	-16.0
Date (yy/dd)	79/ 01	89/ 02	76/ 03	86/ 30	02/ 06	76/ 03	99/ 28	73/ 18	00/ 04	84/ 31	85/ 27	90/ 29
<b>Relative humidity</b>	88.0	88.0	87.0	85.0	84.0	84.0	85.0	88.0	91.0	91.0	88.0	88.0

Local data regularly retrieved by weather stations at the British Columbia Institute of Technology (BCIT) from 2013 shows the weather was higher than the expected normals. Figure 2 presents the outdoor daily average temperatures for each month. The data was all obtained during 2013, but because of technical reasons, the data for 2014 could not be obtained.

Figure 3 shows the maximum, minimum, and average temperatures experienced throughout a typical August day. Practically, all hours of the day could benefit from natural ventilation, with the exception of the uncommon cooler days. The prevailing wind direction recorded from May through September shows to be typically from the south and highest during the warmest hours of the day. This can be seen in both the wind-rose chart and the average speed and direction chart. The probability chart shows the most common speeds experienced were in the 0.5 to 1.0 m/s range (Figure 4).

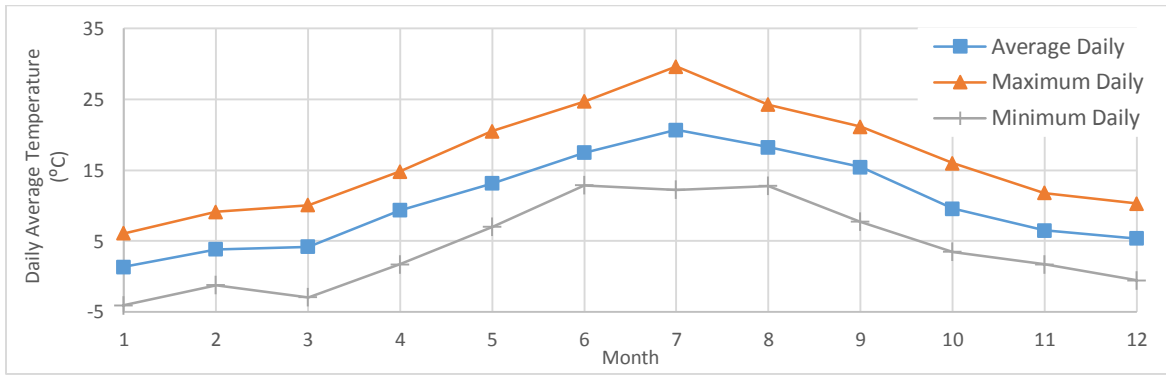


**Figure 2: Outdoor daily average monthly temperature for 2013 at a local weather station.**

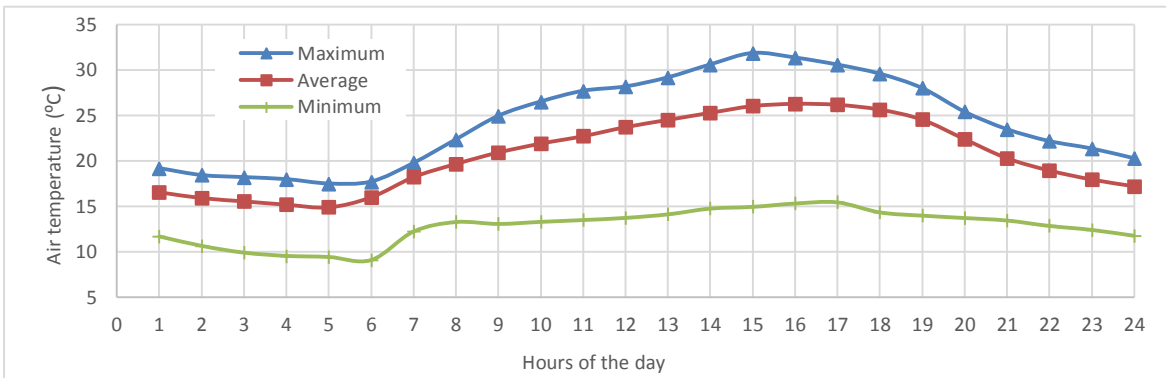


**Figure 3: Daily air temperature profile at a local weather station in August of 2013.**

The marine climate zone is not only found in the Pacific Northwest, it is found in many other parts of the world, even with along regions along the coast of the Atlantic Ocean. Olsen and Chen (2003) found that for a building situated in the comparable marine climate of the United Kingdom, natural ventilation induced only by opening windows in combination with night cooling was ideal to meet the cooling needs of the building, particularly in the spring and fall; however, during parts of the summer, natural ventilation alone was unable to meet the cooling demands to allow an acceptable indoor environmental quality, so some mechanical systems were required to cool the building. This shows that while natural ventilation may not always be entirely feasible to create comfortable indoor conditions on the hottest summer days, it can be used to supplement forced air and air conditioning to cool the building with a hybrid ventilation system approach. Especially with newer well-insulated homes being built tighter,

infiltration is less prevalent and becomes further insufficient to provide any significant ventilation, making the use of these mechanical or hybrid ventilation systems more necessary. This adds to the desire to determine strategies that will facilitate natural ventilation more effectively.

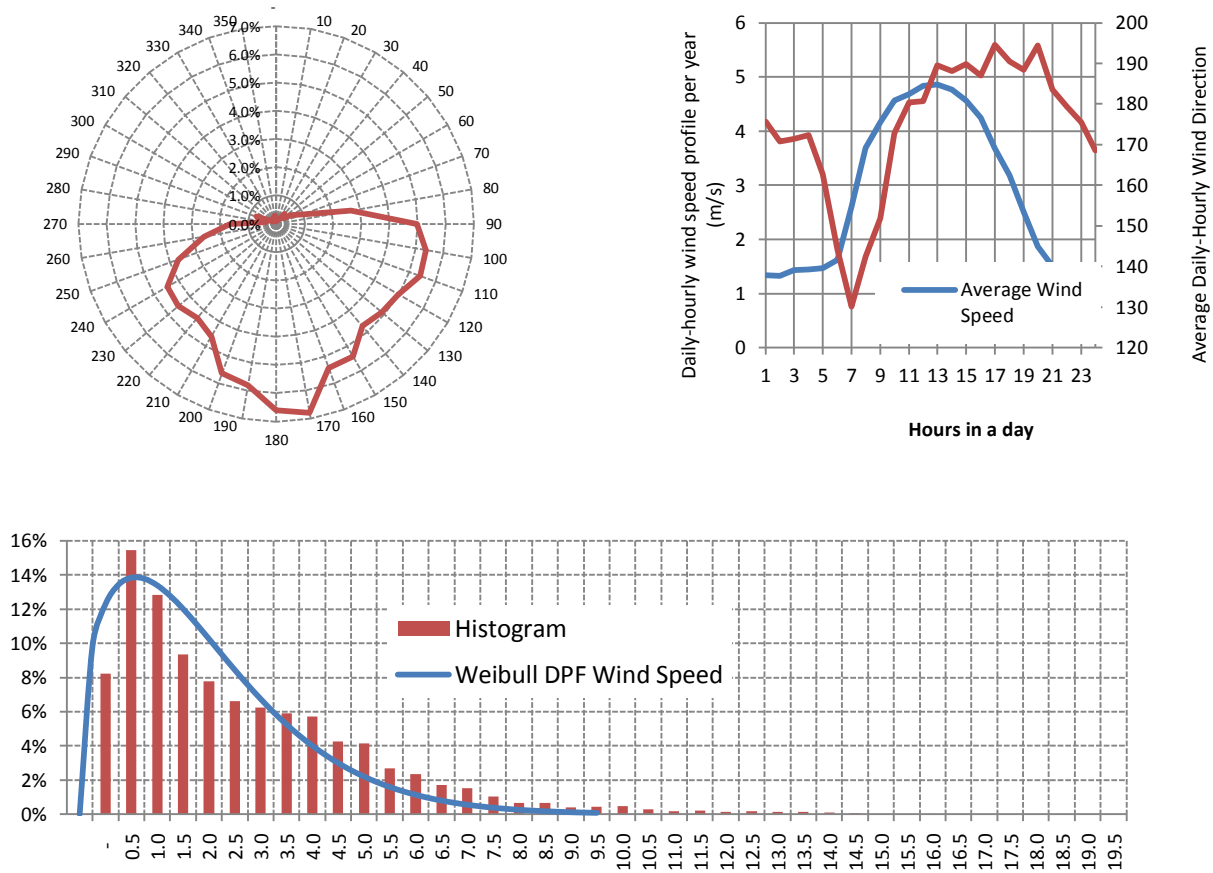


**Figure 4: Wind-rose from local weather station from May to August, 2013 (top left). Daily average wind speed and direction from May to September, 2013 (top right). Probability distribution of air speeds from the local weather station from May to August, 2013 (bottom).**

Even within the mild marine climate zone, there may often be driving forces that are too weak for natural ventilation to be primarily used as a source of ventilation, as well as climates that are too harsh. Santamouris (2013) mentions there must be reasonable consideration given to local wind behaviour, as wind plays a significant role in the potential for natural ventilation in a

home. Average wind intensity in Vancouver is typically lower than that seen in the rest of Canada and many parts of North America (ASHRAE, 2009). This may limit a portion of the natural ventilation a house can facilitate as it forces homes to only rely on the static pressure differentials across the envelope, due to the lack of wind and its corresponding dynamic pressure. An example where the climate may be too harsh includes the heat island effect (Russell, Sherman, & Rudd, 2005),(V.Geros, M.Santamouris, N.Papanikolaou, & G.Guarracino, 2001). This occurs when many buildings and people congregate in a small area, changing the local climate through replacing green spaces with extensive use of concrete and energy intensive structures. This typically results in less wind and increased temperatures because of a higher density of building structures. Due to some of these unfavorable localized conditions, Vancouver's climate may not always offer sufficient conditions to allow natural ventilation to operate; however, in general, the conditions are acceptable and certainly capable to promote natural ventilation the majority of the time.

### **1.1.2. Adaptive thermal comfort**

The effectiveness of natural ventilation relies on the idea that occupants of a naturally ventilated home have control over their environment and can open and close windows, as they choose. Adaptive thermal comfort has been thoroughly researched and much work is being done by researchers worldwide. ASHRAE Standard 55: Thermal Environmental Conditions for Human Occupancy is a standard used in the design of new residential constructions. The standard is meant to specify the conditions (temperature, thermal radiation, humidity and air speed) which allow at least 80% of occupants to feel comfortable, which only includes opinions of "slightly warm," slightly cool," and "neutral". A general acceptability criterion can be seen in

Figure 5. While it is extensively referenced in the comfort of occupants, Brager and de Dear (2000) and Fabi et al. (2012) mention the standard ignores several important factors relating to human comfort such as cultural, social, and contextual factors that do not fit the specific requirements of ASHRAE Standard 55, which ASHRAE implies applies to all building types, climates, and populations.

There are multiple criterions of ASHRAE Standard 55 which can apply to different building systems. Most notable is the adaptive comfort model which applies to naturally ventilated buildings. The occupants in naturally ventilated buildings typically wear a wider range of clothing and they psychologically and physiologically adapt to a wider temperature range of acceptability instead of the artificial environments created in conditioned spaces (Santamouris, *Advances in Passive Cooling*, 2007). de Dear and Brager (1998) investigated this statistically by taking data from the ASHRAE RP-884 database, a compilation of nearly 21,000 data sets of people including the following information:

- thermal questionnaire responses of sensation, acceptability, and preference
- clothing and metabolic estimates
- indoor climate observations (air, operative, and plane radiant asymmetry temperatures, air velocity, dew point)
- thermal indices such as mean radiant temperature
- outdoor climate observations (temperature, relative humidity)

Standardizing the data according to various comfort standards allowed the data to confirm that statistically, occupants in buildings with centrally controlled HVAC had much less

control over their environmental conditions when compared to naturally ventilated buildings, where occupants would engage in controlling their environment.

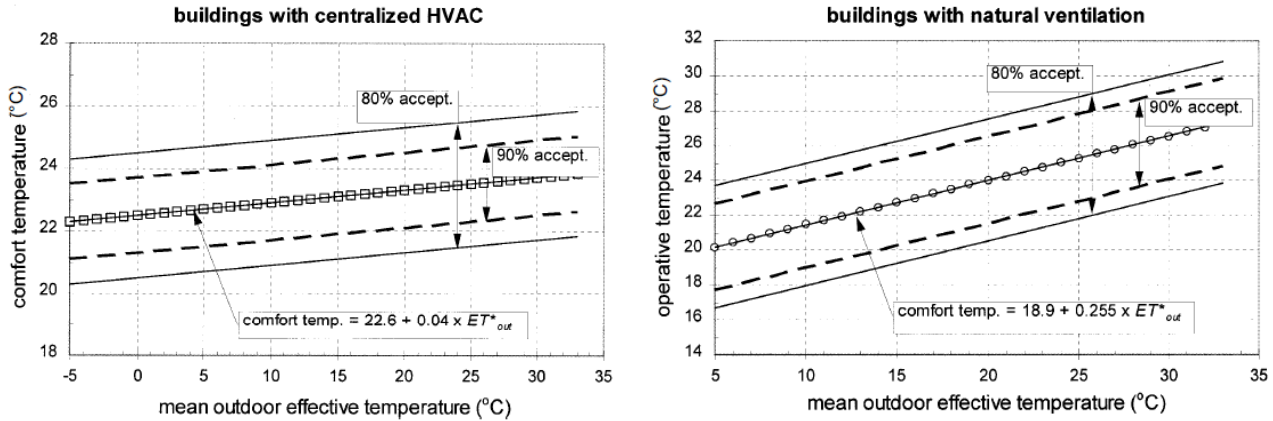


**Figure 5: Comfort conditions in which 80% and 90% of occupants are comfortable. Buildings with centralized HVAC (left) are much narrower than those in naturally ventilated buildings (right) (de Dear & Brager, 1998).**

This need for multiple criteria is made evident by Brager and de Dear (2002). They studied Fanger's PMV thermal comfort model, and found that the model accurately predicted the observed comfort temperatures of occupants for buildings conditioned with HVAC systems; however, the model was much less effective at predicting the comfort temperatures of naturally ventilated buildings. They postulated the difference was likely psychological due to shifting thermal expectations as well as a higher level of perceived control. Kim and de Dear (2012) studied different types of ventilation systems and they found that the greatest overall occupant satisfaction occurred when occupants had control over the HVAC systems as well as the ability to operate windows; however, they also found that occupants were more thermally satisfied when they only had the ability to operate windows, such as in purely naturally ventilated spaces. Kim and de Dear (2012) also discovered that occupants were most thermally comfortable with a hybrid ventilation system. This further supports the idea from the previous section that in some cases, assisting natural ventilation with a mechanical system may be required for thermal

comfort. How much additional ventilation is needed to achieve thermal comfort is an issue that needs to be investigated further.

Another aspect of the local environment that should be considered when assessing thermal comfort is the relative humidity of the space. European Standard EN15251 stated that “humidity has only a small effect on thermal sensation and perceived air quality in the rooms of sedentary occupancy.” Algorithms generated by the EU Project Smart Controls and Thermal Comfort intended to reduce energy use by air conditioning systems showed that the effect of relative humidity on thermal comfort was significantly smaller than the operative temperature of the space (Nicol & Humphreys, 2010).

## **1.2. The use of passive technologies for cooling**

There has been extensive research on the effectiveness of various passive technologies which range from simple to complex and innovative, each with their own benefits and limitations that are often dependent on climate or design. Some of the easiest and most common approaches in sustainable building design include properly-sized overhangs to limit the influx of solar radiation; however, these must be implemented during construction. Other simple technologies include wind scoops to collect and direct additional wind indoors, as well as solar chimneys to supplement stack effect and buoyancy-driven air flow (Tantasavasdi, Srebric, & Chen, 2001). Solar chimneys are especially effective in the absence of wind, and their effectiveness diminishes as the outdoor wind increases. The use of wind towers can supplement this by increasing the ventilation in the presence of wind (Bansal, Mathur, & Bhandari, 1994). Proper optimization and shape of wind towers and solar chimneys (Figure 6), often accomplished using computational fluid dynamics (abbreviated CFD), can substantially increase wind-induced

ventilation (van Hooff, Blocken, Aanen, & Bronsema, 2011). When designing a solar chimney, there must be much consideration to several factors outlined in a review by Khanal and Lei (2011). The geometry of the chimney plays a significant role in the ventilation performance and includes, most notably, the inlet and outlet sizes, and the dimensions of the absorptance region. Using mathematical and full scale models, Bassiouny and Koura (2008) found that maximizing the width of the absorptance region resulted in the most significant increase of air flow when compared to altering the inlet area; however, the size of the inlet area was a critical aspect of the geometry. Ventilation benefitted from a larger inlet but suffered if the inlet was too large due to increase flow back into the space. In the typical design of a solar chimney (Figure 6), the angle is fixed and cannot be optimized for any solar altitude. Optimization instead considers the solar altitude over a full year and depending on the latitude of the solar chimney, the idea tilt angle was numerically and experimentally found to be a function of the latitude of the chimney and ranges between  $45^{\circ}$  and  $60^{\circ}$  (Mathur & Mathur, 2006). The sunlit absorbing surface should also have a high absorptance to emittance ratio.

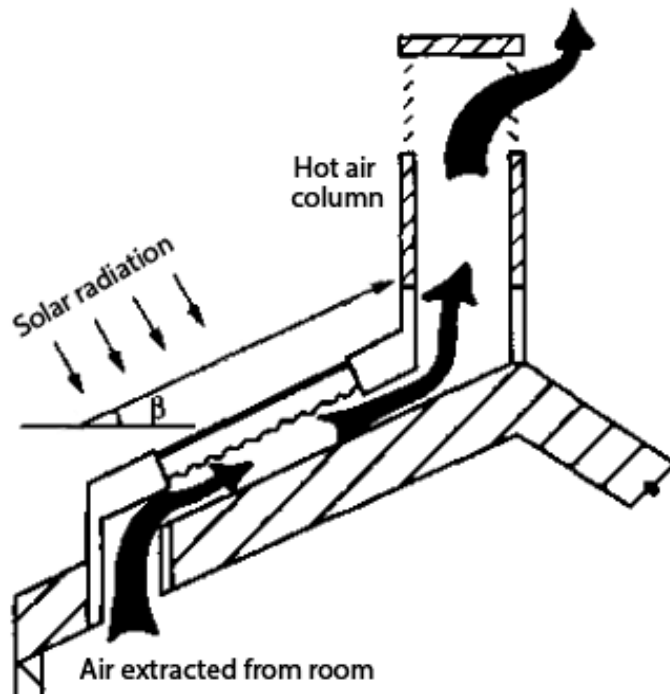


Figure 6: A solar chimney absorbs solar radiation, heating air and causing it to rise out of the chimney while extracting air from the space, promoting ventilation (Bansal, Mathur, & Bhandari, 1994).

### 1.3. Significance of window characterization

On the facade of a building, window type, placement, sizing, and attributes can have significant effects on the overall ventilation of a building. As seen in Figure 7, there are many different types of windows available to choose from, and it is important to know how each behaves in different situations and geographical locations. Design decisions can be influenced by aesthetics, expected weather behavior, options for variable operation, or simply occupant preference. For example, bottom-hung windows may offer increased rain protection over a sliding or casement window but they may direct air jets to unfavorable spaces. Casement windows can catch and direct wind indoors or shield a portion of it depending on the wind direction. Horizontal pivoted windows allow greater single-sided ventilation potential due to the height difference between the lower and upper sections of opening.

Properties of different window types when opened at a typical angle	Side hung, opening to inside	Bottom hung, opening to inside	Sliding, opened pane always covers part of window	Horizontal pivoted, lower part opening to outside	Top hung, opening to outside
					
Weather protection	-	+	-	O	O
Max. achievable ventilation rate	+	-	O	+	O
Adjustability of opening size	+	-	+	+	+
Flexibility for placement of furniture	-	+	+	O	+

**Figure 7: Evaluation of different window opening types and some of their properties under typical use. Description of symbols: - poor; O medium; + good (Roetzel, Tsangrassoulis, Dietrich, & Busching, 2010).**

The air flow path through the envelope can dictate the direction of flow in the interior. In most cases apart from sliding windows, the interior jet of air may be directed towards an outlet, reducing the effectiveness of the ventilation. Alternatively, the jet may be directed towards occupied spaces, reducing thermal comfort, or they may also disrupt a temperature stratification, potentially mixing the air in smaller spaces when the stratification was intended to more effectively exhaust warmer air. As a result, knowing how these jets behave on the interior space can be significant in the design stage of a passive house.

## 1.4.Objectives and scope

The scope of this research was to conduct a systematic study on the effectiveness of natural ventilation to maintain acceptable thermal comfort in a net-zero energy house located in the mild marine climate of the Pacific Northwest. This includes assessing the overall construction and design of the house as well as the important aspects that most affect the process of natural ventilation. Potential technologies and the effects they could have on the house are also included in this research. There was due consideration to various key factors affecting natural ventilation, including many of those listed in Table 1 and others which are addressed in the following literature review. While natural ventilation can be used throughout most of the

year in the climate studied, the time period studied is limited to the summer and shoulder seasons' and the corresponding weather conditions, as these are the seasons which mechanical systems are most heavily used. Computer-based models developed were compared and finely tuned with real data to assess their effectiveness to accurately simulate the real conditions experienced. Specifically, research was conducted to investigate and discover what aspects of the house made it perform so well, and in doing so, develop a methodology for assessing net-zero houses. Further goals included quantifying the effectiveness of some passive technologies used to facilitate natural ventilation, as well as investigating some risk factors related to thermal comfort. The objectives of this research are the following:

- To monitor the characteristics and performance of a net-zero energy home thoroughly utilizing natural ventilation.
- To investigate the effects of climate, architectural design, and construction on achieving natural ventilation in the Pacific Northwest.
- To investigate, in depth, the characteristics of awning windows and horizontal skylights, and the role they play to facilitate natural ventilation.

In doing these, the research may also accomplish the following:

- Investigate if and how accurately a net-zero energy house can be modeled using the coupling of whole-building energy modeling and CFD softwares.
- To investigate the feasibility of quantifying the effect of some passive technologies and strategies using aforementioned computer software models in enhancing natural ventilation, thermal comfort, and energy performance in net-zero energy houses.

In order to accomplish these objectives, the specifics of the project included monitoring and recording the environmental conditions of a net-zero energy house in Burnaby British Columbia, throughout the summer and into the early fall of 2014. The house, known as the Harmony House, was designed to incorporate natural ventilation, as cooling of the house was intended not to rely on mechanical systems during the summer months. To record data, the house was outfitted with a number of sensors to record temperature, relative humidity, and air speeds at various strategically-determined areas within many of the rooms. The operation of some windows and doors was also recorded to analyze their effect on the ventilation of the house. With the importance of window design with regard to natural ventilation, a test involving pressurizing and depressurizing the house was planned to record characteristics of the windows most significant in the ventilation of the house. To thoroughly understand the characteristics of the air within the Harmony House, the data recorded from field monitoring of the house and subsequent tests on the windows were inputted into models developed in two different softwares. The first software was an energy modeling software to conduct a whole-building dynamic simulation. Secondly, air flow modeling was done using CFD by inputting boundary conditions obtained from the whole-building analysis, as well as field monitoring. The CFD allowed for detailed air flow visualizations and temperature profiles to be observed within the house to assess its natural ventilation potential under various common scenarios. The results are expected to show the precise dynamics and phenomena of air flows through the house and define the interior conditions within the house and reveal why and how the house performed well and kept temperatures low, despite high outdoor conditions. This may benefit architects and engineers interested in passive design using natural ventilation by providing insight on how natural ventilation behaves in net-zero energy houses. The results may also offer methods to assess and

quantify design choices meant to improve cooling, decrease energy consumption, and achieve higher thermal comfort.

## **1.5. Thesis arrangement**

This thesis has been separated into sections describing the major areas of work that was conducted. Section 2 is an overview of the Harmony House; the house selected to be the case study for this research. Some of the relevant features of the house are discussed, as well as the general movement and mechanics of air entering the main atrium. Section 3 is the literature review which covers many of the important aspects affecting natural ventilation in a passive house, most significantly the main driving forces (wind and air buoyancy) and the interactions between them. There is also a heavy emphasis on the pressure differential across the building façade and the effects of window configuration on this pressure differential and the consequential flow of air in or out of building. Furthermore, it discusses some of the common methods of assessing natural ventilation in the breadths of monitoring, measuring, and modeling, with the latter concerning dynamic thermal models and computational fluid dynamics. Section 4 briefly describes the main problem and introduces the proposed solutions as well as to what extent the research will cover. The methodology of Section 5 explains the processes undertaken to solve the problem presented. It includes several stages of experiments (including both, planned and executed) that were done. The modeling component of the research is also discussed as the process of validation and coupling is explained, as well as explaining the metrics for assessing the thermal comfort in the models and the implementation of technologies to be tested. Section 6 discusses the results of the methodology and attempts to explain the outcomes

observed. Sections 7 and 8 conclude the results of the research and note the limitations and suggest areas for further work that can be conducted.

## **2. HARMONY HOUSE**

### **2.1.Introduction**

Harmony House EQUilibrium™ Housing Project was a project created to build a net-zero home with energy requirements satisfying that of the (CMHC) Canada Mortgage and Housing Corporation's EQUilibrium™ - National Sustainable Housing Demonstration Initiative, while achieving a healthy indoor environment. By using several energy-friendly architectural design choices, the home produces more energy, all renewable, than it consumes. The house, located in Burnaby British Columbia, utilizes air buoyancy, stack effect, and the local wind to intake cool fresh outdoor air and exhaust warmer air through large operable skylight openings which allows for free cooling almost year round. Most of the air exchanging takes place in the main atrium living area. The atrium is a large, open area with operable windows in the lower portion and is closely connected to a side door in the kitchen. Other paths to the outdoors, such as the front door or other operable windows, are typically closed. In addition to these, doors connected to the atrium mostly remain closed, further isolating the space from other factors. Air intake is primarily through the operable windows and the kitchen door and it exits through the above skylights. All openings are controlled through regular use by the occupants, with the exception of the skylight; in the presence of rain, it automatically closes. The architect's intent for the house is to not use any air conditioning in the house during the summer and instead rely on natural means to draw in cooler air. Figure 8 illustrates the architect's design intent for natural ventilation. According to anecdotal feedback from the homeowners, this design works and the house is performing as expected.

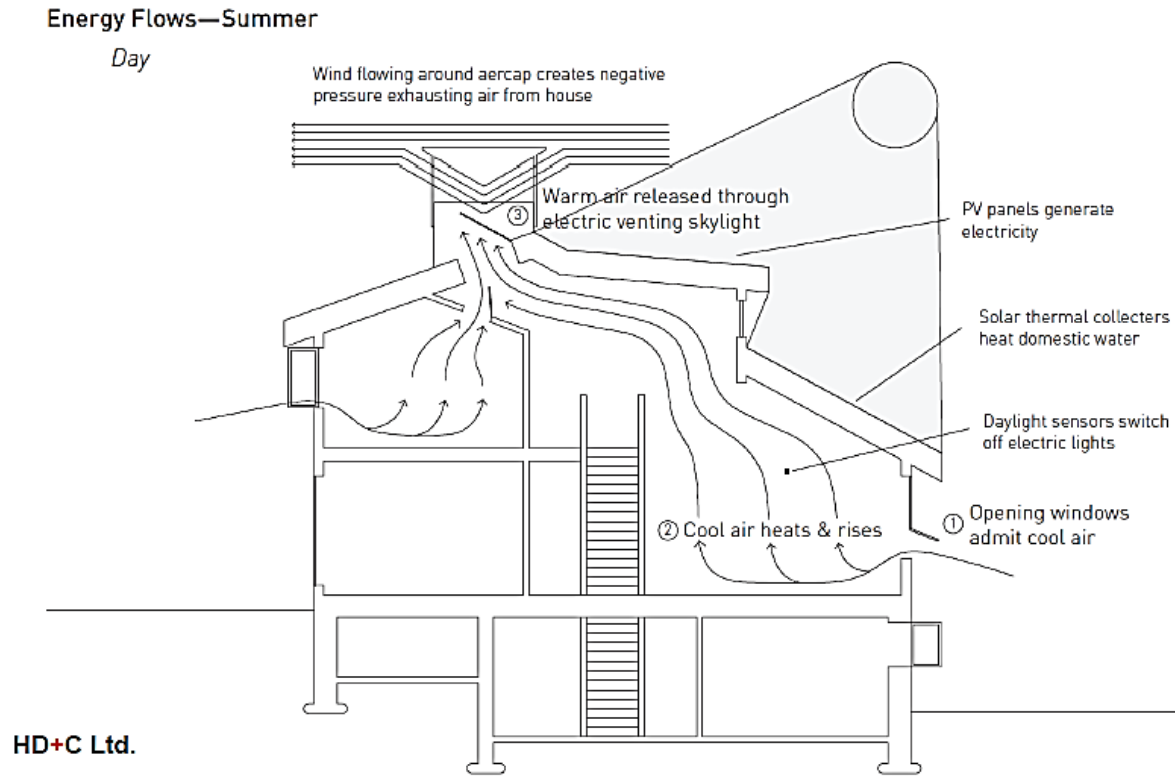


**Figure 8: Design Concepts by the architect on the natural ventilation of the house during summer months.**

An indoor floor plan of Harmony House can be found in APPENDIX A – Floor plan and sensor location. The basement was converted into a rental suite so access was prohibited. During the design phase of Harmony House, an "Aerocap" venturi-shaped chimney cap was planned and built; however, it was not installed due to some final decision changes. This Aerocap will be discussed in further sections.

## **2.2. Air behavior within the atrium**

The mechanism of air entering a space can significantly affect its behavior once in the space. Factors such as window size and configuration, space size and obstacles, incoming air velocity, and temperature differentials can all play roles in the ventilation of the space. Driven

by wind or buoyancy, incoming air creates a jet separated from the rest of the stagnant air in the room by a boundary layer. The jet dissipates away from the opening and the fresh air begins to mix with the air already in the space. The incoming air displaces the stale air which is exhausted out another orifice. In the case of the Harmony House, the defining characteristics are well known and have been observed so the mechanisms at various locations within the main atrium are relatively predictable (Figure 9).

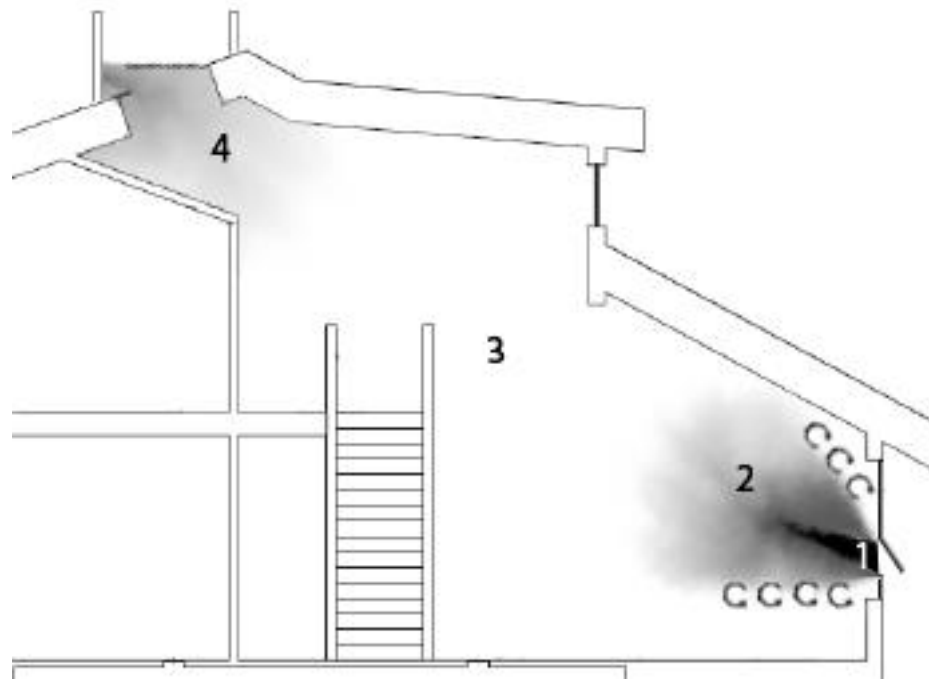


**Figure 9: The four main regions of air within the Harmony House's main atrium. The behaviour of air is different at each location.**

### **2.2.1. Zone 1: Potential core region**

Immediately downstream of the inlet is the potential core region (Awbi, 2003) which is characterized by a jet with a constant centerline velocity which usually extends outwards 5 – 10 times the length of the opening cross-section. This jet can be directed depending on the type of opening (Nitawichit, Khunatorn, & Tippyawong, 2008) and for the external-opening awning

windows installed in the Harmony House, the jet is typically directed upwards. In this region, there is no mixing of the incoming air and the indoor air.

### **2.2.2. Zone 2: Flow decay region**

As kinetic energy is dissipated into the surrounding air, the potential core disappears and the centerline velocity decays proportionally according to Equation 1 in the decay region.

$$\frac{U_m}{U_0} \propto \frac{1}{x^n} \quad \text{Eq. 1}$$

The fraction of the centerline velocity  $U_m$  to the centerline velocity in the potential core  $U_0$  is inversely proportionally to the distance  $x^n$  where  $x$  is the distance from the end of the potential core and  $n$  is some value dependent on the characteristics and configuration of the window, typically between 0.33 and 1.0. A fully developed turbulent flow expands the flow at some constant spread angle separating the jet from surrounding air by a shear layer and the centerline velocity decays at a faster rate in this area, according to Equation 2.

$$\frac{U_m}{U_0} \propto \frac{1}{x} \quad \text{Eq. 2}$$

### **2.2.3. Zone 3: Terminal region**

Further from opening, the rate of decay increases at an exponential rate until the flow is stagnant with the surrounding air and ultimately becomes thoroughly mixed.

$$\frac{U_m}{U_0} \propto \frac{1}{x^2} \quad \text{Eq. 3}$$

In the summer, using natural ventilation to cool the indoors introduces cool air. Though the temperature difference between the outdoor and indoor air is not significant, there still is an effect on the incoming air. Incoming air from the outside is acted on by buoyant pressure  $P_b$  equal to Equation 4.  $\Delta H$  is the difference in height between the inlet and outlet, and  $g$  is the acceleration due to gravity.

$$\Delta P_b = \rho_0 g \frac{T_{in} - T_{out}}{T_{in}} \Delta H \quad \text{Eq. 4}$$

For cooler air, this will induce incoming air to move downwards in most cases, as the indoors are almost always kept at higher temperatures than the outdoors. Only on the warmest days will the incoming jet be directed upwards if entering horizontally.

#### **2.2.4. Zone 4: Extraction region**

As the pressure differentials across the lower openings induce air into the house, through the conservation of mass combined with the fact that rising warm air causes buoyant pressure on the ceiling and up through the skylight, air is able to exhaust out of the house when the skylights are open. This warm air removes a significant amount of energy from the house.

### **2.3. Features and operation**

For cooling in the warmer months of the year, the house was installed with an air-to-air heat-pump cooling system; however, the architect who designed the house asked the owners to refrain from using it and since their occupancy, they have not used the air conditioning systems and their comfort through the summer had not been compromised. As indicated in Figure 8, a venturi-shaped cap called the Aerocap was designed and built for the house to enhance wind-

induced natural ventilation, but was never installed due to enclosure rain leakage concerns by the owners. The benefits this Aerocap may have provided are later investigated in this research.

To minimize direct solar heat gain at the occupied areas, the house is well shaded and windows are provided with adjustable blinds, except for the upper section of the corridor above the occupancy level on the top floor. This upper section includes the short chimney to let the sun warm the upper interior surfaces, in turn warming air by conductive heat transfer and generating a buoyant effect as the warm air rises. At the lower occupied levels, a high performance enclosure reduces the conductive heat transfer into the house. Because of the house's design and construction, a good balance exists between heat gains from solar radiation and the cooling effect of incoming air, so it is expected that the indoor temperatures remain stable. The challenge in the design was to make the house act as a 'thermal buffer' and give sufficient control to the house's occupants to regulate the environment just by opening or closing windows and skylights. Anecdotally, surprisingly comfortable conditions were experienced while placing sensors in the house during unusually warm summer days; air effectively circulated driven by wind pressures and buoyancy forces enhanced by the solar gains throughout the house.

The kinematic energy of the cooler incoming air would quickly dissipate upon entering the house and it would warm by convective heat transfer as it cools down the house, contributing to the buoyant forces leaving through the skylights. The skylights at the top of the chimney channel the buoyant warm air out of the house, therefore higher air speeds are expected at the chimney section than at the mid-height of the atrium and at the living area.

In addition to maximizing solar gains to reduce heating energy consumption in the winter, the house is oriented to capture the effects of the prevailing winds (Figure 4a and Figure

4b). A combination of positive and negative pressures at the lower windows and the skylight, respectively, drives the air flow; however, because wind is erratic and can be abruptly calm or strong, gusts are expected.

### **3. LITERATURE REVIEW**

As mentioned previously, Harmony House is a net-zero energy house engineered to incorporate natural ventilation as the primary source of ventilation and cooling. As a result, a thorough understanding of the mechanics of natural ventilation must be understood. The significant aspects of natural ventilation investigated in this thesis include wind and buoyancy and their effects on air flow through cross-ventilated spaces, particularly with spaces that have openings at various heights, such as in the Harmony House. This ensures that the space utilizes stack effect to help achieve natural ventilation. Furthermore, when investigating the effects of wind and buoyancy, they must be considered both together and independently to determine the effects they may have on each other. While there is a large range of parameters affecting wind and buoyancy; only some could be considered. Among these include thermal mass and its role in moving air, pressure differentials across the building envelope and within the building, and the orifices in the building envelope permitting natural ventilation to happen. The latter includes discussion of window types and their ability to allow air into a space and their resistance to air flow. This section will investigate previous studies varying from small-scale and full-scale experiments to computer-simulated results and how they have been effectively used to accurately predict natural ventilation.

#### **3.1. Natural ventilation and related mechanisms**

Natural ventilation is the process of introducing outside air into a space, typically replacing the older, often warmer air, all without any use of mechanical ventilation. This process is passively initiated through a pressure difference across the inside and outside of the building envelope. Pressure differences can arise from high pressure induced on the building facade by

wind, as well as low pressures induced by stack effect. The density of warm air is lower than that of cool air, causing it to rise in the presence of cool air. With a lower window allowing cool air to enter and a high window allowing warm air to leave, this creates a constant flow of fresh cool air into the space. The introduced cool air must be heated to instigate the stack effect; this energy typically comes from solar gains which heat the interior mass of the space. The following investigates these processes in depth.

### **3.1.1. Wind, buoyancy and their interactions**

In his own review of many papers covering the topic of the fluid mechanics of natural ventilation, Linden (1999) argued when a windward lower window in combination with a leeward upper window were the inlet and outlet, respectively, wind was fully able to promote natural ventilation, especially in cases where the air remained stratified. This stratification is particularly possible for low or null wind speeds; however, the stratification can be disturbed if wind speeds become too high, creating an interior of mixed air. While natural ventilation still occurs, it is much less efficient in this case. The process by which this occurs is complicated and depends on the strength of the stratification caused by temperature differentials, as well as the flow distribution of the space. This process was mathematically modeled by Cooper and Linden (1992).

They found expressions for a dimensionless 'interface height' variable, expressed in Figure 10 as heights,  $h_1$  and  $h_2$ , which determined the height as a fraction of the total height of the space, at which the boundary between two fluids of different densities exist. This number was dependent on the geometry of the space, as well as the incoming 'strength' of each fluid, which was dependent on density and inflow rate. In cases of strong incoming fluids, the



differences usually result in small temperature differences between head and foot levels while allowing the space to be sufficiently cooled; however, if hybrid cooling systems are implemented improperly, temperature differences can be as much as 10 degrees Celsius (Spencer & Zhai, 2007). A high neutral pressure plane (NPP) is also significantly beneficial in achieving ventilation throughout a building. All orifices below the NPP typically experience inflow from the outdoors instead of older air from other areas of the building, so a high NPP will maximize the number of orifices receiving air (Flourentzou, Van der Maas, & Roulet, 1998). This especially makes skylights useful due to their allowance of openings for outflow at the highest possible elevation.

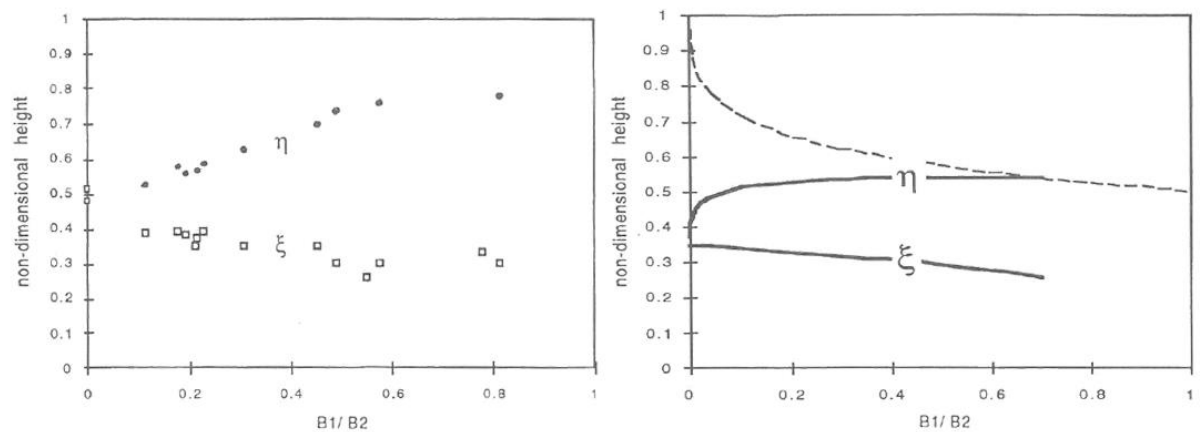


**Figure 11: Interface heights as a function of fluid strength ratio. Experimental results (left) show good agreement with mathematical model (right).**

When considering wind on the facade of a structure, there are two main components that must be examined. Khan, et al. (2008) describes the first as the mean driving pressure, which is simply the average pressure exerted on the face of the building around an opening of interest. The second component is the fluctuating component, described in detail by Straw, et al. (2000). The fluctuating component consists of three sub-components. Continuous air flow is the

fluctuation of wind incident on the facade causing broad banded ventilation, or varying ventilation dependent on wind conditions. Pulsation flow is the ventilation caused by pressure differentials between the interior and exterior, resulting with perpendicular flow from high to low pressure. Finally, eddy penetration is the ventilation due to eddies that form around an opening. The effect of fluctuating wind was investigated by Jiang and Chen (2002). Using a large eddy simulation (LES) model to simulate the results of a work conducted on buildings in Japan (Katayama, Tsutsumi, & Ishii, 1992), it was found that constant wind speeds upon the facade of a building and through an orifice can result with high air speeds penetrating deep into a space. Fluctuating wind; however, loses energy as direction changes, resulting in lower internal air speeds. Jiang and Chen's work reasonably agreed with the on-site work. The frequency of fluctuating wind conditions is much higher than that of constant speeds, so these high speed cores developing in naturally ventilated spaces do not often occur.

When examining the combined effects of wind and buoyancy, a CFD study conducted by Nitatwichit et al. (2008) found that the effect of buoyancy was most significant when wind speeds incident on a building were low,  $0.25\text{ m/s}$  in the study. They concluded this by creating a typical Thai state school in a model. Energy was added to the system by warming the walls to various temperatures and different air speeds were set as inlet boundary conditions. Their results were numerically verified with similar work done previously by Posner, et al (2003). Khan et al. (2008) continued to say that while stack effect dominates as the main mechanism for natural ventilation in low wind, in the summer the effectiveness of stack effect reduces due to the temperature differences between the interior and exterior being too low. While the temperature difference across the façade does not significantly impact the resistance of air flow into a space, it is very telling of the behaviour of the air once it enters the space (Heiselberg, Bjorn, &

Nielsen, 2002). It also is significant in introducing low energy air into the space to absorb energy and carry it out of the house. This further suggests that natural ventilation should be optimised by balancing contributions from buoyancy and wind but these quantitative analyses offer little insight to the physical interaction of wind and buoyancy. A mathematical study by Li and Delsante (2001) instead found analytical solutions for calculating natural ventilation. Deriving parameters from previous work, they concluded that flow rates can be easily determined when acting alone, but do not add linearly when acting simultaneously. Previous mathematical modeling by Hunt and Linden (1999) found that the air speeds induced by buoyancy can be expressed as a function of the difference of interior and exterior fluid densities. Air speeds induced by wind; however, can be expressed as a function of the difference of interior and exterior pressure. The interaction of these two speeds when complimenting each other do not add linearly, but rather using Pythagorean addition,  $|U_{total}| = \sqrt{|U_w|^2 + |U_B|^2}$  , as represented in Figure 12.

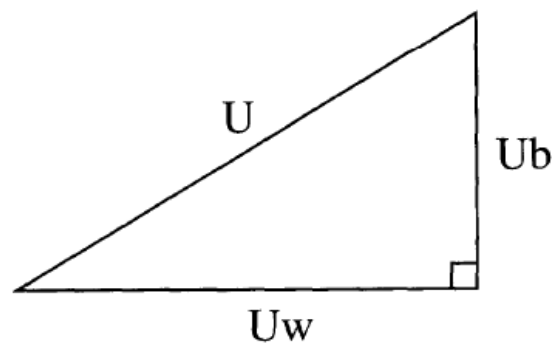


**Figure 12: Pythagorean Addition of speeds induced by wind and buoyancy (Hunt & Linden, 1999).**

In some cases, the wind's interaction with natural buoyancy may adversely affect air flow; this effect is researched in a study by Gan (2010). In a CFD study, Gan found that wind can assist buoyancy on the windward side of a building while simultaneously oppose it on the

leeward side. A solution he proposes to prevent the adverse wind effects is to depressurize the building by closing windows on the windward side of the building, or using some technologies such as wind turrets or turbines atop the building. Alternatively, the Aerocap could be beneficial in this regard. Aynsley (2007) adds that to promote proper ventilation of a space, the inlet area must be smaller than the outlet area. This prevents the likelihood of flow out of the inlet, as is seen in single-sided ventilation.

### **3.1.2. Contributions of thermal mass**

Natural ventilation is facilitated by the buoyancy caused by air temperature differentials. These temperature differentials are induced by cool and warm air, the warmer air typically having been heated by solar gains within the house. In order to store and release this solar energy, significant thermal mass is necessary and must be properly sized to store and disperse energy at appropriate rates. Thermal comfort should be achievable throughout the late hours of the day and into the night. Gagliano et al. (2014), conducted an on-site experiment in Catania Italy. The researchers found that the most effective thermal mass should have a time lag of about 8 hours for west-facing walls and 12 – 14 hours for east-facing in order to allow natural ventilation to proceed overnight; however, this time lag may not be appropriate in other climates, particularly outside Catania's climate zone. Many studies have also studied the appropriate time lag and come to similar conclusions (Spencer & Zhai, 2007), (Balaras, 1996), (Ma & Lin-Shu, 2012), (Yam, Li, & Zheng, 2003), (Gregory, Moghtaderi, Sugo, & Page, 2007). The latter of these continued that a more insulating building envelope would keep more stable temperatures indoors. They also found a relation between the area of sunlight-penetrating windows to the

amount of thermal mass required to store the heat, signifying the importance of window sizing, placement, and accessories to optimize the use of thermal storage for natural ventilation.

While generally, the use of thermal mass has been shown to increase ventilation flow rates, the results of some studies have shown otherwise. Using CFD to study the characteristics of wind any buoyancy-driven cross-ventilation through various window opening types in a classroom, Nitatwichit et al. (2008) found that air exchange rates actually decreased with increasing wall surface temperatures showing that in this case, the buoyancy caused by thermal mass acted against the wind-driven flow and overall, it reduced air flow rates. Another experiment, by Lo and Novoselac (2011) involving a full-sized house, was conducted to measure cross-ventilation using fluctuating pressure boundary conditions. Upon taking measurements of external pressures and inlet and outlet flow rates, a CFD model was generated to simulate temperature differences of up to 20°C between the incoming air and the surfaces of walls. While the fluctuation of pressures on the facade moderately affected the flow rates, the effect from the increased surface temperatures showed no change in ventilation rates over the wide range temperature differences tested. While the flow rate was unaffected, there was a significant impact on the internal mixing of the air, which could disrupt any developing air temperature stratifications.

### **3.2. Effects of openings and pressure differentials across the envelope**

When considering the equations many whole-building simulation tools use to conduct their analyses, it is essential to thoroughly understand the openings to any space and how the simulation softwares will handle them. Most notably are the factors that affect the rate of air flow into the space, as it is highly dependent on how the discharge coefficients are defined. For

example, the error in the discharge coefficient will proportionally scale with the error of the air flow, so an accurate discharge coefficient is crucial for reliable results.

### 3.2.1. The orifice equation and the discharge coefficient

It can be easily seen that the rate of air flow through an infinitesimally small section is the product of the flow velocity and the area of that section which that velocity acts upon. Summing up these values over the entirety of an opening in the building facade will result in the total flow rate through that opening.

$$Q_i = \sum_i A_i V_i \quad \text{Eq. 5}$$

Generalized for an opening, this becomes

$$Q = A_c V_c \quad \text{Eq. 6}$$

where  $A_c$  is the cross-sectional area of the opening.  $V_c$  is the average air velocity through the opening. These are expressed as maximum area  $A$  and theoretical velocity  $V_{th}$  possible multiplied by coefficients  $C_c$  and  $C_v$ , respectively.

$$A_c = C_c A \quad \text{Eq. 7}$$

$$V_c = C_v V_{th} \quad \text{Eq. 8}$$

$C_c$  represents the contraction coefficient which is the ratio of the area at the vena contracta and the area of the orifice inducing the vena contracta.  $C_v$  is the velocity coefficient and is the ratio of the velocity to the maximum theoretical velocity possible  $V_{th}$ .

$$V_{th} = \sqrt{\frac{2\Delta P}{\rho_0}} \quad \text{Eq. 9}$$

$\Delta P$  is the pressure change across the opening and  $\rho_0$  the density of the air. The discharge coefficient is introduced as the product of both the contraction and velocity

coefficients. This substitution is done because the coefficient of contraction and the velocity coefficients are very difficult to define in practice (Iqbal, Afshari, Wigo, & Heiselberg, 2015), (Heiselberg, Svidt, & Nielsen, 2001).

$$C_d = C_c C_v \quad \text{Eq. 10}$$

The orifice equation can be rewritten as

$$Q = AC_d \sqrt{\frac{2\Delta P}{\rho_0}} \quad \text{Eq. 11}$$

The orifice equation is derived from Bernoulli's Principle, which states that for incompressible flows, an increase of velocity will result in a loss of pressure. Bernoulli's equation summarizes this as

$$\frac{1}{2}\rho v^2 + P_s + \rho gh = P_{total} \quad \text{Eq. 12}$$

That is to say, the kinetic pressure and static pressure (and the atmospheric pressure) sum to a constant total pressure  $P_{total}$  along any streamline.

### 3.2.2. Factors affecting the discharge coefficient

The most ambiguous aspect of the orifice equation is that of the discharge coefficient. It generally cannot be measured directly and is strongly related to a number of variables and the interactions between them. Many papers have investigated some of the variables and the results have been fairly contradictory. In many investigations, real multi-directional air flow is simplified to a one-dimensional problem and any gradients (temperature, pressure) are converted into bulk properties. Most studies conclude the discharge coefficient to fall between 0.3 and 0.8 (Allard, et al., 1992).

Measuring the variables that affect the discharge coefficient have been conducted using many different methods. Typically, the orifice equation is used; however, the orifice equation can only be considered valid under some general assumptions. Assumptions made in its must hold, as well as some qualitative assumptions. Outlined by Karava, et al. (2004), these include the following:

- The air must be fully-developed turbulent flow
- The pressure distribution on the exterior must not be affected by any orifice
- Any kinetic energy is dissipated such that kinetic pressure is neglected, and thus, the pressure difference across the building envelope is considered entirely static

A fully developed turbulent flow suggests the flow is stable, or steady state, and boundary conditions such as wind or temperature are unchanging. Because the orifice equation (Equation 11) is a function of the internal and external pressure, these must be properly defined before the orifice equation can have any merit. The external pressure is directly affected by openings in the facade, especially in cases of cross ventilation. Ideally, removing the opening entirely and taking the external pressure to be the pressure on the facade of the building at where the opening was removed is a solution to this problem; however, Sandberg (2004) investigated this effect in a cross-ventilated structure using a combination of wind tunnel testing conducted by True, et al (2003) and CFD. The wind tunnel test involved a 16 *cm* long cylinder with a 15 *cm* diameter oriented along the direction of wind. Openings were created on both ends of the cylinder. The ratio of the openings were adjusted, thus changing the porosity, and Sandberg was able to conclude that pressure coefficients could not be obtained using the sealed body assumption for porosities too small or too large. Small porosities resulted in more flow than could be explained by the pressure differential, while large porosities allowed kinetic energy to

flow through and out of the cylinder without dissipating into heat due to internal friction, often eliminating the low-pressure wake on the leeward side of the building. The aforementioned sealed body assumption assumes that the pressure distribution on the outside of the house is not affected by any windows or openings (Figure 13), so it is clear why this would be ineffective for large porosities. Typically, the sealed body assumption applies to most structures with below 30% opening area on the exterior (Karava P. , 2008).

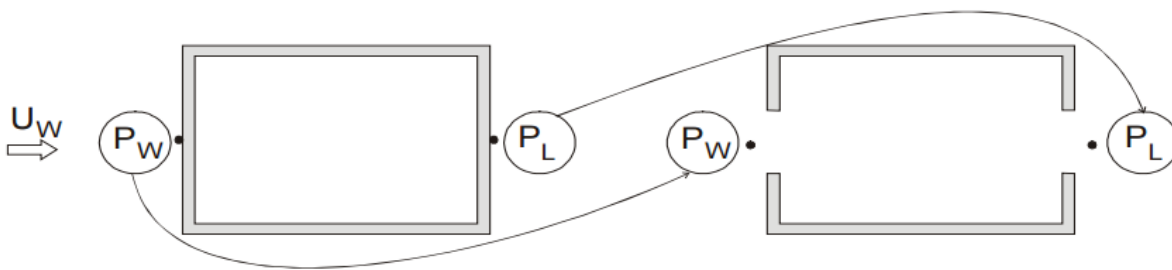


**Figure 13: A visual representation of the sealed body assumption(True, Sandberg, Heiselberg, & Nielsen, 2003).**

The constancy of the discharge coefficient has also been questioned under varying boundary conditions. It is obvious that the configuration and geometry of an opening can be significant in its determination, but these held constant raises questions about the effect of wind, temperature, and pressure differentials. A forced air experiment was conducted by Heiselberg et al. (2001) in order to determine the effects of these temperature and pressure differences on the discharge coefficient across two common window types. A large room was divided into two sections by a 6 meter wide, 3 meter high wall. Installed in the wall were a bottom hung window and a side hung window. With one side temperature controlled, air was forced through the opening from the cold side to the warm side and the pressure differential was recorded and flow characteristics observed. As seen in Figure 14, over a range of several pressure differentials, the discharge coefficient was found to be constant for pressure differentials above approximately

10 Pa, an issue when considering that natural ventilation typically takes place at pressure differentials below this. Large temperature differentials caused the discharge coefficient to reduce, except in cases where the opening area was small. The discharge coefficient was found to be highly dependent on the window type, opening area, and temperature difference, though predictions under isothermal conditions were generally accurate.

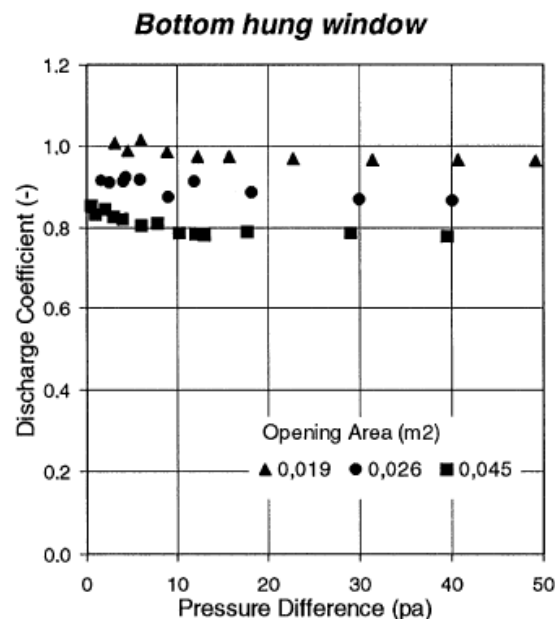


Figure 14: The pressure differential across a window is typically constant at pressures above 10 Pa (Heiselberg, Svidt, & Nielsen, Characteristics of airflow from open windows, 2001).

The discharge coefficient was held uniform throughout a study on cross ventilation by Kato et al. (1992), suggesting the geometry of the opening was the most significant factor affecting the coefficient. The LES study involved a small room model simulated under various boundary conditions to observe the differences in air characterizations. The model had five configurations:

1. Windward and leeward wall connected by a narrow duct.
2. Thick walled room with orifices on each wall.

3. Thin walled room with orifices on each wall.
4. Thick walled room with orifices on each wall with interior wind break.
5. Thin walled room with orifices on each wall with interior wind break.

Approaching wind following the power law was incident on the models and the simulation showed that openings for inflow and outflow within a room must be far enough away from each other to accommodate the dissipation of the kinetic energy. Larger openings require this distance to increase; however, the use of wind breaks helped dissipate some of the kinetic energy. The resulting higher static pressure difference across the envelope showed air flow rates decrease due to less kinetic energy carrying through the model. The researchers continued to note that often, with the orifice equation, the total pressure is substituted for the static pressure so in cases where kinetic energy is conserved, this is a poor method to determine the air flow rate. Their LES model was validated using wind tunnel testing which showed good agreement with their results. The accuracy of their results is in contrast to a similar study by Sawachi et al. (2004). Using a full-scale building, air flow was characterized within a room but their measurements of discharge coefficient were highly dependent on wind conditions. With a multitude of varying wind directions, their measurements of discharge coefficient ranged between 0.26 and 0.68, but was generally stable for wind speeds near perpendicular to the facade. As seen in Figure 15, the wind speed also affected the discharge coefficient significantly, but the effect was different for the inflow and outflow openings. The discharge coefficient for the inflow opening increased linearly throughout the range of wind speeds tested. For the outflow opening, the discharge increased more rapidly; however, only up until a certain wind speed, at which point the discharge coefficient leveled off. Another study aiming to improve knowledge on factors affecting the discharge coefficient involved pressure-driven air

flow in a full-scale building. Tracer gas was used to measure air flow rates in the absence of wind and it was found that the generally accepted value of 0.6 was sufficient in air flow prediction. The effect of wind caused so much uncertainty that no reliable results could be determined (Flourentzou, Van der Maas, & Roulet, 1998).

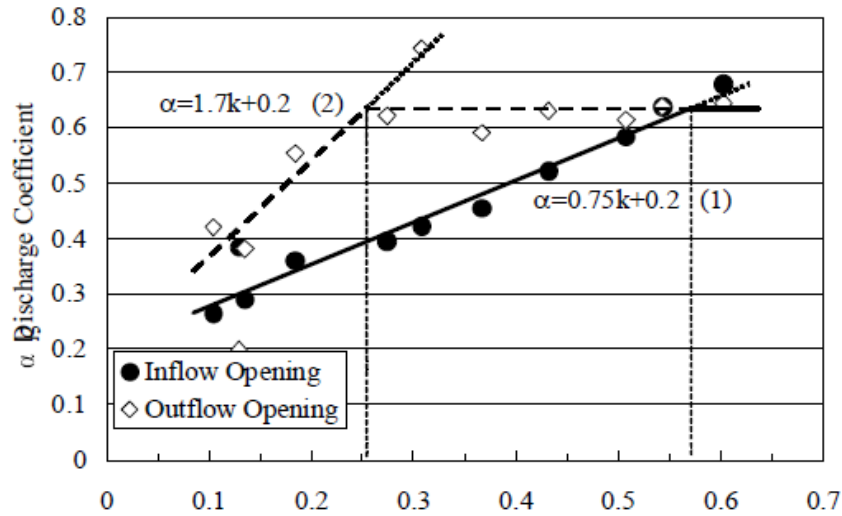


Figure 15: The discharge coefficient as a function of k. k represents the ratio of the average air speed in the opening to the ambient outside wind speed (Sawachi, et al., 2004).

### 3.2.3. Previous studies on window types

It is clear the geometry of an opening is a critical factor in the characteristics of air flow, and thus, the discharge coefficient. Windows are available in several configurations, shapes, and sizes, as well as some other defining characteristics such as frame depth and the sharpness of surrounding edges. Often, studies focus on simple sharp-edge orifices that would usually be seen in a sliding window; although, other configurations are common and should be considered in air flow studies. Six configurations were investigated in a study on the cross-ventilation potential in a typical space. A CFD model of a basic room was created with various simplistic openings of the different configurations, including window types: awning, casement, louvered, sliding, and

side hung, as well as a door. Using primarily wind-driven flow to the inside of the room, the windows were shown to behave differently with respect to air flow rate, jet velocity, and jet penetration. For example in the case of the awning window, wind-driven cross ventilating flows had direct impacts on the occupied zone. In low temperature differentials, high velocity jet was projected towards the ceiling. As the indoor temperature was increased, the jet would quickly drop to the floor because of its thermal buoyancy. Similar results were seen for the casement and side-hung window configurations, showing a risk for draught; however, the awning window was shown to have the highest resistance to flow, and thus lowest discharge coefficient, of all tested window configurations (Nitatwichit, Khunatorn, & Tippyawong, 2008).

While the geometry of sliding windows is generally straightforward, awning, casement, and side-hung windows present new challenges because the act of opening them presents obstacles that obstruct the path which air can take. This effect can be different among all the degrees which the window can open. Yang et al. (2010) tested both a bottom-hung and side hung window using a physical small-scale model accompanied by CFD, as well as full-scale CFD. The window was tested under opening angles of 5°, 10°, 15°, 30°, 45°, 60°, 75°, and 90°. As expected, the pressure across the window increased sharply for cases of low opening angle. The discharge coefficient increased with increasing opening angle according to the power law  $C_d = 0.0256 * \theta^{0.7432}$  for a window with a length-to-height ratio of 20:9. The value of the discharge coefficient may vary significantly as this ratio changes.

Challenges are further presented in the determination of the opening area of complex windows. Sliding windows generally have areas equal to their length multiplied to their width. Awning, casement, and side-hung windows, again, must be handled with more consideration to their opening area. The geometrical area can be obtained by adding up the areas on the sides of

the open window and the areas between the window and the building construction, as seen in Figure 16 (Heiselberg, Svidt, & Nielsen, 2001).

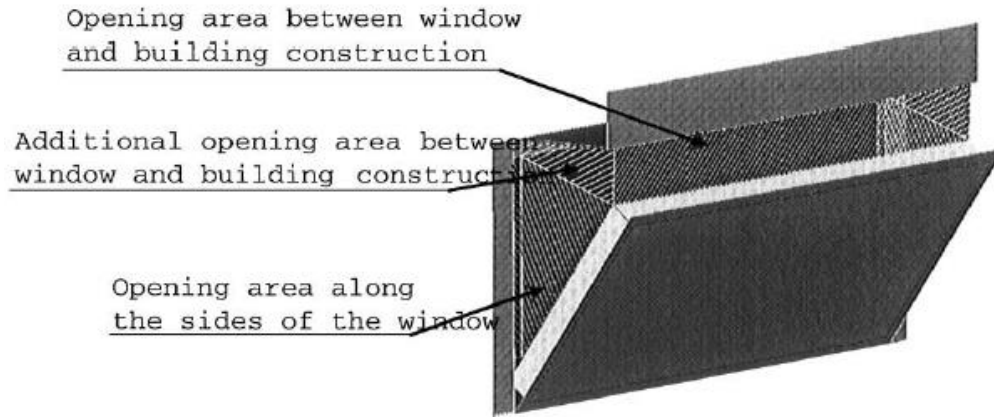


**Figure 16: The method to obtain the geometrical opening area of an awning, side-hung, or casement window (Heiselberg, Svidt, & Nielsen, 2001).**

While Heiselberg et al. (2001) used a geometry-based equation to determine the area of the window, there are other methods used by researchers that may vary the resultant air flow rate, even if the same window is considered in their measurements. A method used by the IES software, MarcoFlo, uses Equation 13 for the opening area of for all hung windows.

$$A_{op} = C_v * f_a * A \quad \text{Eq. 13}$$

The opening area is said to be a product of the openable area  $A$  and the fraction capable of opening,  $f_a$ , and some constant  $C_v$  which is dependent on the type and dimensions of the awning window according to Table 4.

**Table 4: The values of  $C_v$  for a top-hung window (Integrated Environmental Solutions Limited, 2007).**

Opening Angle	$C_v$				
	$L/H < 0.5$	$0.5 = L/H < 1$	$1 = L/H < 2$	$L/H > 2$	
10	0.34	0.24	0.17	0.10	
20	0.52	0.39	0.30	0.23	
30	0.60	0.50	0.43	0.36	
45	0.65	0.58	0.54	0.50	
60	0.67	0.63	0.60	0.58	
90	0.68	0.65	0.65	0.64	

A method used for a similar bottom-hung window used Equation 14 for determining the effective opening area  $A_{ow}$ .

$$A_{ow} = C_k(\alpha) * A_w \tag{Eq. 14}$$

$A_w$  represents the area of the window when fully opened, while  $C_k(\alpha)$  is a dimensionless constant given by Equation 15.

$$C_k(\alpha) = 2.60 * 10^{-7} \alpha^3 - 1.19 * 10^{-4} \alpha^2 + 1.86 * 10^{-2} \alpha \tag{Eq. 15}$$

This approximation, shown in Figure 17, showed high accuracy when compared to measured values for residential windows of aspect ratio between 1:1 and 2:1 (Prestandard prEN 15242, 2005).

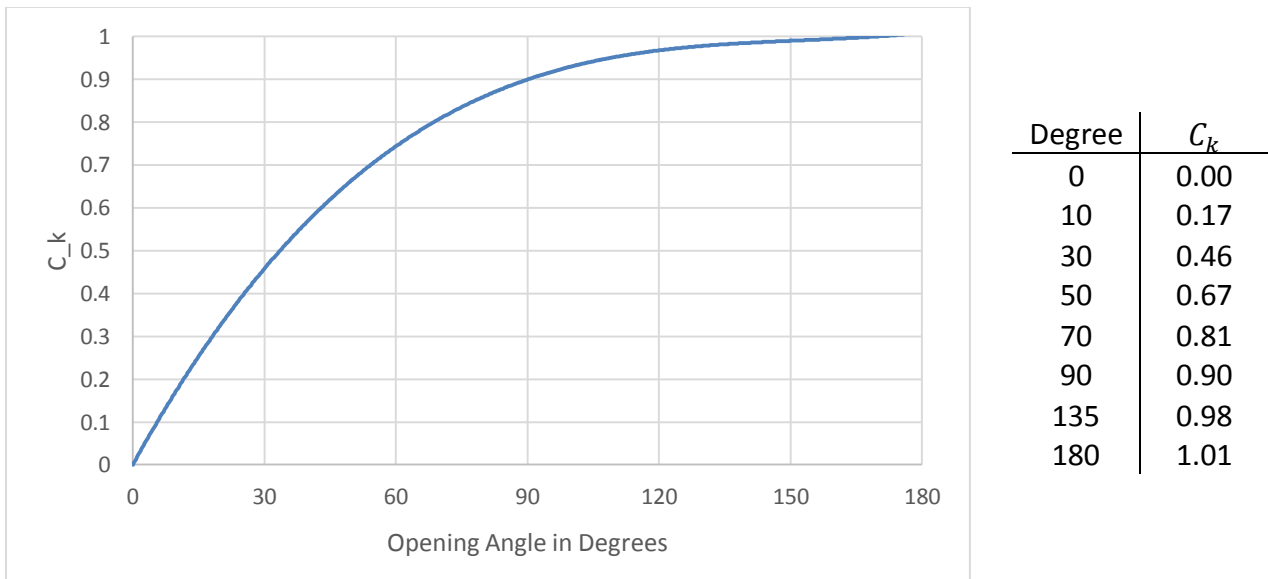


Figure 17: Values of  $C_k$ , adapted from (Prestandard prEN 15242, 2005).

### **3.3.Previous studies on natural ventilation assessment**

While it is well accepted that natural ventilation is beneficial to both the occupants of a home as well as the energy footprint the home exerts, it is not easily quantified. There are "almost infinite combinations of different climatic contexts, urban geometries, climate variables and design objectives" (Oke, 1988). Because of the case-specificity of assessing natural ventilation in any home, it is tedious to apply extensive modeling and testing to each one. Anecdotal evidence has shown that the rules-of-thumb engineers and architects often rely on to reduce energy consumption has generally been a poor approach to make.

There are many methods to assess the natural ventilation potential for any space. All of which have been researched and tested in many sorts of ventilation and related building science studies to help characterize and quantify the phenomena. Each approach has its own benefits and limitations that may cause one to prefer one particular method over another. In many cases, the use of multiple models is used to minimize these limitations and take the strengths of one model to apply to another. For example, the use of small and full-scale models is commonly coupled with CFD simulations which allows the validation of the CFD model, giving accurate characterizations of the physical system. The most common methods for the assessment of natural ventilation will be discussed.

#### **3.3.1. Field monitoring**

Field monitoring refers to the monitoring of a space or building over extended periods of time usually under natural operation. If done correctly, the results can be valuable but with the complexity of any building, maintaining control of the many aspects can be more problematic than its results are worth. A building, whether a large office building or small

residential home, will have people entering and leaving often throughout the day, creating fluctuating conditions that leave correlations difficult to detect. Furthermore, with many orifices for air to enter or leave from, it can be difficult or impossible to characterize air flow with any accuracy and the number of monitoring equipment needed for even basic monitoring in a residential house can be expensive. The value of field monitoring comes from the less-detailed data that can be obtained, such as temperature distributions and other scalar values; whereas more complex aspects like air flow characterization is much more difficult to obtain. General trends can typically be observed which, coupled with available HVAC systems monitoring, can give good insights to the performance of a building. Simultaneous weather monitoring is also important to properly assess natural ventilation, as it factors into the mechanism of natural ventilation considerably. Field monitoring is also often accompanied by surveys, as they describe detailed occupant experiences throughout the period of time that was measured (Hassan & Ramli, 2010); however, this is dependent on the detail the questions in the survey.

### **3.3.2. Field measurements**

Like field monitoring, field measuring is done on-site however it is not done under typical building operation. Monitoring is entirely passive and captures the sum and effects of all of the building processes. Measurements are done in a more controlled environment, which can be excessively difficult to achieve with occupants entering or leaving the building, or disrupting tests in a number of ways. Closing the building is ideal during testing as it allows much more ease to change variables of interest or isolate components of the building for close examination. While usually lasting much shorter periods of time compared to field monitoring, these tests are useful in that they propose ideas and methods to increase comfort in the house using energy-

saving practices(Iba, Hokoi, Ogura, & Ito, 2013). The results of these measurements can also be used to validate numerical and computational models.

### **3.3.3. Small and full-scale models**

Due to the economic benefits, it can be effective to analyze a building by using small-scale models. Typically conducted in wind tunnel laboratories, these allow nearly full control of most of the relevant boundary conditions, leaving little to chance occurrences like unexpected wind or building disruption, which can occur in cases of full-scale experiments; however, this benefit, while significant, is not without limitations. The Grashof number is a dimensionless variable which represents the ratio of the buoyancy forces to the viscous forces and applies to physical systems where convection is concerned, such as in natural ventilation. The Reynolds Number is a similar dimensionless variable of the ratio between the momentum forces and the viscous forces and is often referred on when characterizing fluid flow as turbulent or laminar. As Ding et al. (2005) and Chen (2004) state, these two numbers are not conserved when scaling a full sized model down to a scale mock-up, causing consistency problems. If not accounted for, the inaccuracy of these numbers can cause the results of small-scale experiments to be unreliable. In many cases however, wind tunnel tests on models can result in effective data that closely resembles true phenomena that occurs in buildings,(Katayama, Tsutsumi, & Ishii, 1992), (Kato, Murakami, Mochida, Akabayashi, & Tominaga, 1992),(Kobayashi, Sandberg, Kotani, & Claesson, 2010), (Takizawa, Kurabuchi, & Ohba, 2014).

### **3.3.4. The benefits of computational simulations for assessment**

With the potential to significantly reduce energy consumption in buildings, natural ventilation is underutilized in new constructions and when it is considered, it is rarely engineered beyond some rules-of-thumb. Much because of the planning required, many architects choose not to plan, in depth, their design choices and as a result, their buildings underperform. These issues could be fixed with attention given to simulating energy consumption and air flows in the design phase, when optimization and changes to the construction can still be made. Simulation-based support can be an effective method to analyse the thermal conditions within naturally ventilated houses (Loonen, Hoes, & Hensen, 2014), but typically, this has been limited to upscale or public buildings with greater importance to human health and comfort, such as in hospitals. There exist a number of tools to assist this but most notable are whole-building dynamic thermal models and computational fluid dynamics.

The most desirable attributes on a tool to model natural ventilation would need the ability to, as summarized by Menchaca Brandan (2012):

- couple the dynamics of air flow and heat transfer
- quickly perform transient simulations with weather data
- model the transient effects of thermal mass
- require only the parameters relevant to natural ventilation
- allow easily modifiable to compare different scenarios
- perform fast simulations
- be accessible to architects and designers
- provide accuracy in terms of thermal comfort

Common computational tools available include empirical, analytical, multizone, and CFD models. A comparison of some of the advantages of these tools can be seen in Table 5.

**Table 5: Comparison of capabilities of multizone and CFD to model natural ventilation. Adapted from Menchaca Brandan (2012).**

	Empirical/ Analytical	Multizone models (COMIS/CONTA M)	Multizone models With E+ or TRNSYS	CFD
Couples air flow thermal dynamics	Low	No	Yes	Yes
Models thermal mass effects	Low	No	Yes	No
Accuracy in predicting thermal comfort conditions	Low	Low (average values per zone)	Low	High
Expertise required to use	Low	Low	Intermediate	High
Time to run a simulation	N/A	Seconds	Hours	Days (weeks if transient)
Time/effort to modify input	Low	Minutes	House/days	Days
Appropriate for which design stage	None	Early	Intermediate	Intermediate/ late

A complete simulation should include a parametrical analysis in order to determine the parameters and boundary conditions that may drastically change the model if not determined accurately. For a natural or hybrid ventilation system, good modeling comes with the coupling of a good ventilation model and dynamic thermal model (International Energy Agency; Energy Conservation in Buildings and Community Systems, 2002).

### **3.3.4.1. Empirical and analytical models**

Empirical and analytical models can be useful for general descriptions of the processes involved in the physics and operation of a building, particularly for smoke characterization or natural ventilation in large spaces, such as in basic atria. They are based on the fundamental equations of fluid dynamics and heat transfer but are usually quite broad and do not encompass

much detail of the building. Important aspects of a space, such as geometry and wind, are rarely factored into the equations due to the relative complexity in those variables. Some of this information may be preserved in empirical models, as they are often developed from data obtained from experimental measurements and computer simulation to obtain particular coefficients to make the models work within a particular scope (Chen Q. , 2009). Empirical and analytical models also assume constant indoor air temperature, temperature stratification, and air density (Allocca, Chen, & Glicksman, 2003), among other broad assumptions. Consequently, these models can be limited in their applicability.

#### **3.3.4..2. Dynamic thermal models**

Dynamic thermal models simulate the whole-building performance of a house or building by using single nodes, typically one in each room or building zone. Each node has a wide variety of properties involving the energy flows within the model, including solar gains, internal gains, average air, radiant, operative, and surface temperature, average pressure, among other relevant properties. Air flow is exchanged between nodes at rates dependent on the pressures of each adjacent node as well as the size and discharge coefficient of orifices connecting them and envelope leakage. Dynamic thermal models offer limited detail because, similarly with empirical and analytical models, these nodes do not account for any variation within zones and all air is considered stagnant and mixed, which is rarely the case in reality. All information regarding temperature stratification, varying wall temperatures, and even variations in pressure, is lost. The advantage of dynamic thermal models is their ability to incorporate sub-hourly weather data into simulations. This allows the simulation of building performance throughout a whole year, as well as the fluctuations throughout the day due to its strengths with simulating

radiation from the sun and within the building. They also offer high customization in many input options. Windows and doors can be placed wherever preferred, in any size. Furthermore, the individual operation of every opening can be defined with high precision, meaning properly defining the schedules of the building can mimic the true operation of the building with good accuracy. With a large database of building components to choose from, there is a high level of detail possible in the physical construction of the building.

Dynamic thermal models are useful in the modeling of natural cross-ventilation typical in office buildings or homes that are composed of non-vertical rooms and simplistic designs, but with the increasing use of atria and vertical spaces, the effect of buoyancy is becoming more significant in building design. Because they treat zones as uniform and having spaces with no air variation within them, dynamic thermal models are less effective at simulating the effects of buoyancy and stack effect, such are the conditions within atria. The 'top' of the zone contains the same air conditions as the 'bottom' which, in reality, can differ by several degrees. This is a significant source of error for natural ventilation design. A solution proposed by Tan and Glicksman (2005) involved dividing an atrium into at least two smaller zones (Figure 18). The inclusion of this design choice had a strong beneficial impact on their model's results and they were able to conclude that dynamic thermal models were useful for the prediction of wind and buoyancy-induced natural ventilation.

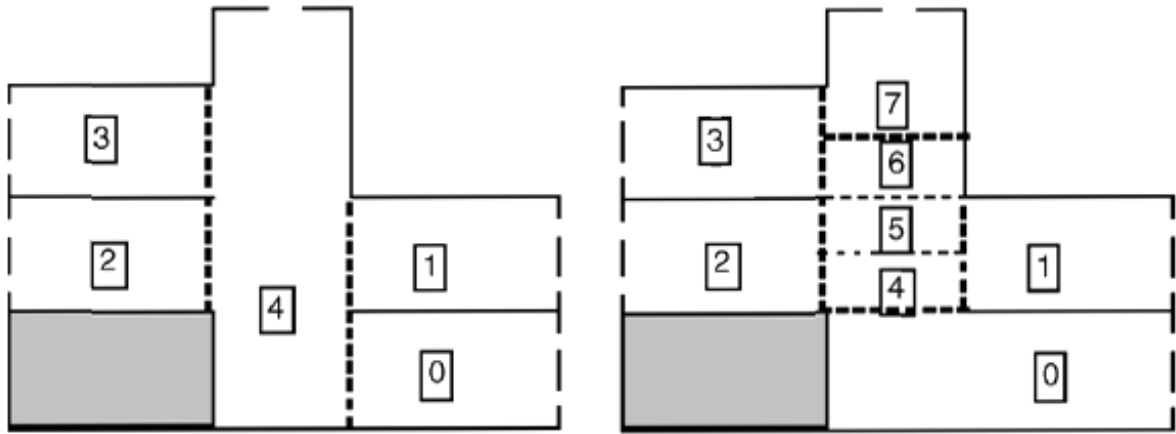


**Figure 18:** A solution to vertical spaces in multizone models is to divide one zone into multiple, as seen with zone 4 (left) split into multiple zones 4, 5, 6, and 7 (Tan & Glicksman, 2005).

While natural ventilation can be highly complex with multiple openings connecting a single space, the equations dictating the dynamics of the model are mostly only concerned between two nodes. Ventilation rates are calculated based on the pressure difference across external orifices using pressures induced by wind and stack pressure effects. The flow rate is expressed as a variation of the orifice equation discussed earlier (Equation 11):

$$q = C(\Delta P)^n \quad \text{Eq. 16}$$

where  $q$  and  $\Delta P$  represent the volumetric flow rate and the pressure difference, respectively, through and across the opening. The exponent  $n$  varies between 0.5 (turbulent flow) and 1.0 (laminar flow) (DesignBuilder Software Ltd., 2015). While the orifice equation discussed previously used the discharge coefficient  $C_d$ , some dynamic thermal models use a more encompassing general flow coefficient  $C$ , which is dependent on the size of the opening. The effects from wind are present through the positive pressure they exert on the upwind facade of a building. The surface pressure from wind  $P_W$  is considered using Equation 17.

$$P_W = \frac{1}{2} \rho C_p v_z^2 \quad \text{Eq. 17}$$

$C_p$  is the wind pressure coefficient and is a function of wind direction, orifice location, and local exposure. The value  $v_z$  is mean wind velocity at the height of the orifice. In reality, the determination of the wind pressure coefficient is much more complex, as outlined by Grosso (1991). More parameters must be considered in addition to those already mentioned, such as the wind velocity profile and plan area density, which is more complex than many simulations typically model. The building's aspect ratio also can significantly affect the wind pressure coefficient.

### **3.3.4.3. Computational fluid dynamics**

Fluid mechanics is a branch of physics that deals with the properties and dynamics of static or dynamic fluids. The Navier-Stokes Equations are a system of partial differential equations that are the best numerical approximation to the motion of fluids and are aptly able to predict fluid motion. Due to the chaotic nature of turbulent fluids both in nature and in controlled environments, the equations require a high level of computation in order to be solved and cannot be done by hand. Computational fluid dynamics (CFD) is the application of numerical analysis using computers to solve these equations (Figure 19).

CFD is an incredibly useful tool and can be used in many applications in buildings and architecture, including contaminant transport, HVAC design, interior air quality, and both interior and exterior fluid dynamics. The time required to develop a CFD models is often high and requires building the model from the ground up with as much detail as deemed necessary. The geometry of objects and their properties must be inputted which can be time-consuming for a complex building or space and the time of computation can be high, particularly when many

simulations need to be run in series. The equations are solved by dividing a computational domain into a number of individual cells, or elements and applying the balance equations to each cell iteratively until the results converge within some predefined threshold to a solution. Depending on the preferred or required detail, the number of elements can be several million and more elements will yield a better results; however, calculation time will take longer.

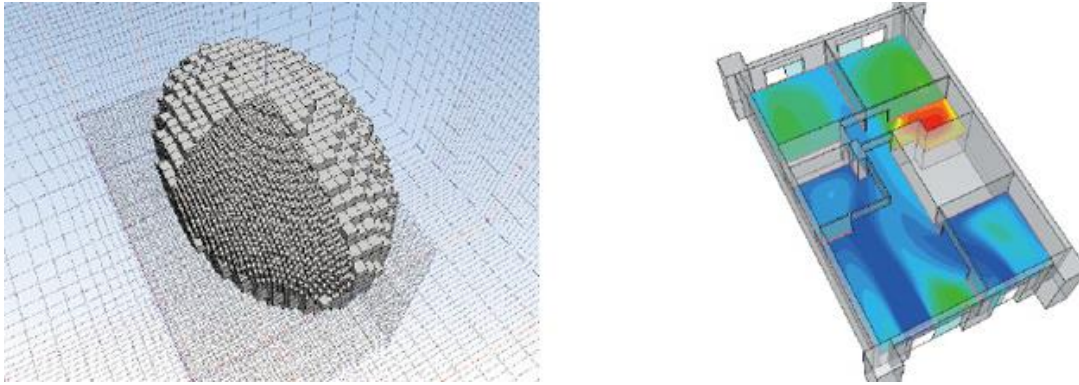


Figure 19: A shape divided into many elements (left). A CFD simulation of a simple space (right). (CRADLE-CFD).

### 3.3.4..3.1. Turbulence modeling

With several turbulence models to choose from, Reynolds-averaged Navier Stokes (RANS) based standard  $k - \varepsilon$  model is commonly used. This model is based on the characteristic quantities of turbulence: turbulent kinetic energy ( $k$ ) and its dissipation rate ( $\varepsilon$ ) and are given by Equations 18 and 19, which are functions of instantaneous velocity  $u$ , and position  $x$ .

$$k = \frac{1}{2} \overline{u'_i u'_i} \quad \text{Eq. 18}$$

$$\varepsilon = \nu \overline{\frac{\partial u'_i}{\partial x_j} \frac{\partial u'_i}{\partial x_j}} \quad \text{Eq. 19}$$

The idea of compressibility of fluids is also an important characteristic of a fluid, as the equations that describe it can change. A fluid can be considered incompressible if its density remains relatively constant. This is expected for low velocity (<100 m/s) flows, low temperature (under several hundred degrees, Celsius) variation, single phase, non-combusting fluids (CRADLE-CFD). In the scenario of natural ventilation, fluids remain well below these thresholds. Thus, the balance equations governing fluid flow for incompressible fluids are functions of the turbulent kinetic energy, dissipation rate, eddy viscosity  $\mu_t$ , density  $\rho$ , thermal expansion coefficient  $\beta$ , and Prandtl Number  $P_{rt}$ , as well as some other constants. These balance equations are seen below.

$$\frac{\partial \rho k}{\partial t} + \frac{\partial u_i \rho k}{\partial x_i} = \frac{\partial}{\partial x_i} \left( \frac{\mu_t}{\sigma_k} \frac{\partial k}{\partial x_i} \right) + G_s + G_T - \rho \varepsilon \quad \text{Eq. 20}$$

$$\frac{\partial \rho \varepsilon}{\partial t} + \frac{\partial u_i \rho \varepsilon}{\partial x_i} = \frac{\partial}{\partial x_i} \left( \frac{\mu_t}{\sigma_\varepsilon} \frac{\partial \varepsilon}{\partial x_i} \right) + C_1 \frac{\varepsilon}{k} (G_s + G_T) (1 + C_3 R_f) - C_2 \frac{\rho \varepsilon^2}{k} \quad \text{Eq. 21}$$

Where,

$$G_s = \mu_t \left( \frac{\partial u_i}{\partial x_j} + \frac{\partial u_j}{\partial x_i} \right) \frac{\partial u_i}{\partial x_j} \quad \text{Eq. 22}$$

$$G_T = g_i \beta \frac{\mu_t}{P_{rt}} \frac{\partial T}{\partial x_i} \quad \text{Eq. 23}$$

$$R_f = - \frac{G_T}{G_s + G_T} \quad \text{Eq. 24}$$

$$u_t = C_u \rho \frac{k^2}{\varepsilon} \quad \text{Eq. 25}$$

The constants  $\sigma_k$ ,  $\sigma_\varepsilon$ ,  $\sigma_t$ ,  $C_1$ ,  $C_2$ ,  $C_3$ , and  $C_\mu$  are obtained experimentally and are expressed in Table 6.

**Table 6: Constants used in the standard and RNG  $k - \varepsilon$  models.**

	$\sigma_k$	$\sigma_\varepsilon$	$C_1$	$C_2$	$C_3$	$C_\mu$	$\sigma_t$
Standard $k - \varepsilon$ model	1.000	1.300	1.440	1.920	0.000	0.090	0.900
RNG $k - \varepsilon$ model	0.719	0.719	$C_1(\eta)$	1.680	0.000	0.085	n/a

$$C_1(\eta) = 1.42 - \frac{\eta \left(1 - \frac{\eta}{4.38}\right)}{1 + 0.012\eta^3} \quad \text{Eq. 26}$$

$$\eta = \frac{k}{\varepsilon} \sqrt{\frac{1}{2} \left( \frac{\partial u_i}{\partial x_j} + \frac{\partial u_j}{\partial x_i} \right) \left( \frac{\partial u_i}{\partial x_j} + \frac{\partial u_j}{\partial x_i} \right)} \quad \text{Eq. 27}$$

Some improvements to the standard  $k - \varepsilon$  model have given rise to the Re-Normalization Group (RNG)  $k - \varepsilon$  model. This turbulence model differs from the standard  $k - \varepsilon$  model by the methods which the constants are obtained. Instead, it uses Fourier analysis, and the constants are also listed in Table 6. Other  $k - \varepsilon$  models have been developed over time; however, the standard and RNG  $k - \varepsilon$  models are the most widely used  $k - \varepsilon$  turbulence models in buildings.

Many studies have investigated the benefits of various turbulence models, namely these standard and RNG  $k - \varepsilon$  models. The standard  $k - \varepsilon$  model typically gives satisfactory results, but the RNG  $k - \varepsilon$  model is much more widely used by researchers. Iqbal et al. (2012) and Iqbal et al. (2015) found that the standard  $k - \varepsilon$  turbulence model was sufficiently accurate, while the former found it was less suitable for pressures under 0.5 Pa. Similar results were found by other researchers, though they directly compared the results to the RNG  $k - \varepsilon$  model. Cook, Ji, and Hunt (2003) concluded that the standard model over-predicted the rate of entrainment into a buoyant plume, whereas the RNG model was closer with the experimental and analytical results. Evola and Popov (2006) found that the standard model was poor at predicting

the air velocity around horizontal surfaces, but was a good model for cross-ventilating flows. This aside, the RNG model provided more accurate results in single-sided ventilation and cross ventilation flows, and was found to provide good confidence in determining the pressure distribution around a building when tested for wind-driven natural ventilation. In a study comparing several turbulence models, the RNG and standard model were both found to perform poorly in capturing inflow characteristics, in favor of the standard  $k - \omega$  and SST turbulence models (Cheng-Hu, Kurabuchi, & Ohba, 2005). A comparison of five different  $k - \varepsilon$  models by Chen (1995) showed inaccuracies in predicting penetration depth among the 2S and standard  $k - \varepsilon$  models. A general analysis of the five models can be seen in Table 7. Chen made the recommendation that the RNG model was best for indoor air flows. Similar thoughts are expressed by Tan and Glicksman (2005), Seifert et al. (2006), and Yang et al. (2010).

**Table 7: Summary of the performance of the  $k - \varepsilon$  models for predicting indoor air flow. A=excellent, B=good, C=fair, D=poor, E=unacceptable (Chen Q. , 1995).**

Flow Type	Parameters	$k - \varepsilon$	LB $k - \varepsilon$	2L $k - \varepsilon$	2S $k - \varepsilon$	RNG $k - \varepsilon$
Natural convection	Mean vel.	B	A	B	B	B
	Turbulence	C	C	D	D	C
	Temp.	B	D	B	B	B
	Heat trans.	C	B	A	C	C
Forced convection	Mean vel.	C	C	C	E	C
	Turbulence	D	D	D	D	D
Mixed convection	Temp.	A	A	C	A	A
	$x_e$	C	B	B	D	A
Impinging jet	Mean vel.	C	C	C	A	A
	Turbulence	D	D	D	C	C

Another common turbulence model is Large Eddy Simulation (LES). The LES model uses ‘filtered’ Navier Stokes equations and as a result, models the dynamics of large eddies only, ignoring the smaller ones. LES models require much finer mesh densities and thus can take 20 times longer converge on a solution when compared to RANS models (Cable, 2009). While they

have been shown to offer accurate results,  $k - \varepsilon$  models have proved to be sufficiently accurate in short computational times and thus, were chosen for the basis of all CFD simulations.

### 3.3.4.3.2. Boundary conditions

As mentioned previously, the boundary conditions are critical in developing a working accurate model. A parametric analysis can reveal much about the factors related to natural ventilation in a computer model and the effect they have on that model. There have been many CFD studies done in a variety of different building science studies so there is good knowledge on how to develop a CFD model, especially in studies related to natural ventilation.

The ambient wind conditions are parameters that can be input in several ways and play a significant role on the external pressures acting on the façade of the building. Some studies may model the wind around a building, giving input conditions for a second set of simulations performed on the interior, specifying conditions directly at the inlet of the building (Cook, Ji, & Hunt, 2003). This method however, can limit the detail of the flow through the opening. It may also neglect the contribution of natural ventilation by buoyancy if the inlet velocity or flow rate is specified instead of the pressure. Ambient wind can also be specified by a function of a reference velocity  $V_0$  and height  $H_0$  and roughness coefficient  $\alpha$  (Heiselberg P. , 2002).

$$V_i = V_0 \left( \frac{H_i}{H_0} \right)^\alpha \quad \text{Eq. 28}$$

Other functions can be used as well. Evola and Popov (2006) used Equation 29 as a boundary upwind boundary condition for the effects of wind.  $\kappa$  is the Von Kármán constant and is approximately equal to 0.41.

$$V(h) = \frac{V_0}{\kappa} \ln \left( \frac{H_i}{H_0} \right) \quad \text{Eq. 29}$$

For the outlet, the most common and reliable condition is the fixed static pressure condition which allows no pressure differential across the outlet and air is free to exit the computational domain (Allocca, Chen, & Glicksman, 2003), (Seifert, Li, & Axley, 2006), (Tominaga, Mochida, Murakami, & Sawaki, 2008), (Menchaca Brandan, 2012), (Iqbal, Afshari, Wigo, & Heiselberg, 2015).

The boundary conditions at surfaces is important for describing how flow will ‘catch’ onto a wall it is in contact and flowing by. Free-slip conditions typically are applied to the boundaries of the computational domain that are not inlets or outlets such that there is no shear friction for any of the fluid touching the boundary; whereas, no-slip conditions are applied to most objects as it defines the fluid to have no velocity relative to the object at the fluid-object boundary. In literature, the no-slip condition is heavily preferred as the slip condition on objects (Cook, Ji, & Hunt, 2003), (Allocca, Chen, & Glicksman, 2003), (Seifert, Li, & Axley, 2006), (Nitawichit, Khunatorn, & Tippyawong, 2008), (van Hooff, Blocken, Aanen, & Bronsema, 2011), (Iqbal, Nielsen, Afshari, & Heiselberg, 2012), (Menchaca Brandan, 2012), (Iqbal, Afshari, Wigo, & Heiselberg, 2015).

The minimum size of the computational domain is dependent on the object or building being investigated. Domains used include 2.5 times the height of the building, and 4 times the width wide, and four times the length long (Tan & Glicksman, 2005). Other conditions suggest 4 times the height of the building and 8 times the length in the leeward direction (Evola & Popov, 2006). While there is some ambiguity in the exact size, the general consensus is to model the computational domain to be 4 – 8 times each dimension of the building.

From the software used, other recommended settings were typically applied. The heat transfer conditions at the boundary of the computational domain should be set to adiabatic; however, because the house is modeled so far from this boundary, these conditions play little role in the behavior of the house in the model. The fluid-solid boundary should be set to log-law heat transfer. This allows the heat transfer coefficient to be determined by the software based on an empirical formula. It is also the recommended setting for the software for cases relating to natural ventilation. Heat transfer between solids should be set as conduction.

#### **4. PROBLEM STATEMENT**

Single-family residential homes are not designed with enough focus given to their climate and microclimate. Often only rules-of-thumb are used occasionally in the design phase to incorporate natural ventilation and the effectiveness of these design choices are usually unproven and can underperform. Implementing useful design strategies is difficult because some designs may over or underventilate, causing thermal discomfort and the need for mechanical heating or supplementary ventilation fans for cooling. Methods to assess and identify design decisions that work well and optimize those that can be improved can benefit architects attempting to build homes which consume less energy. One example of a case where an assessment of natural ventilation could have offered optimized design is presented by Tzikopoulos et al. (2005). They conducted a study on 77 sustainable buildings and found that energy efficiency was negatively affected by many techniques intended conserve energy by using natural ventilation. Applying a proper assessment of these design choices can help uncover an appropriate use of natural ventilation technologies, helping to achieve thermal comfort throughout the year. While these designs will differ greatly between different climates, the Pacific coast offers an ideal marine climate which architects could utilize to leverage natural ventilation to achieve minimal energy consumption for much of the year, while maintaining or improving thermal comfort and indoor environmental quality. The problem with this situation is that there needs to be more systematic studies on the assessment and merits of natural ventilation design, specifically relating to construction and the effects of passive technologies. The question arises: how does one assess the merits of natural ventilation in a house that had natural it intended to be used in its daily operation? This research aims to offer insight into the value of some passive design choices and the methods used to assess them in a case study house known

as the Harmony House. Monitoring and interpretation of data are the basis of the methodology and are essential to the evaluation of the effectiveness of natural ventilation in the house. Computational simulations further offer accurate visualizations and a greater understanding of what components contribute most significantly to cooling by natural ventilation.

## **5. METHODOLOGY**

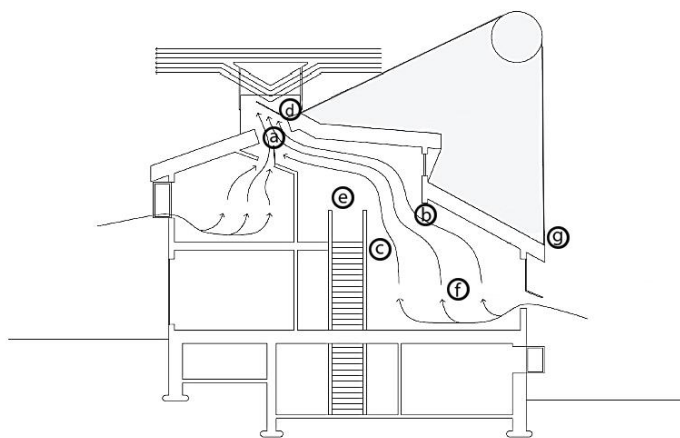
To quantify the performance of the house, a series of tests were developed. This section describes the tasks that were undertaken to assess a case study house, known as the Harmony House and discussed in Section 2, for its potential to use natural ventilation for thermal comfort. There are three main areas of work that were done: monitoring, testing, and modeling. The monitoring section of the research was of the Harmony House and the testing was to finely characterize the windows to investigate their effect on the ventilation of the house. This testing was initially planned to be conducted on-site at the Harmony House, but was moved to a test shed to be conducted at the British Columbia Institute of Technology; although, CFD was ultimately used to evaluate the windows. The planned tests will be discussed to understand the inspiration of using CFD to conduct the tests. The modeling of the Harmony House was done using both a dynamic thermal whole-building simulation software, as well as in CFD. Results of the measurements and testing were used to calibrate and validate the models the two models.

### **5.1. Monitoring during occupancy**

The first set of measurements conducted at Harmony House were performed in the summer of 2014 for a period of approximately four months from late June through October; however, due to technical problems, there were some interruptions in the data acquired. The purpose was to record the house under natural operation and conditions while the owners resumed their regular schedules in the house. This brought some challenges in designing this monitoring stage to be undistruptive and unobtrusive.

### 5.1.1. Instrumentation and placement within the case study house

In order to observe the conditions of the house, numerous sensors were placed throughout the house. The sensors recorded temperature, mean radiant temperature, relative humidity, air speed, and the open or closed state of some windows, skylights, and doors. Multiple data loggers were used, all of which were set to record temperature and relative humidity, internally. To record the mean radiant temperature, four of the data loggers were also fitted with custom globe thermometers. According to the recommendations made by M.A. Humphreys (1977), these were constructed from standard 40 mm diameter table-tennis balls painted matte-grey, fitted on temperature sensors. They were placed in areas of expected high occupancy and greater interest, such as the main atrium, and as opposed to a back guest bedroom or bathroom (Figure 20). They were also placed to capture thermal stratification along the atrium height. The time recording intervals was set to 10 minutes for these data loggers to allow small changes to be observed, yet allow significant data to be collected before necessary data retrieval due to limited memory within the loggers. The loggers allowed roughly 8,000 instantaneous recordings of date and time, air temperature, operative temperature, and relative humidity.



- a - Skylight anemometer
- b - Beam anemometer
- c - Central anemometer
- d - BlackGlobe thermometer
- e - HOBO East corridor thermometer
- f - Living room thermometer
- g - Outdoor weather station thermometer

**Figure 20: Location of many of the sensors installed in the Harmony House.**

Six state loggers were used to record the states of two of the four lower windows, both skylights, the door to the main bedroom, and a door in the kitchen leading to the back yard, all of which were connected to the main atrium. It is important to note that while state sensors recorded whether a window or door is open or closed, it did not record the extent to which the window or door was open, and a minimally ajar door would be registered as open. The state loggers recorded the precise time at which the state was changed. A data acquisition box was used to collect data from three omnidirectional anemometers, as well as the temperature of a fifth 6" globe thermometer. The time interval for these sensors was 15 seconds, allowing very sudden changes to be recorded, particularly in air speed. The temperature-measuring sensors were placed throughout the atrium and in some other rooms of the house to give a good representation of the temperature profile within the house. The anemometers were placed in areas of expected significant air flow; however, options were limited due to the length of the available cables. These locations included one near the skylights to measure outward flow speeds, one in a central area to measure the presence of possible drafts, and also one along the main air flow path between the skylight and the lower windows to measure the presence of jet streams. The locations of all sensors are outlined in APPENDIX A – Floor plan and sensor location and a list of the sensor models can be seen in Table 8. Outdoor temperature, humidity, wind speed and direction, and solar radiation conditions were recorded on-site using a WeatherLink monitoring station.

**Table 8: List of equipment used in the instrumentation of the Harmony House.**

Sensor	Quantity	Measures	Operating Range and Accuracy	Manuals
Campbell Scientific Inc. BlackGlobe Temperature Sensor for Heat Stress	1	Operative temperature	OR: -5°C to 95°C Acc: <±0.2°C	(Campbell Scientific, Inc., 2015)
Onset HOBO U12 data loggers	6	Temperature, humidity	OR: 0°C to 50°C Acc: ±0.35°C	(onset HOBO Data Loggers, 2015)
Onset The TMCx-HD Temperature sensor w/ globe	4	Operative temperature	OR: -40°C to 100°C (air) Acc: ±0.25°C	(onset HOBO Data Loggers, 2013)
HOBO UX90 State Logger - UX90-001	6	Open/closed state	N/A	(onset HOBO Data Loggers, 2015)
TSI Inc. 8475 Series air velocity transducer	3	Air speed	Acc: ±1.0% of full scale	(TSI Inc., 2012)
34972A data logger with Agilent 34901A Multiplexer	1	Voltage inputs	N/A	(Agilent Technologies, 2012)

### 5.1.2. Calibration of equipment

The air speed anemometers as well as the BlackGlobe globe thermometer were purchased shortly before the house was instrumented and were factory calibrated. It was uncertain whether the HOBO loggers were all calibrated. To test them without a completely controllable environment, the HOBO sensors were all placed in the same environmental conditions and recorded for a period of time in order to measure the deviations among the sensors. The temperature ranged between 10°C and 25°C and offered many abrupt temperature changes over the span of two days. Among the HOBO sensors used, there was, at most, a 0.5 °C temperature difference between the highest and lowest measurements, which falls slightly outside the expected error of the model. There was variation between the response times of the

temperatures, particularly noticeable in the abrupt temperature changes; however, these changes are uncommon in typical indoor conditions. A sample segment of time can be seen in Figure 21.

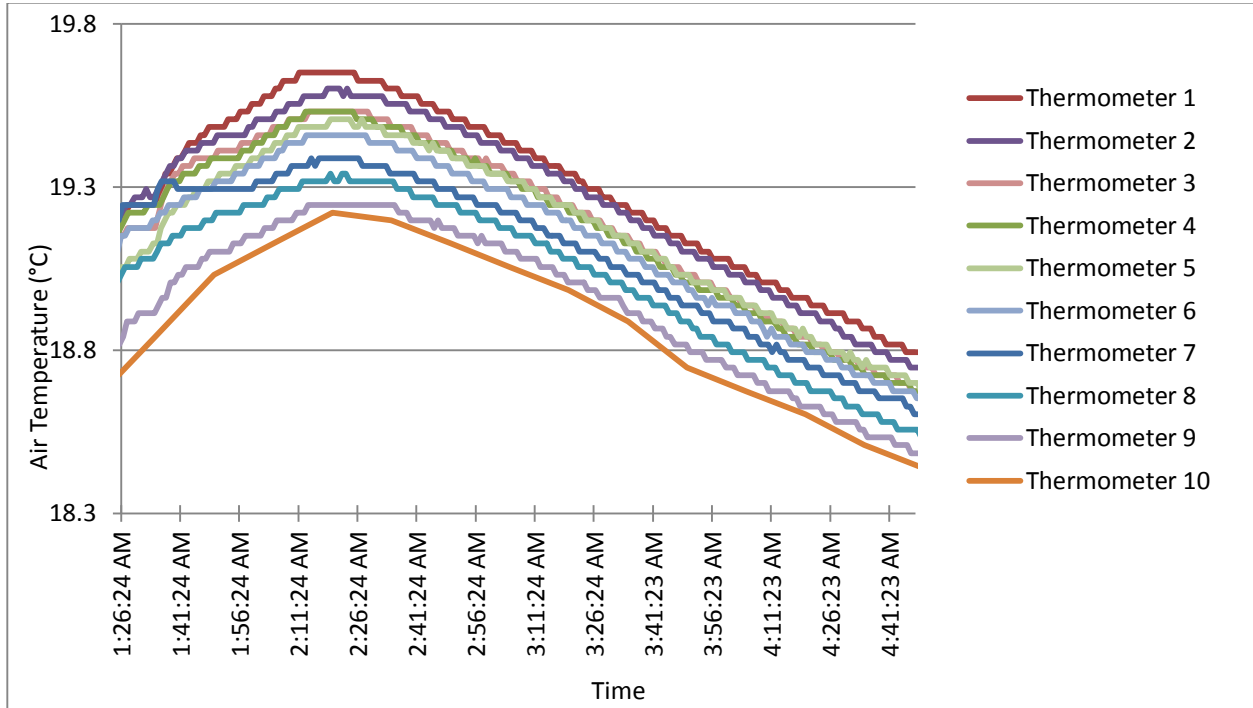


Figure 21: The temperature deviations of the HOBO sensors. Variation among the sensors was at most 0.5°C

### 5.1.3. Timeline of data acquisition

The house was outfitted and measurement began in early July 2014 and continued until late October 2014. Data was collected periodically throughout this time to prevent overwriting or system errors that could be fixed during visits to the house. A range of environmental conditions were recorded, including consecutive days of hot weather to days of rain where data was of no practical use. Near the end of October, all instruments were removed from the house with the exception of the weather station, which belonged to the owners and continued to record weather conditions.

## **5.2. Testing the window discharge coefficients**

As mentioned in the literature review, an important aspect of modeling natural ventilation is the proper characterization of the windows connected to the space. The windows at the Harmony House were intended to utilize natural ventilation, and thus were designed and installed in areas to promote wind-driven ventilation and stack effect. To help characterize the window types installed, a test was developed to measure the air flow through the windows on-site. Because the four lower windows are where air primarily came into the atrium, the discharge coefficients of the windows were important to obtain as they represented significant variables in the standard orifice equation. While characterizing sharp-edged rectangular orifices has been done throughout literature (Allard, et al., 1992), (Heiselberg, Bjorn, & Nielsen, 2002), (Karava, Stathopoulos, & Athientis, 2004), (Evola & Popov, 2006), the characterization of different window types is lacking. The windows installed at the Harmony House were awning windows, which behave very differently than a common sliding window. There is no assumption that can be used for an awning window's discharge coefficient; and thus, another level of complexity was added. To characterize the air flow through this window type, a blower door was used to create pressure differentials across the envelope at known volumetric flow rates; the discharge coefficient could then be determined at various opening angles based on these pressure differentials and the orifice equation.

### **5.2.1. On-site window testing**

The total pressure, consisting of the dynamic and the static pressure, plays an important role in the characterization of any window. To measure this, several pressure manometers were used. The manometers consist of two tubes attached to positive and negative terminals on the

manometer. The other terminal of the positive tube is placed in the area of greater pressure and the negative in the area of less pressure. The tubes were placed sufficiently far away from any orifice such that they were unaffected by the air flow through the orifice yet not so far that the pressure recorded would have been different than at the opening, following the sealed body assumption (Karava P. , 2008). This also ensured still-air and uniform pressure on each side. An approach was used by Lo and Novoselac (2011) which had the pressure measurements made 30-100 cm away from the window of interest.

Due to stack effect, warm air rising out of the upper skylights caused cool air to enter through the lower South-facing windows, creating a pressure difference across the wall, with the higher pressure being on the outside of the house. The wind was also typically incident on this side of the house as previously shown in Figure 4. To record for both static and dynamic pressure, two manometers were used simultaneously, though for such small windows on a low-porosity wall, the dynamic pressure was expected to be greatly overpowered by the static pressure (Sandberg, 2004), provided the measurements were recorded while wind was calm or sufficiently low. One manometer was meant to measure the total pressure on the external wall, so its pressure tubes were oriented normal to the exterior wall, which was the expected direction of incoming wind. The other manometer was fitted with a static pressure tip attachment, also oriented normal to the wall, to measure the static pressure at the facade close to the window. The difference between the readings could be interpreted to be the dynamic pressure. For the upper skylight, only one manometer was used. Because the orifice was shielded with a square parapet to block the majority of the wind, the air flows were typically small and the dynamic pressure was immediately neglected; and thus, only static pressure was measured. The manometers measuring the pressure across the lower windows had their external positive pressure tubes

placed approximately 40 inches away from the window in order to not be affected by the flows through the windows. The same was applied to the skylights; however this was less necessary due to the aforementioned dynamic pressure being neglected and the shielding of the wind by the parapet. The negative pressure tubes were placed indoors away from their respective windows. A blower door was fitted into a doorframe between the laundry room and the outdoors and all faceplates were removed from the face of the blower door to allow a high rate of air flow into or out of the house. The goal was to achieve the full range of air flow required without changing faceplates between tests to minimize the error that may come from switching them.

Anemometers were placed at the openings in positions where they were to remain stationary throughout all tests. This was to record air speeds through the window at known ventilation rates for various window opening angles and configurations. This would later be used to determine flow rates of the house under natural conditions, as there was no other way available to measure flow rates without disrupting the flow, itself.

The methods used in this test required an airtight envelope, so fenestrations, vents and grilles were sealed. Only the middle and upper floors were sealed, as access to the lower basement suite was unavailable. The background leakage would then be recorded by running the blower door to pressurize the house to various pressures up to 50 Pa. A different leakage rate would be determined for each point and a curve would be fitted to the data to extrapolate to any desired pressure differential, in accordance with procedures by Lo and Novoselac (2011), and Heiselberg (2002). The Harmony House was designed to be exceptionally airtight, with a goal of 0.75 ACH at 50 Pa.

With the background leakage now known, the skylights were to be tested for their discharge coefficient. Opening one of the two main skylights to 15°, the maximum opening angle of the window, the house would be pressurized at various pressure differentials. The flow rate recorded from the blower door could be corrected by the leakage data recorded earlier, and plotted against the corresponding pressure difference across the skylight. The resulting plot could have a curve fit according to the orifice equation to determine the discharge coefficient for the individual skylight at any angle. The same procedure would be conducted for the other skylight to confirm the results to be similar for each skylight. It was also important to test the case where both skylights were open, as this was the most common configuration used when the skylights were operated.

The skylights would then be closed and the lower windows would be tested using the same methodology, beginning with one single lower window opened. Two windows open would also be tested, as the discharge coefficient, like for the skylights, could change depending on the adjacent windows simultaneously opened.

Finally, with the anemometers mentioned previously still in place, all equipment would be removed and the house would be allowed to operate normally. Without the blower door, flow rates could be determined by correlating anemometer readings to the flow rates measured during the testing with the blower door. A similar procedure was conducted by Lo and Novoselac (2011) in which they calibrated pitot tubes responding to wind intensity and were able to correlate a wind speed into a volumetric flow rate. A list of the equipment used for the test can be seen in Table 9.

**Table 9: A list of instruments used in the test. Calibration was achieved where necessary according to operation manuals.**

Sensor	Quantity	Measures	Operating Range and Accuracy	Manuals
Campbell Scientific Inc. BlackGlobe Temperature Sensor for Heat Stress	1	Operative temperature	OR: -5°C to 95°C Acc: $\leq \pm 0.2^\circ\text{C}$	(Campbell Scientific, Inc., 2015)
Onset HOBO U12 data loggers	2	Temperature, humidity	OR: 0°C to 50°C Acc: $\pm 0.35^\circ\text{C}$	(onset HOBO Data Loggers, 2015)
Onset The TMCx-HD Temperature sensor	2	Operative temperature	OR: -40°C to 100°C (air) Acc: $\pm 0.25^\circ\text{C}$	(onset HOBO Data Loggers, 2013)
TSI Inc. 8475 Series air velocity transducer	3	Air speed	Acc: $\pm 1.0\%$ of full scale	(TSI Inc., 2012)
34972A data logger with Agilent 34901A Multiplexer	1	Voltage inputs	N/A	(Agilent Technologies, 2012)
Dwyer MS-121 LCD pressure transmitter	3	Pressure differential	OR: 0 Pa to 50 Pa Acc: $\pm 1\%$ for 50 Pa	(Dwyer, 2015)
Retrotec Blower Door 5101 Classic	1	Flow Rate, Pressure differential	Acc: $\pm 5\%$	(Retrotec, 2015)

### 5.2.2. Off-site window testing

To allow full control of the variables necessary to determine the characteristics of the window, a second procedure was developed following the construction of a test shed structure. The methodology of the experiment would follow almost identically to how the on-site window testing occurred; however, a controllable environment would allow better results and more variability in the experiments that could be conducted, such as easily changing the interior (or even exterior) temperature, no outdoor wind uncertainty, and other ventures could be investigated such as the integration of a solar chimney or testing air flow characteristics of various skylights. Like a similar experiment by Heiselberg et al. (2002), the room would be constructed such that the inlet and outlets did not have any direct influences on air flow through the windows. Pressure would be generally uniform within the room and would be recorded at

locations of equal height to the window, and sufficiently far from the opening. Heiselberg et al. tested pressure differentials ranging from 0.1 to 60 Pa across four windows, sometimes all simultaneously open. The higher pressure differentials were only tested on small opening areas due to the uncertainty and instability of high pressure differentials on large openings. The proposed test was planned to only consider pressure differentials up to 50 Pa and as low as the available equipment would allow with good accuracy. The windows were supplied by the same manufacturer that supplied the windows used in the Harmony House. The aspect ratio was approximately 2:1 for the windows in the Harmony House and the window supplied had an aspect ratio of 1.5:1, though the area of the window supplied was only 8% larger. The size of the enclosure was planned to be large enough to allow incoming air to stagnate, reducing the effects of jet streams. Heiselberg et al. used a  $91\text{ m}^2$  space while another experiment by Heiselberg et al. (2001) used a  $101\text{ m}^2$  space.

### **5.3. Model development**

Two simulation models were used in the study to model the Harmony House, with each model having its own advantages. The first was a dynamic thermal model to capture the whole-building indoor thermal environment, thermal comfort, and the air flows in and out of orifices in the envelope. Second, a CFD model was used for an accurate thermal-fluid characterization of the air flow within the main atrium of interest. The models were coupled manually by selecting representative days and times from the data recorded on-site and comparing indoor and outdoor temperatures, and air flows with the models with the intent of capturing detailed thermal-fluid dynamics of the indoor environment.

### **5.3.1. Dynamic thermal model**

The hourly dynamic energy simulations were performed using DesignBuilder (DB) software. DB is one of the most comprehensive user interfaces for the EnergyPlus dynamic thermal simulation engine. The model used the Canadian Weather for Energy Calculations (CWEC) year data from Energyplus weather data files. Air circulation was modeled using a multi-zone air flow network approach in which spaces were characterized as single nodes, exchanging energy between adjacent nodes while simultaneously considering both wind and stack effects. Wind pressures on the house are obtained by relating the surface averaged wind pressure coefficients ( $C_p$ ) on the different enclosure surfaces to hourly free-field dynamic pressures from the wind at various building heights. Buoyancy is not directly modeled; however, treating the atrium as stacked thermal zones adequately represents thermal stratification. The use of DB allowed a good characterization of the buoyancy effect in the atrium and through the chimney. It also helped to accurately represent the dynamic thermal responses of the house to outdoor climate cycles with consideration of solar heat gain, thermal mass, and time lag. The validation of the model is discussed in a future section.

### **5.3.2. CFD model**

To study the precise temperature and air flow profiles of the Harmony House, a steady-state CFD model was developed using scSTREAM with measurements and materials obtained from official blueprints and floorplans. The advantage of a dedicated CFD tool is the ability to simulate the mechanism of natural ventilation without knowledge of air flow rates through facades, external and internal pressures, discharge and pressure coefficients, and many other important details that the software is instead able to account for. The CFD model of the house

followed a coupled approach in which the urban wind flow and the indoor air flow were modeled simultaneously within the same computational domain. The coupled approach adequately represents the air flow through openings under a given wind conditions. For the simulations performed, an RNG  $k-\epsilon$  turbulence model was used for its effectiveness in predicting exterior surface pressures (van Hooff, Blocken, Aanen, & Bronsema, 2011), interior and turbulent flows with separation and reattachment (Zhai, Zhang, Zhang, & Chen, 2007), and general recommendation for use with indoor air flows (Chen Q. , 1995), (Tan & Glicksman, 2005).

### **5.3.3. Validation process of the computer models**

With the dynamic thermal model and CFD model both completed, the requirement for validation was essential to give merit to results that were later obtained. The validation was a two stage process beginning with the dynamic thermal model which was critical as it is the one to be used for adaptive thermal comfort prediction and its comparison with measurements from the recorded data. Firstly, to be able to predict adaptive thermal comfort, it was critical to determine if the dynamic thermal model was able to produce, from an energy balance, accurate indoor thermal conditions and thermal stratification in the atrium. Secondly, the dynamic thermal conditions in the atrium from the thermal simulation should be close enough to the measured values recorded on-site. Measurement data was carefully selected for validating the dynamic thermal model. The validation was planned in six steps. A visualization of the process can be seen in Figure 22.

**Step 1** – Warm, average, and cool days were selected from the recorded data based on their outdoor temperatures for comparison with days in the simulation weather file that closely matched those warm, average, and cool days.

**Step 2** – A CFD test shed model (closely resembling the experiment that was planned) was designed to determine the flow characteristics of the openings, specifically the lower windows and skylights at various opening degrees. The methodology follows the procedure developed by Hult, et al. (2012) and is discussed in a later section. The resultant discharge coefficients were inputted into the dynamic model to generate more accurate simulations.

**Step 3** – Weather files used in the dynamic thermal model were edited to produce an artificial, constant wind by replacing the native data with 0 *m/s* (calm), 1 *m/s*, and 2 *m/s* wind speeds incident on the southern façade. The range of air speeds was selected based on the most frequent air speeds recorded at the local weather station (Figure 4). Simulations were run and from the results, daily highs were selected during warm, average, and cool days that matched those selected in Step 1. Corresponding surface temperatures from each respective day were input into the CFD model of the house which was to be run under the same artificial three wind speeds. Steady-state simulations in the CFD model were run to completion.

**Step 4** – For cross-validation of dynamic thermal and CFD models, air flows at the windows and skylights were compared, as well as atrium air temperatures at the various measured heights. In fine-tuning, closely comparable air flows and temperatures should be expected between these models under the corresponding boundary conditions.

**Step 5** – The CFD model was validated by comparing the air speeds and temperatures at the locations indicated in Figure 20 with data recorded on-site on days that matched the boundary conditions used in the CFD simulation.

**Step 6** – The dynamic thermal model was validated by comparing peak indoor temperatures with the recorded temperatures on the days selected in Step 1.

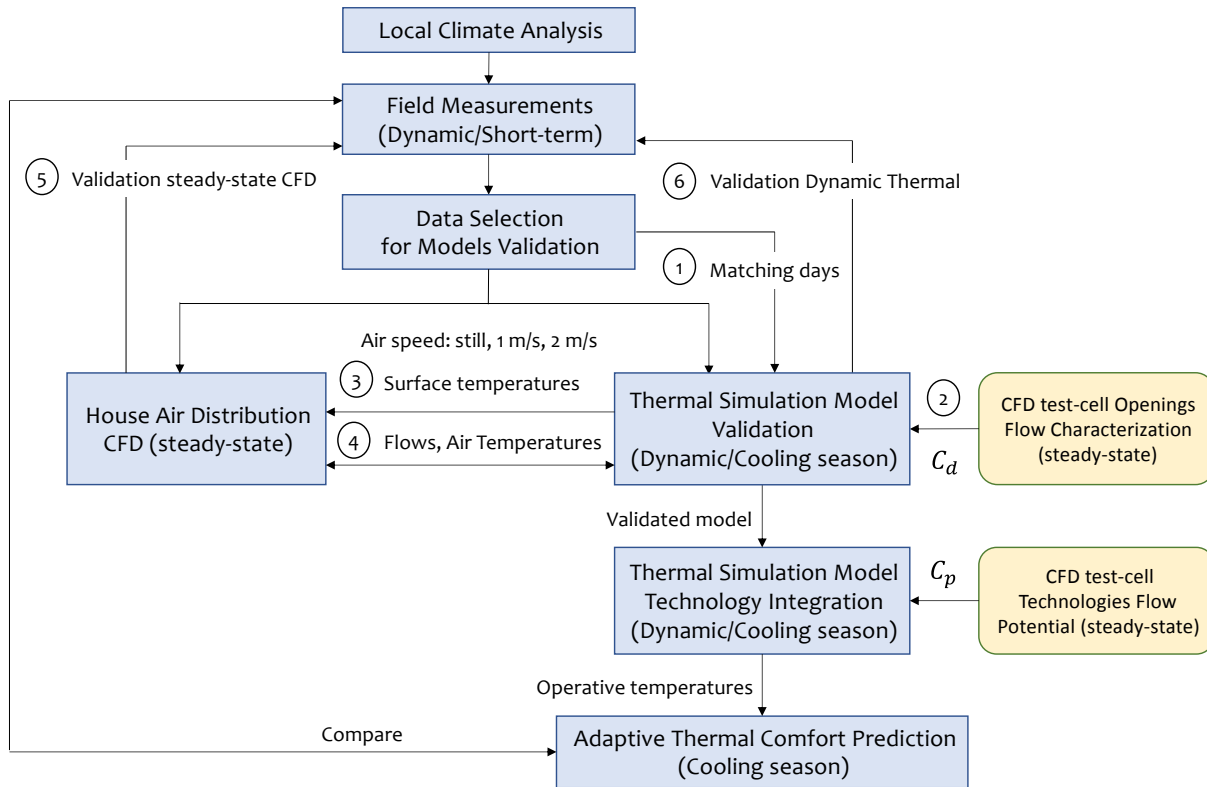


Figure 22: A flow chart of methodology used to assess the thermal comfort of the Harmony House.

Once these six steps were completed, the models were considered validated and could be used for the assessment of thermal comfort in the house.

### 5.3.4. Determination of discharge coefficients

As mentioned previously, dynamic thermal models typically handle the interaction of air flow between two spaces by the area of an orifice connecting them as well as the discharge coefficient. This can be a major drawback as the discharge coefficient can be hard to define. As seen in Section 3.2.2, the discharge coefficient has a wide range of values and the air flow scales linearly with the discharge coefficient, so modeling the air flow properly can be especially difficult. With the majority of windows installed in the Harmony House being awning windows,

the discharge coefficients typically used in energy simulations cannot be assumed to represent a good characterization of air flow resistance. To measure more representative discharge coefficients to input into the energy simulations, CFD results were taken from a work by Hult, et al (2012) and were recreated with the CFD software used in this study. The results were then compared for the purpose of validating the methods used for this particular experiment. Using a constant flow rate, Hult et al. used the orifice equation to determine the area-discharge coefficient equivalent  $(A * C_d)_{eff}$  at various opening angles for awning windows of a width-to-height aspect ratio of 2 by measuring the average pressure on each side of the orifice at some distance away.

Upon confirming validation, the same process was completed for various configurations of windows for simple, detailed, and mixed scenarios for the aspect ratio of windows installed at the Harmony House. The simple case was composed of flat planes while the detailed case takes wall thickness and window geometry into consideration. The results were compiled and implemented into the dynamic thermal model, with varying values for each individual window type.

### **5.3.5. CFD cell resolution testing**

The most common procedure for determining an appropriate cell resolution is to start with expectedly large cell sizes and run a simulation. Changing the overall cell size to be slightly smaller and running the same simulation will typically yield slightly different results. Repeating this procedure until the change in results is below some threshold will verify that the cell size is sufficiently small enough to yield accurate results (Lo & Novoselac, 2011), (Hult, Iaccarino, & Fischer, 2012).

The same procedure is followed with the CFD model of the Harmony House; however, it is done in a piecewise manner. Capturing the surroundings of the house may not require a fine grid resolution but the awning windows are often only open to such a degree that the distance from the window sill to the bottom of the window may as small as, or smaller than an individual cell edge. Modeling the whole area with such a fine grid would cause simulation times to be unreasonably high so an alternative method must be used. scSTREAM offers the option of finer grid refining in defined areas so individual openings can be given finer meshing.

To determine the appropriate cell size for each window, the relevant windows were modeled in a test cell inspired by Hult, et al. (2012). Windows that were not recorded to be typically open were ignored, leaving just the lower windows and the two main atrium skylights. Because the cell size must be much smaller than the size of the opening, only maximum opening angles were tested, for both the skylight and awning windows. Furthermore, both detailed and simple scenarios mentioned previously were tested to determine the differences in using either in the Harmony House model.

#### **5.4.Prediction of adaptive thermal comfort of occupants**

Once the dynamic thermal model was well validated and producing accurate results corresponding to recorded measurements and CFD simulation, the schedules of the dynamic thermal model were changed to reflect typical use in the house. Again, these schedules were predicted based on the state sensors and general trends recorded throughout the entire recording period. The previous weather file (with altered wind speeds) was replaced with an unedited weather file to simulate the real conditions that could be experienced in a year. Thermal simulations were run and indoor operative temperatures were obtained at the living area on the

first floor for the months of May through September to predict thermal comfort under the various technology scenarios. It is worth noting that the operative temperature is calculated by the software as an average of the air temperature and the mean radiant temperature in a space, both of which are derived from the energy balance equations in the thermal model, which of course include the natural air flows through the openings driven by the wind and the stack effect. The prevailing mean outdoor air temperature for each day was calculated using a formula from ASHRAE 55 seen in the Equation Eq. 30, with  $\alpha = 0.6$  and for up to twenty terms.

$$T_{pma} = (1 - \alpha)[t_{e,(d-1)} + \alpha t_{e,(d-2)} + \alpha^2 t_{e,(d-2)} + \alpha^3 t_{e,(d-3)} + \dots] \quad \text{Eq. 30}$$

where:  $\alpha$  is a constant  $\in (0,1)$

$t_{e,(d)}$  is the daily average temperature on day  $d$

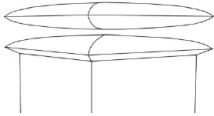
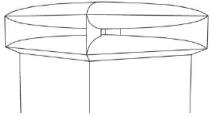
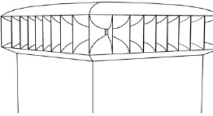
Using the prevailing mean outdoor air temperature is an effective method of determining the comfort of people in naturally ventilated spaces. This is because the formula puts weight in the days preceding the day in question, much like how the comfort of those in naturally ventilated spaces is affected by their perception of days prior (Humphreys, Nicol, & Roaf, 2015). The equation puts the emphasis on days immediately preceding, with less weight on each successive day, creating the exponentially weighted running mean of the outdoor daily mean temperatures over the previous number of days. The adaptive thermal comfort of the atrium and the bedroom were investigated.

## 5.5. Chimney-cap technology integration

One of the uncertainties surrounding the construction of the house was to what extent the addition of the Aerocap (Figure 23) could have contributed, or some other similar passive technologies. To study the potential the Aerocap had, work by van Hooff et al. (2011) was investigated, and so two technologies were selected for this research: the Aerocap and van Hooff

et al. “venturi-shaped roof”. Van Hooff et al. used CFD combined with wind tunnel testing for validation to measure the qualitative effects of this venturi-shaped roof installed atop of a building. This streamlined aerodynamic shape would create greater negative pressures at the orifice which it was situated atop than the ‘blocky’ shape of the Aerocap. Because this is a technology that relies on wind, the wind pressure coefficients were determined for a series of wind directions. The results of their work can be seen in Table 10. Configuration A resulted in the lowest coefficient of pressures under all wind angles so this “best-case scenario” was tested as if it was situated atop the Harmony House by inputting the coefficients of pressure into the dynamic thermal model. The increased cooling potential in the atrium space was the subject of this addition to the model.

**Table 10: Coefficients of pressure for venturi-shaped roofs (van Hooff, Blocken, Aanen, & Bronsema, 2011).**

Roof Configuration Image				
Wind Angle	A (no guiding vanes)	B (guiding vanes at 90°)	C (guiding vanes at 10°)	D (no venturi-shaped roof)
0°	-1.21	-0.37	-0.22	-0.30
15°	-1.20	-0.12	-0.15	-0.33
30°	-1.27	0.25	-0.03	-0.30
45°	-1.35	0.24	0.07	-0.30



**Figure 23: The completed “Aerocap” planned to be place atop the Harmony House(Sustainability Television)).**

## 6. RESULTS AND DISCUSSION

### 6.1. Occupant behavior and comfort conditions

With the completion of the data recording period, the data was analyzed and synchronized so that operation and trends could be observed ( Figure 24). The complete data for the months of July, August, and September can be seen in APPENDIX B – Compiled data. As expected, there was a clear periodicity as nearly all environmental measurements followed daily peaks and troughs. Some state sensors recording operation of windows and doors recorded periodic behavior as well.

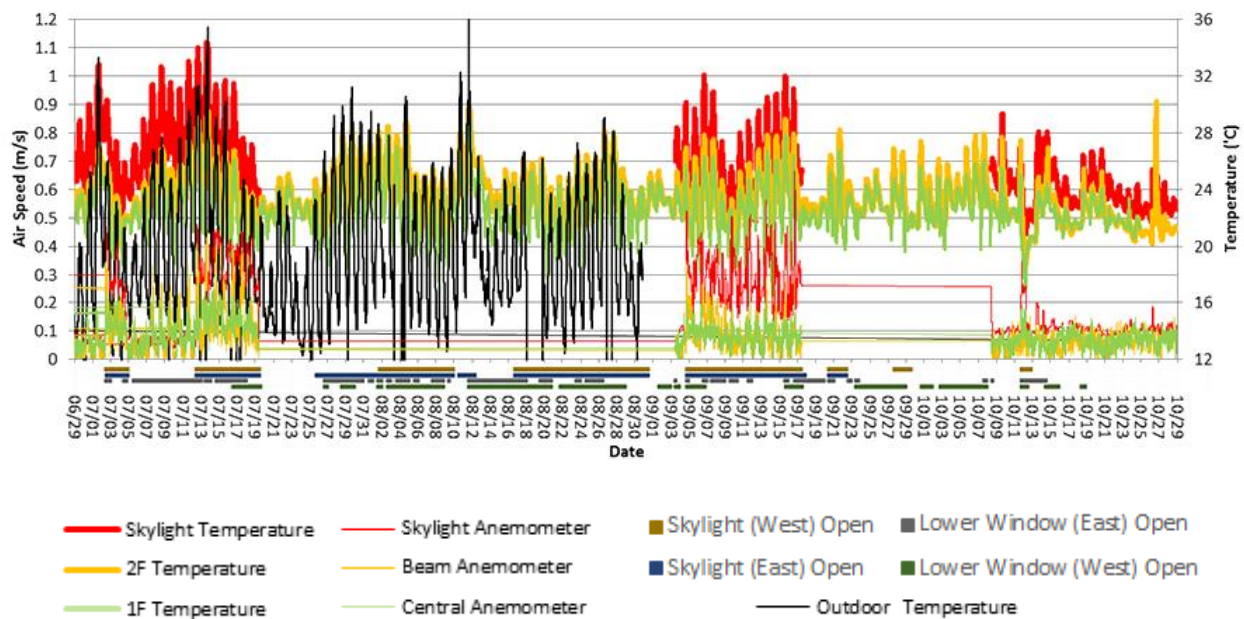


Figure 24: Several months of recorded data. The data is difficult to interpret in such a large scale so smaller segments must be investigated to make any conclusions.

A full instrumentation of the house would need many more sensors, and would likely need to be installed permanently and unobtrusively. The temperature profile of the house was

still measured in many areas because while air does tend to mix well within enclosed spaces, in larger spaces stratification was observed.

The usage of anemometers is difficult in monitoring a house due to the inability to effectively conceal the sensors without compromising their ability to accurately measure air speeds. In addition to the high cost of accurate sensors, they are not versatile to be placed in many locations due to being relatively bulky, fragile, and sensitive to proper installation.

The HOBO Loggers fitted with custom globe attachments constructed from painted table-tennis balls were shown to perform nearly as well as an actual dedicated globe thermometer instrument, with the added benefit of unlimited placement; whereas, the globe thermometer instrument was limited to the length of cable connecting it to the data acquisition box.

On-site weather conditions recorded by a weather station offered data in the following categories: indoor and outdoor temperature, indoor and outdoor relative humidity, air pressure, wind speed and direction, solar radiation, rain rate and accumulation, and the dew point temperature. Only some of these factors were considered in the data analysis. The station was situated on a second floor balcony outside of the master bedroom. Some CFD simulations confirmed that this location was not optimal for reliable wind data as the house affected the wind significantly in areas close to the house. However, the wind speed readings did reveal which days wind was present, even if direction and speed was unreliable.

## 6.2. Results of off-site window testing

Despite a test shed being designed, estimated, and planned for construction, the shed was not built due to time and logistics problems. Obtaining the discharge coefficients of the windows was shifted to using CFD based on validated work by other researchers.

### 6.2.1. Summary of the compiled data

The number of individual sets of data was over 40, with at least 30 being used to some extent in this research. With so many temporary sensors in place, the likelihood of stoppages in data recording was considerably high and inevitable to occur. The most useful data occurred when most sensors were functioning correctly. Figure 25 represents the timeline of where data was successfully recorded and where malfunctions caused holes in the data.

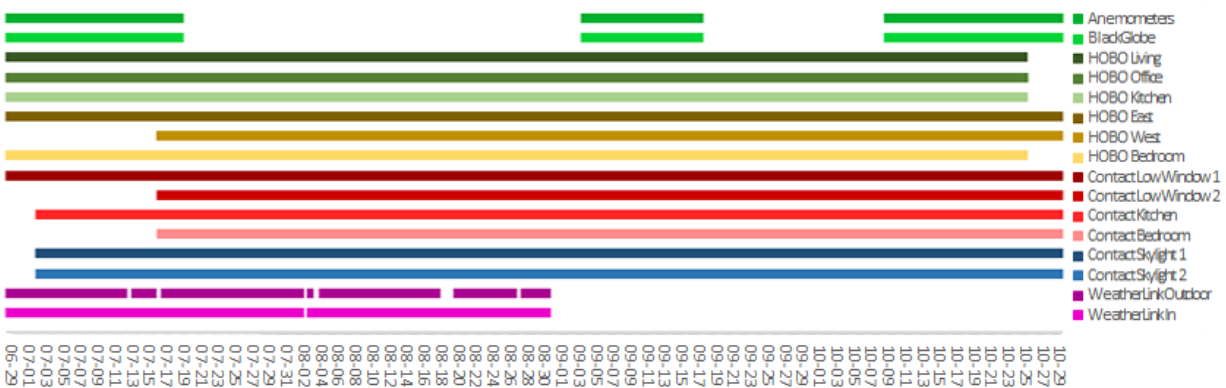


Figure 25: Status of the sensors used. Shaded regions represent time when the sensors were online. Non-shaded regions represent holes in data due to sensor malfunction or delayed installation.

While the HOBO Loggers performed fine with no errors or interruptions in the data, the most significant issue experienced was the failure of the Data Acquisition Box. Due to malfunctioning, the acquisition box consistently failed to record data until it was manually reset, which could not occur often as to not disrupt the occupants living in the house. This caused a

large and critical loss of data for the air speed anemometers and BlackGlobe globe thermometer placed near the skylight. This aside, there were still sections of data for which most sensors functioned properly, and the temperature outdoors was particularly high, allowing a good observational period to explore how natural ventilation functioned in the house.

### **6.2.2. Trends observed in recorded data**

Overlaying the data on a single plot allowed the many sets of data to be investigated simultaneously. Many trends were clearly evident and relationships between various aspects of the house were observed.

As seen in Figure 26, aggregated data from the air speed anemometers, temperature sensors, and state sensors were plotted over the course of a small time frame in July to more clearly display some observed trends. One of the most notable and significant trends observed with respect to natural ventilation was the effect of opening the skylights. Air flows would increase by as much as  $0.6\text{ m/s}$  at the sensor closest to the skylights because flow paths were created to allow the stack effect to occur. Less drastic changes in air speed at the central location suggested the kinetic energy of the air was quickly dispersed upon entering the atrium, allowing for adequate mixing of air. The other anemometer partially in the path of the incoming air also experienced increased flows then the skylights were opened.

With the outdoor temperature fluctuating on a daily interval, the indoor temperatures fluctuated as well; however, to a lesser extent which suggests thermal mass played an effective role in the thermal comfort of the occupants. Warm temperatures were retained through the night hours, even well after the outdoor temperature fell well below the indoor temperature. Thermal stratifications were seen as higher temperatures were recorded for sensors located at

higher heights. The lowest of the displayed temperature readings was located in the living area on the lower floor; the highest was the BlackGlobe operative temperature located in the skylight opening which typically measured temperatures higher than those outside due to both the increased solar gains in the chimney and thermal buoyancy.

Figure 26 further shows that despite warmer outdoor conditions, the house remained cool and comfortable. This is explained by the thermal mass in the house; as warm air entered the house, the large amounts of physical mass absorbed the heat, allowing the interior air temperature to remain cooler than the outdoors while still exchanging the old air inside with fresh air from the outdoors.

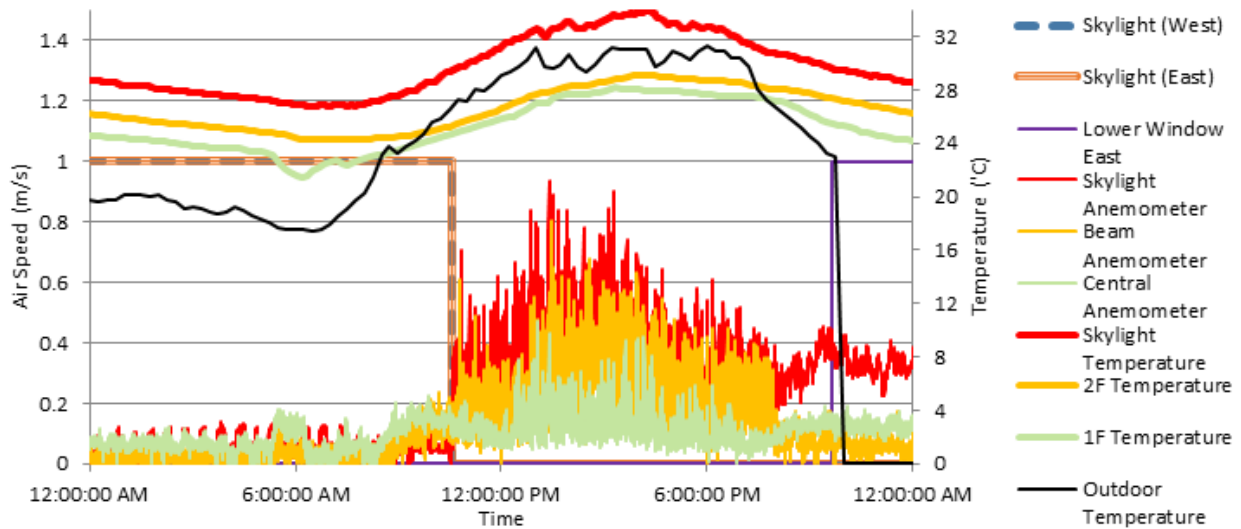


**Figure 26: July 12, 2014 from the compiled data.**

While Figure 26 shows the conditions within the house on a particularly warm day, and how thermal mass keeps the house cool, Figure 27 instead shows the direct effects of the skylights by examining days where the temperature was not abnormally hot. While air speed and skylight temperature data is not available, they can be assumed to be similar to other times when

the skylights were opened; their precise values are not essential for this part of the analysis. The climate conditions seen in Figure 27 show moderate temperatures, less than those seen in Figure 26 and exterior air temperatures rarely raised above the indoor temperatures. Due to the construction of the Harmony House, solar gains caused the interior temperature to increase despite cooler outdoor conditions. This heat was able to rise out of the house, drawing in cooler air and preventing the house from continuously heating up from the solar gains. This is a clear example of ideal conditions which allow the house to operate and utilize the skylights for cooling.

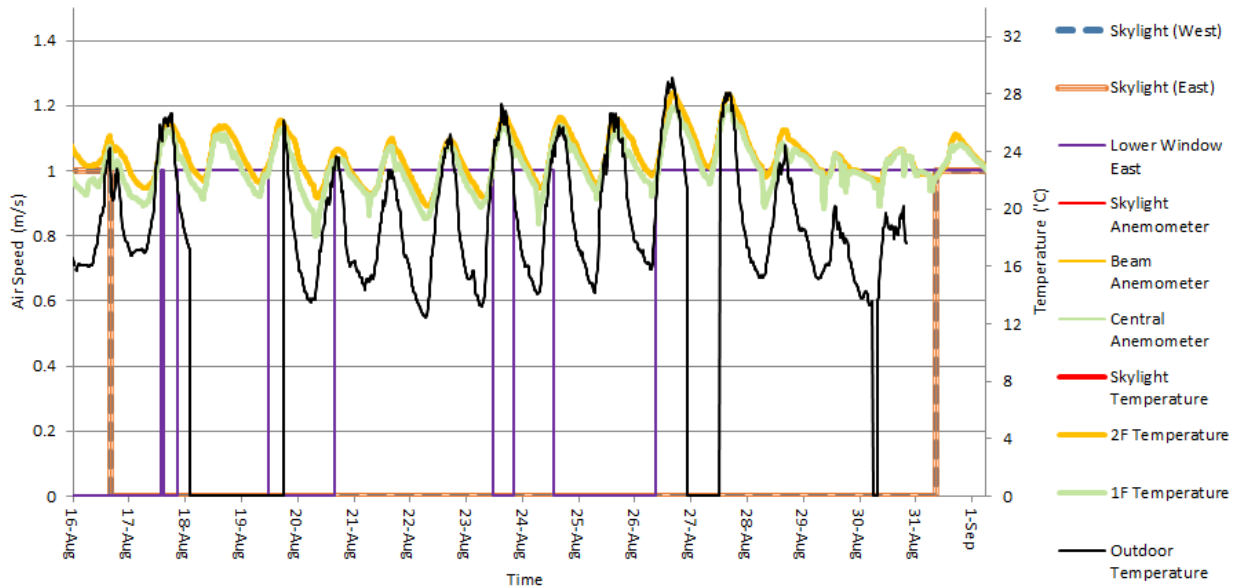


**Figure 27: A two week segment featuring full use of the skylights and the cooling effect they provide. Note that some of the data seen in the legend is not shown as this data was recorded during the shutdown of some equipment.**

Another example of the skylights offering cooling can be seen between two sets of data with similar outdoor conditions; however, only one day made use of the skylights to help cool the house. As seen in Figure 28, both July 9 and July 17 featured outdoor air temperatures peaking at around 25°C. While the skylights remained close during and throughout the days

prior to July 9, they were open for and prior to July 17, offering a good opportunity to compare the conditions between the two days. The operative temperature in the occupied areas was about 2°C lower with the skylights open, while the temperature in the chimney was as much as 4°C lower. This suggests the house performed best and ventilated the most air during typical summer conditions. While still effective, the house was less efficient at cooling when the outside temperature was unusually hot; however, as seen in the compiled data in APPENDIX B – Compiled data, this is generally uncommon.

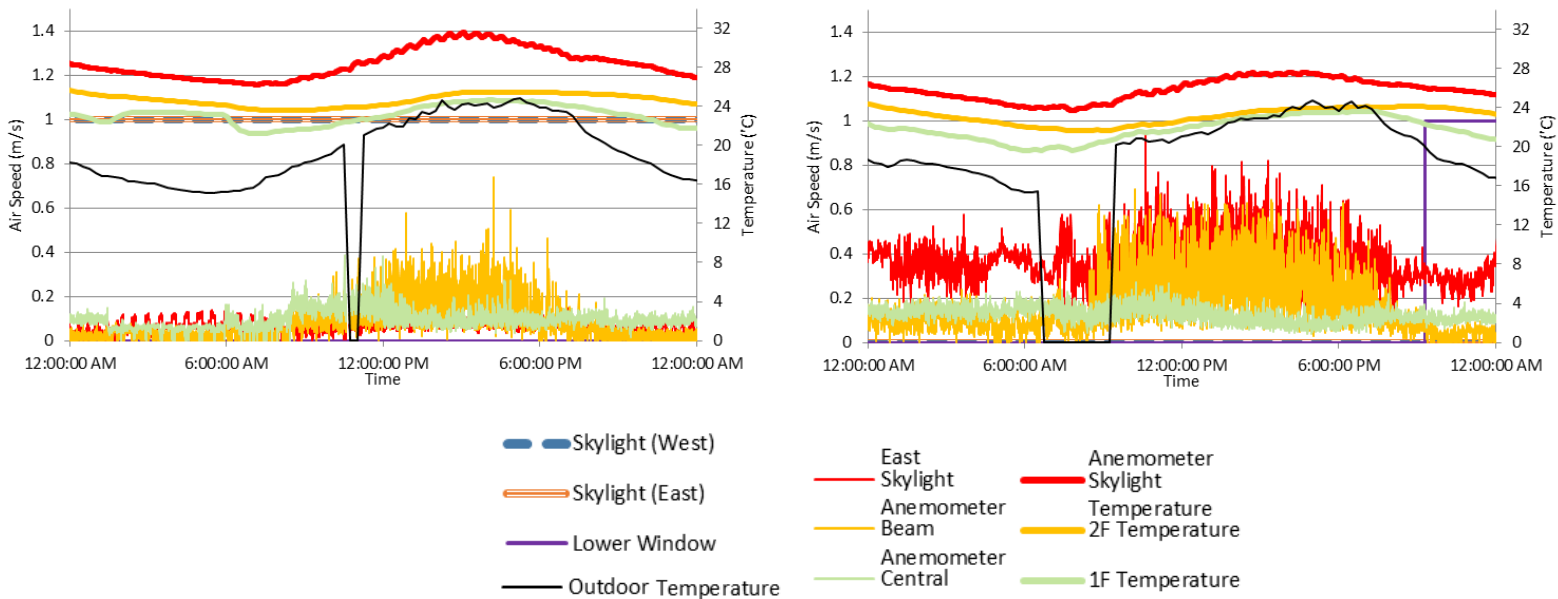


**Figure 28: The interior climate data and the outdoor temperature for July 9, 2014 (left) and July 17, 2014 (right).**

Some of the data proved to be uninterpretable for reasons unforeseen. The contact sensor installed on the kitchen door showed erratic behavior almost every day, as the occupants often used the door to access the back yard. Because the contact sensor would only register as ‘closed’ if the door was completely closed, the situation often occurred where the door was essentially closed, however, not completely, and the sensor would record the door as being ‘open’. This was a limitation that must be considered with the results.

While ASHRAE does not include relative humidity in any thermal comfort analysis, relative humidity was passively investigated to determine any trends or relationships between comfort in the house and the relative humidity. It was previously mentioned that European Standard EN 15251 stated that relative humidity plays a minute role in thermal comfort; however, the relative humidity was still recorded during the monitoring phase of the research. Figure 29 shows that despite fluctuating outdoor relative humidities outdoors, the house was able to keep the relative humidity indoors quite stable. Furthermore, the occupants of the house reported no issues relating to relative humidity, so these findings support the notion stated by EN 15251. While this may be true for relative humidities in the typical comfort ranges of about 50%-60%, the house never allowed the relative humidity to reach excessively low or high values so no conclusions can be made on these extremes.

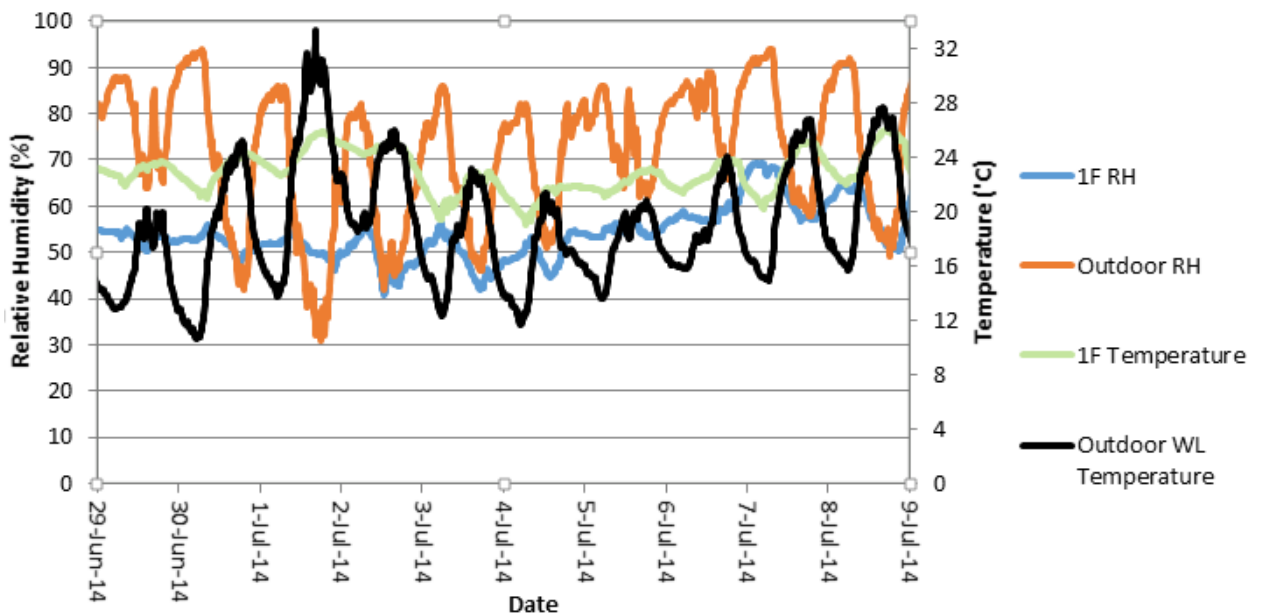


Figure 29: The outdoor and indoor relative humidity recorded, plotted with the outdoor and indoor temperatures.

### **6.3.Results of on-site window testing**

Though the on-site testing was attempted, it could not be completed. After thoroughly sealing off the orifices and vents of the house, a blower door was installed and run for background leakage. Preliminary results did yield leakage rates; however because the house was occupied and the state of the basement suite was unaccounted for, the rate was inconsistent upon repeating the experiment. Furthermore, when opening the smallest window involved in the test, the blower door used could not pressurize the house with any stability. Opening any other orifices would have caused massive pressure losses that the blower door would not be able to correct. As a result, the test was stopped and the off-site testing was planned.

### **6.4.Dynamic thermal model of the Harmony House**

A scale model of Harmony House was built using the DesignBuilder software (DesignBuilder Software Ltd., 2015). The floor plan was constructed according to the CAD drawings submitted for the building permit to approve construction. Aspects such as building footprint, height, wall, and window size and placement were all obtained from this document supplied by the architect. The R-values and corresponding components of the walls, ceiling, floor, and glazing were all taken from presentation documents explaining the construction of the building and manually inputted into the software using the software's built-in component libraries where applicable. Some materials not available in the component libraries were researched for their characteristics and added to the library for use. A view of the model in the DesignBuilder interface can be seen in Figure 30.



**Figure 30: Visualization of the dynamic thermal model of the Harmony House.**

All rooms were separated into their own zones with individual nodes. Due to multizone air flow network simulations' poor handling of vertical spaces, the house, and more importantly, the main atrium was divided into multiple sections (Figure 31), all connected by open holes but classified as different zones to allow air to flow freely between the zones and not be treated as one single node (Tan & Glicksman, 2005). Doing so also allowed solar radiation to transmit through the upper floor zone to the zones below. By using this method, temperature stratification could be recorded at the three separate levels. The software used also lacked any input for window characteristics; every window was modeled as a square orifice with a discharge coefficient of 0.65. As mentioned previously, proper window characterization is critical for generating accurate simulations. Vents were input in place of windows and secondary windows of equal size were installed alongside the vents at the same height. This was done because most of the physical opening area in awning windows begins at the sill of the window due to the geometry at small opening angles. The windows were shaped like horizontal "letter-boxes"

instead of fitting the window back onto the wall in any location in which it would fit best, which otherwise could have resulted in errors from buoyancy-related problems (Coley, 2008). Improper vertical placement would have introduced height differentials that could potentially affect ventilation rates. The use of these vents allowed the customization of discharge coefficients for each individual vent and the additional windows allowed the lost solar radiation back into the house such that the energy balance of the house was not compromised.

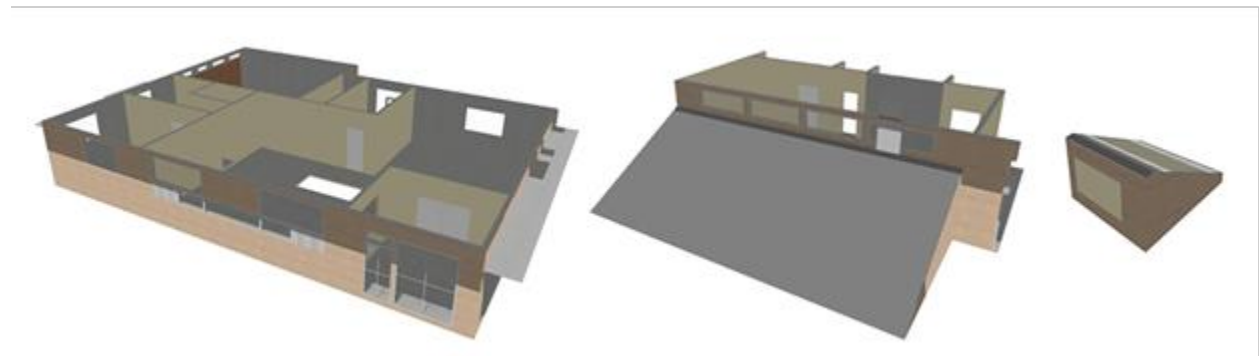


**Figure 31: The three separated zones of the dynamic thermal model: the first floor, the second floor, and the skylight.**

Throughout all simulations performed in the dynamic thermal model, all HVAC systems were turned off, to best match the operation of the environmental controls of the house. The weather file used was obtained from the Canadian Weather year for Energy Calculation(Environment Canada, 2015).

### **6.5.CFD model of the Harmony House**

Like the dynamic thermal model, then CFD model was developed using documentation supplied by the architect. scSTREAM was chosen as the CFD software for its fast computational

time and capability to accurately simulate indoor and outdoor air flows for buildings (Figure 32). CFD also allows for the relatively complex geometry at Harmony House and while dynamic simulations are possible, only steady-state simulations were performed.



**Figure 32: Photograph of the Harmony House (left). Meshed CFD model of the Harmony House (right).**

The physical dimensions of the house are 60 feet wide, 46 feet long, and about 33 feet tall and thus the entire computational domain of the simulations used was 300 feet wide, 450 feet long, and 190 feet tall (Figure 33), or roughly the dimensions of the house multiplied by factors of 5, 10, and 5, respectively, surpassing the recommendations made by Tan and Glicksman (2005) and Evola and Popov (2006). With wind simulated to be incident on the southern façade, the  $y_-$  boundary was set to a constant air speed conditions. The  $y_-$  boundary was set to a fixed static pressure of  $0 Pa$ . The  $x_+, x_-$ , and  $z_+$  boundaries were set to freeslip conditions to nullify friction and prevent any pressure losses across the boundary. The simulations were run until convergence criteria was met.

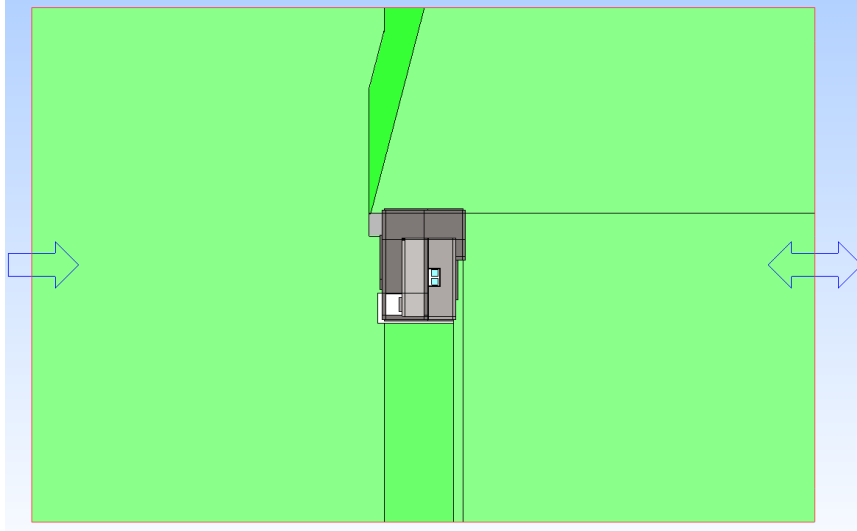


**Figure 33: An overhead view of the computational domain used.**

### **6.5.1. Optimal size of CFD cell resolution**

As will be discussed later, the CFD simulations were run with awning windows. Based on the operation recorded, it was discovered that the most used window controls in the house were the lower four windows on the first floor and the two large skylights atop the atrium. As tested on-site, the lower windows had dimensions of 41" wide, 20" high and were only capable to open to 35°. The skylights were square in shape with an edge size of 45" and were electronically openable to 13°. The pressure across a wall with an awning window was the parameter to be compared amongst simulations because of its stability, ease to measure, and relevance to the Harmony House model. It is worth noting that considering the velocity as the main parameter would require much finer cell resolution (Lo & Novoselac, 2011).

Because the Harmony House model utilizes refined meshing in certain areas, the effect of refine meshing was also investigated. For the lower windows, the cell size was programmed to 10 *cm* in side-length uniformly throughout the whole computational domain and the simulation was run to convergence. 10 *cm* was chosen as it was expected to be exceedingly

large. Rerunning the same scenario with 7 cm, 5 cm, and 4 cm, the results were immediately shown to quickly converge, suggesting a cell size as large as about 5 cm was sufficient to be used. The non-uniform case had an overall cell size of 5 cm, with refinement surrounding the orifice. Smaller refinement was programmed to these sections to verify that the act of refinement did not result in significantly different values. In the case of the skylight window, the opening angle was set to 15°. There was much more fluctuation in the higher cell sizes but the fluctuations appeared to minimize as cell size was reduced. The results of this experiment can be seen in Figure 34. An ideal cell size was found to be no larger than 5 cm in side length, much less than the 10 cm cell size chosen by Lo and Novoselac (2011) on a similar experiment. For the CFD simulations performed, refined meshing was used to reduce computational time. The entirety of the computational domain has 60 cm cells and refined meshing was set closer to the building at 20 cm. Even closer, and encompassing the whole building, the final mesh refinement had a cell size of slightly under 5 cm.

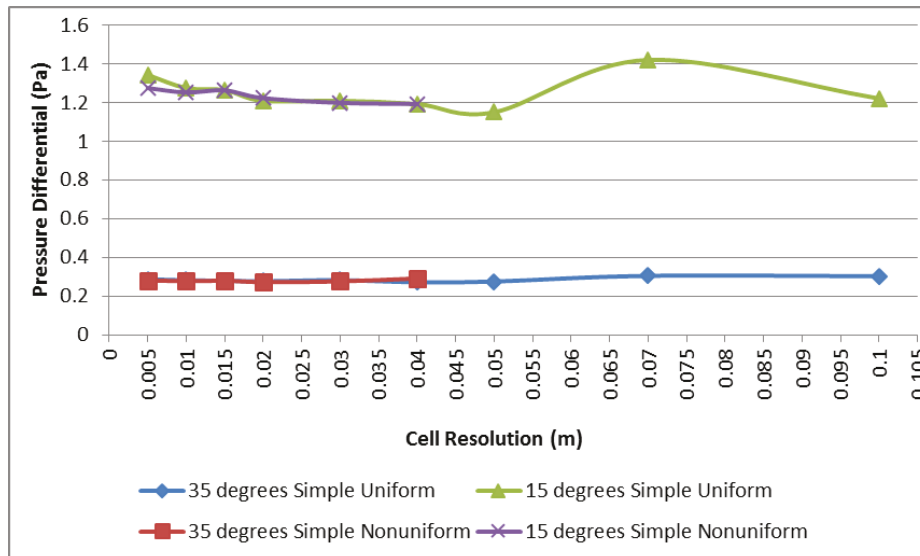


**Figure 34: The determination of the optimal mesh cell size. Uniform refers to a constant cell size throughout the computational domain. Nonuniform refers to a refined mesh cell size around the opening, of a different cell resolution than the rest of the computational domain.**

### 6.5.2. Coefficient of discharge for windows and skylights

Hult et al (2012) created a test cell 3.4 *m* high and 3.6 *m* wide with a wall in the center. The enclosed cell was provided with an inlet 5 *m* upstream and an outlet 5 *m* downstream. In the center wall was a hole 1.2 *m* wide and 0.6 *m* tall. A simple or detailed window was installed into this hole and adjusted to various opening angles, pivoted around the head, or top of the hole. As mentioned previously, the simple window was a plane and the detailed window was three-dimensional and had a finite thickness. The same naming convention also applies to the wall. A constant flow rate of 0.288  $m^3/s$  was supplied at the inlet with free flow at the outlet causing a pressure drop across the wall. This pressure drop was measured very close to the inlet and outlet as to be sufficiently far from the opening. The average of the cross section was taken to account for any case where the pressure was nonuniform; however, in all cases, the pressure was essentially constant across the cross section.

Table 11 and Figure 35 show the results of the test. The pressure across the wall was recorded and the discharge coefficient was calculated according to Equation 11. This discharge coefficient represents the equivalent resistance of flow that would be present for a hole of 1.2 *m* by 0.6 *m* without any awning window attached. Comparing the resultant discharge coefficients with the results of Hult et al., it was found that the two sets of results differed by between 2.6 – 5.9%, suggesting that the results from scSTREAM could be considered validated by Hult et al. work.

The detailed case was tested next to consider the viability of inputting detailed windows into the Harmony House model. The procedure was done in the same way. The results can be seen in Figure 36. The pressure difference across the wall at low window angles was

unreasonably high so the corresponding points were treated as outliers. This is likely because the combined thickness of the wall and of the window combine to create significantly smaller effective opening areas compared to the simple window, combined with the finite size of each cell, resulting in a much higher resistance of flow. Hult et al. suggest that “close agreement between ... data from window manufacturers and [Hult et al.] CFD tests for the simple angled window geometry suggests that the CFD test cell provides an effective method to determine the effective area of a pivoted window”. This logic can be applied to the discharge coefficient as it and the effective area of a window are closely related.

**Table 11: The simulations resulted in pressure differentials across the wall. The results for various opening angles and grid resolutions reveal coefficients of discharge for each opening.**

$\alpha$ [°]	Resolution [cm]	CFD		Hult's paper simple window		
		$\Delta P$ [Pa]	$C_d$	$\Delta P$ [Pa]	$C_d$	$\Delta C_d$ [%]
10	5	4.0657	0.154	3.6537	0.1625	5.2
10	2.5	3.8528	0.158	3.6537	0.1625	2.6
10	1.5	3.9194	0.157	3.6537	0.1625	3.4
30	5	0.7467	0.359	0.6681	0.38	5.4
30	2.5	0.72020	0.366	0.6681	0.38	3.7
30	1.5	0.72017	0.366	0.6681	0.38	3.7
50	1.5	0.3956	0.494	0.3500	0.525	5.9
70	1.5	0.2921	0.575	0.2636	0.605	5.0
90	1.5	0.246	0.626	0.2593	0.61	-2.7

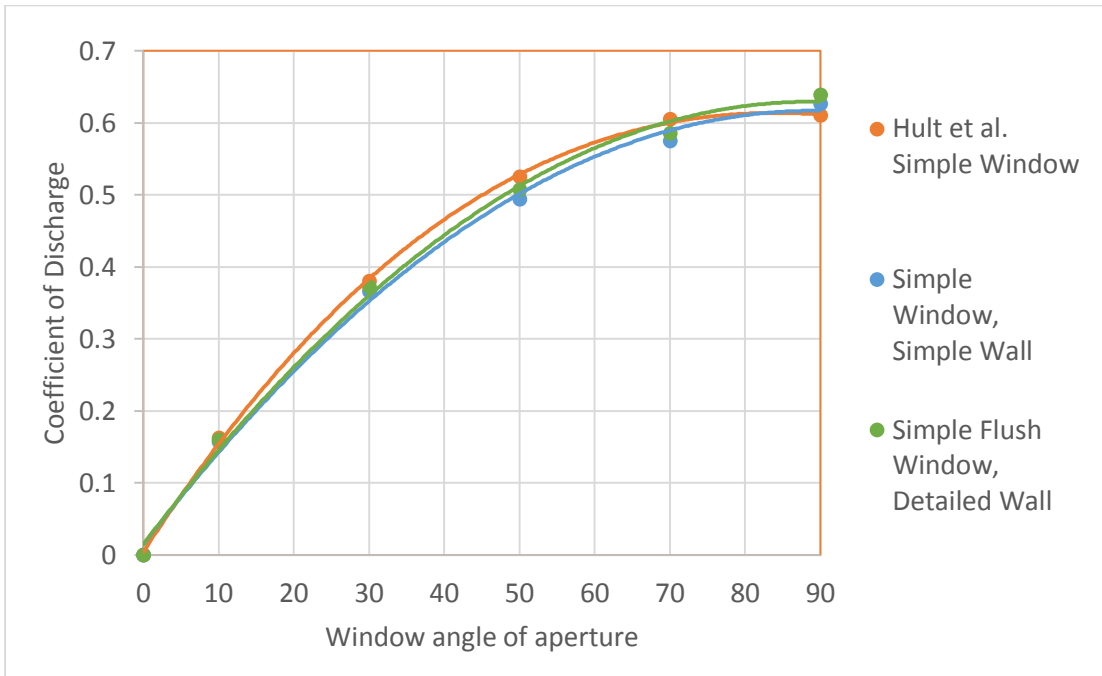


Figure 35: Comparison of simple window discharge coefficient results by Hult et al. (2012) and work done in scSTREAM CFD for model validation.

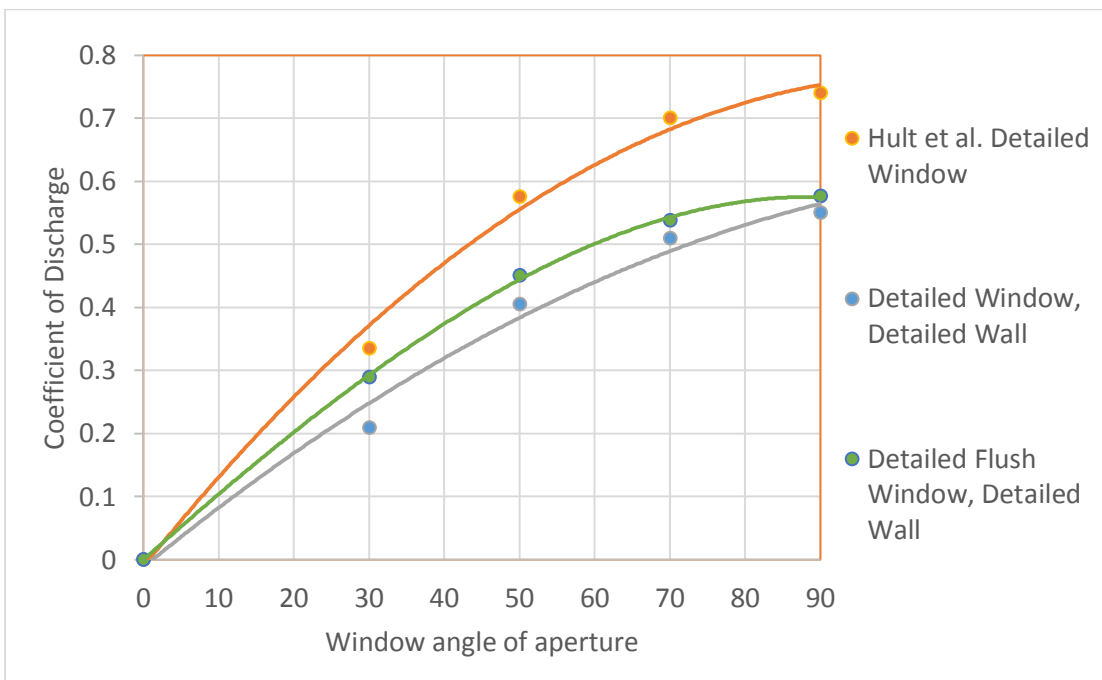


Figure 36: Comparison of detailed window discharge coefficient results by Hult et al. (2012) and work done by scSTREAM CFD for model validation.

The windows in the CFD test shed were altered to the dimensions of the windows at the Harmony House. The specifications of each of the four lower windows were 1.04 m long and 0.50 m high and opened to nearly 90°; however, gravity pulled the windows closed to a maximum angle of 35°. The skylights were square with an edge length of 1.14 m. They could be electronically opened to a maximum of 13°. In testing the discharge coefficients of the windows and skylights in CFD, angles beyond the maximum opening angle were tested to confirm consistency in the results. The test shed in the case for the skylights was rotated by 90° such that air was traveling ‘up’ through the skylight, as opposed to horizontally in the case of the lower windows. The results can be seen in Figure 37. At 35°, the lower windows were found to have a discharge coefficient of 0.391, while the skylights had a discharge coefficient of 0.209 at 13°.

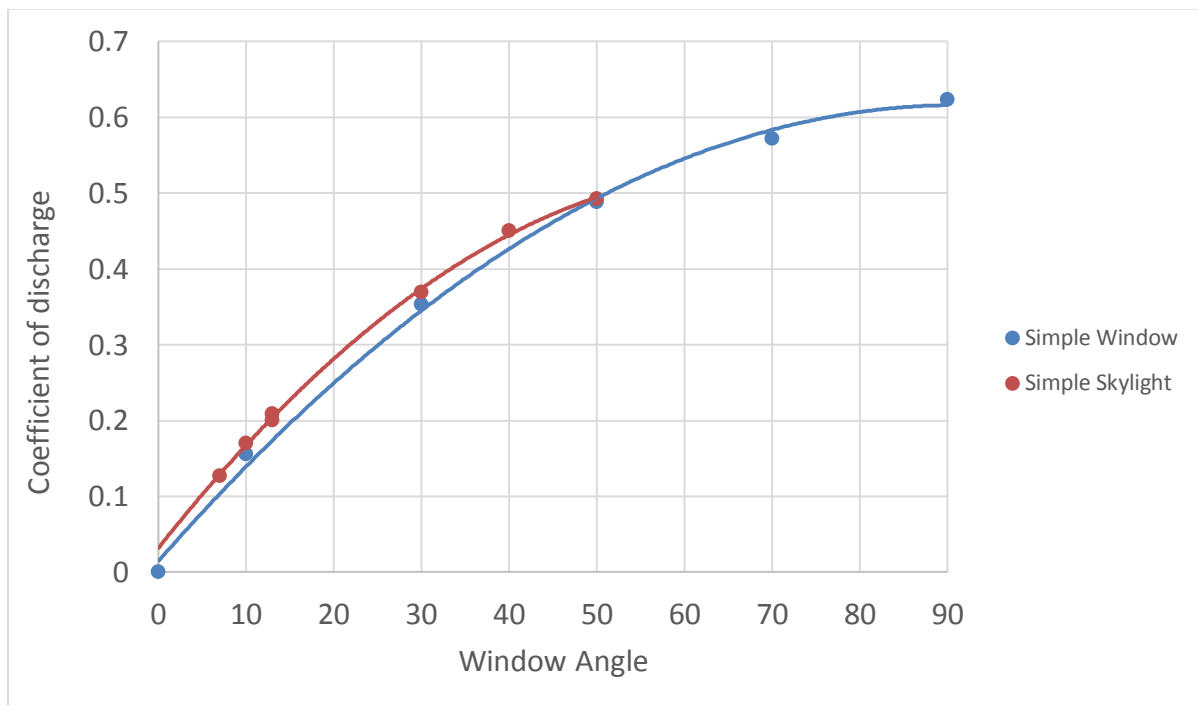


Figure 37: Discharge coefficients for the windows at various opening angles.

## 6.6. Validation of computer models

As mentioned previously, the on-site weather station was situated on the 2nd floor balcony, resulting in unreliable wind data. As a result, the response of the dynamic thermal model to three different wind stimuli was investigated. Based on the local meteorological data, the most common wind speeds were considered, which uncommonly exceeded  $2\text{ m/s}$ . To collect a range of wind speeds, three individual cases were studied:  $0\text{ m/s}$ ,  $1\text{ m/s}$ , and  $2\text{ m/s}$ . The wind was directed to be incident on the southern façade.

To simulate common instances in the operation of the house, all windows and doors were set to be closed using the software's scheduling system. The most commonly used windows (the lower four windows and the upper two skylights) were set to be always open, to isolate the effects of these openings, acting alone. Based on the recordings from the on-site sensors as well as a questionnaire answered by the occupants (APPENDIX E – Results of questionnaire), a common combination of window openings used at the house were to have two of the four lower windows open and both skylights open. This was used as the basis for these simulations. The vents in place of these windows were assigned their respectful discharge coefficients: the lower windows 0.391 and the skylights 0.209.

Representative days of similar outdoor conditions were chosen to compare the interior temperatures of the energy simulation with the recorded data. Table 12 represents the interior peak temperatures throughout different levels of the case study house within the main atrium. The comparison shows good agreement between the temperatures at three heights within the house's main atrium and through the chimney and skylight.

**Table 12: Matched days peak temperatures (°C) between dynamic and recorded results for 1m/s wind.**

Date	Cool day (°C)		Typical day (°C)		Warm day (°C)	
	Data	DB	Data	DB	Data	DB
	18-Jul	06-Jul	16-Jul	24-Jul	13-Jul	22-Jul
1F $T_{air}$	23.1	24.0	26.0	27.4	27.7	28.7
2F $T_{air}$	23.6	24.3	26.7	28.2	29.6	30.2
Sky $T_{op}$	27.1	27.1	31.2	31.5	33.9	34.0
$T_o$	23	21	23	23.5	32	28

Values were chosen based on the peak for that day and the best fits were matched. The first floor air temperature, second floor air temperature, and skylight operative temperature for two back-to-back days of similar outdoor conditions are shown in Figure 38. The day chosen in this case was a “warm” day with a wind speed of 1 m/s. As can be seen, the results of the dynamic thermal model showed good agreement with the recorded data. While peaks of each day served as a good metric for evaluation and comparison, it should be mentioned that the dynamic thermal models were less accurate at predicting overnight lows on the cooler days. This is likely due to the difficulty of modeling the full capability of thermal storage, as the model under-estimated the temperatures at night. This can arise issues in comparing multiple days of data, as the day previous can have an effect on the following day with energy stored in the thermal mass. Also it can be difficult to find several consecutive days with closely matching outdoor temperatures and conditions for comparison.

The other scenarios (warm, average, and cool days) with each wind speed (0 m/s, 1 m/s, and 2 m/s) can be seen in APPENDIX C – Results from the validation of the dynamic thermal model. The results of the simulations show that throughout the warmer months, wind has less of an effect than it does in the shoulder seasons. The difference between 0 m/s and 2 m/s show a decrease in peak temperature in all stratification levels by less than one degree Celsius. This suggests for large spaces with small inlets, buoyancy driven flow dominates. This

is generally what was experienced in the house, as air could be felt entering once windows were opened, even in the absence of wind.

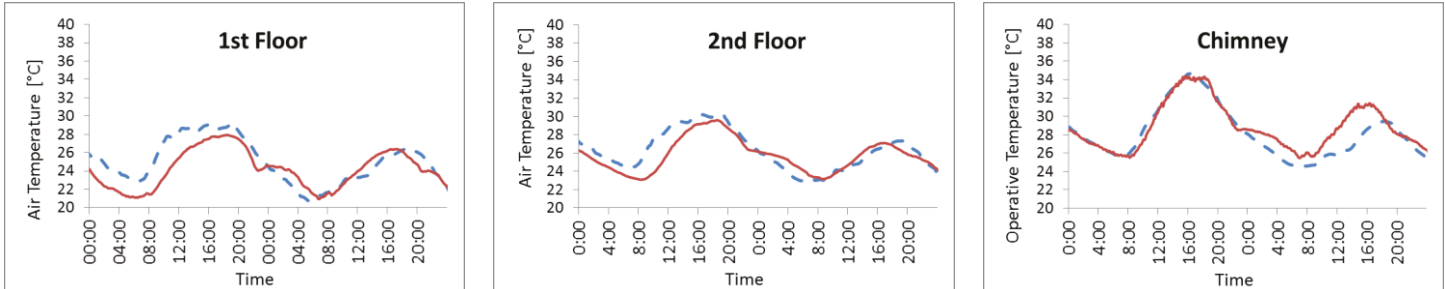


**Figure 38: Comparison of simulated (dotted) and measured (solid) results in temperature for July 13 (recorded) and July 22 (simulated).**

This close match between the energy simulation of the dynamic model (dotted line) and the recorded data (solid line) shows that a dynamic model can be generated to be a good representation of the real conditions experienced in a net-zero energy house like that of the case studied. Extending the comparison to that of a typical day, as well as a relatively warm and cool day, it can be seen that the dynamic model is accurate throughout the temperature ranges typically seen in the summer. Peaks occurring at slightly different times may be explained by having used the method of matching the hours of each day. Comparing two days weeks apart can result in a differing angle of solar azimuth.

With the dynamic thermal model considered to be a good representation of the real conditions recorded, the surface temperatures on each representative day were obtained from the energy simulations (Table 13). The surface temperature of each zone is calculated as the average of all the surfaces in that particular zone considering various internal gains, particularly solar radiation. Individual values were recorded for the first floor, second floor, and skylight, for each of the different simulations with the only variation being the wind speed. These surface

temperatures were input into the CFD model (Figure 39), along with the outdoor dry-bulb temperature for the ambient and incoming air.

**Table 13: Surface temperatures (°C) obtained from dynamic results for 1 m/s wind on a cool, average, and warm day.**

Location	Cool day (°C)	Average day (°C)	Warm day (°C)
1F $T_{wall}$	24.3	27.9	29.8
2F $T_{wall}$	25.3	29.6	31.8
Sky $T_{wall}$	31.0	37.5	40.5

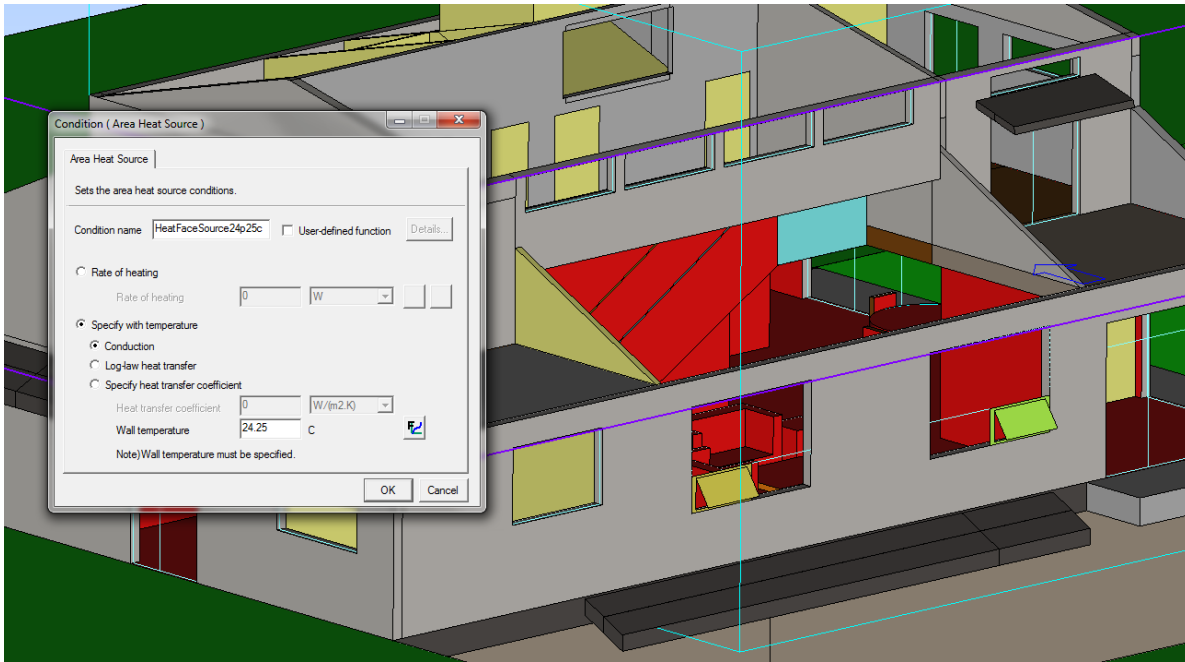


**Figure 39: Inputting a fixed temperature on all surfaces on the first floor (red). Second floor and skylight temperature were also set as fixed, according to the results of the dynamic thermal model.**

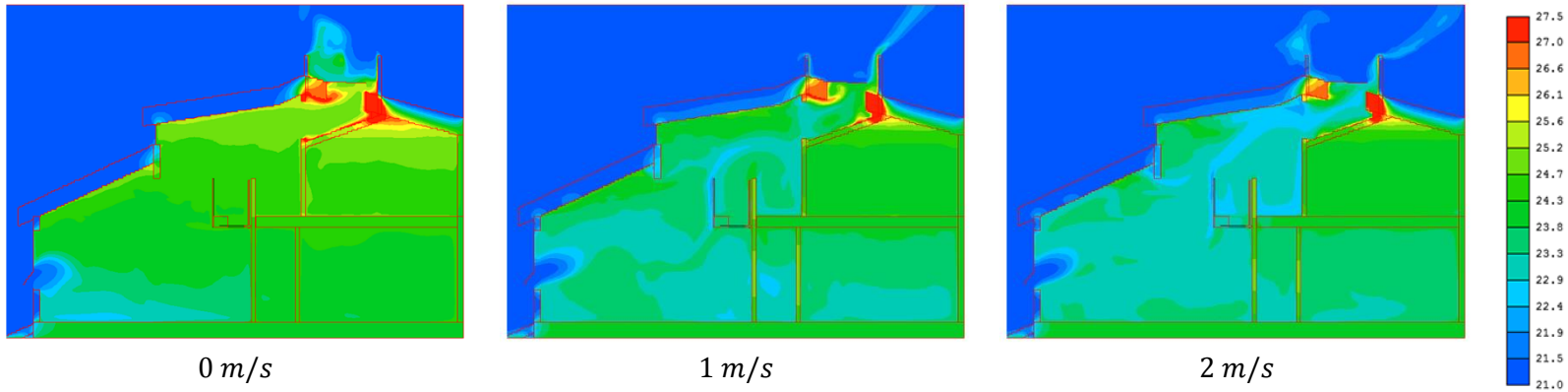


**Figure 40: CFD profile of the house for a cool day, showing clear temperature stratification within the main atrium. The level of stratification and mixing varies depending on the wind speed.**

The same slice throughout the house was used as a metric for comparison in every CFD simulation result. The results from each simulation (Figure 40, full results in APPENDIX D – Results of the CFD model) revealed good agreement with the temperature stratification observed with recorded data and in the dynamic thermal model. The temperature stratification for the case of 1 m/s wind incident on the southern façade on a typical day can be seen in Table 14. The table shows the comparison between the temperatures on each floor and in the skylight, allowing the cross validation of both models with the recorded data.

**Table 14: Temperatures (°C) compared for 1m/s wind typical day. \* marks operative temperature readings.**

Location	Values (°C)		
	CFD	Recorded Data	DB
1F	26.74	26	27.5
2F	27.84	27	29
Skylight	28.18 / n/a*	31.5*	32*

Due to the natural, high-variation of wind speeds ( Figure 24) that are possible in any house, there was a wide range of air speeds recorded at any time. Despite this, trends and averages showed strong correlation with the time of day and operation of windows and skylights.

The three locations of the anemometers on-site were located in the CFD model and a box with a 10 cm side length was formed around it. The average airspeed across the surface of this box was used as a singular value for comparison with the on-site data. This comparison shows that the steady-state CFD simulations accurately predicted the speed of the air in the house and always fell within one standard deviation of the recorded data (Figure 42). The data was collected over a 3.5 hour section of the day during a peak in interior temperature. All parameters of house operation remained stable during these times. One standard deviation was used for error bars because there is uncertainty in the exact window operation during the recorded period. The natural variation in wind was also the cause of these fluctuations. CFD of the air flows (Figure 41) shows increased air flows immediately inside the atrium on the first floor at the potential core region. Once air loses its kinetic energy in the flow decay region, it stagnates in the terminal region and slowly flows upwards until it reaches the opening at the skylight level where it again picks up speed and exhausts out of the house. This process was also explained in Section 2.

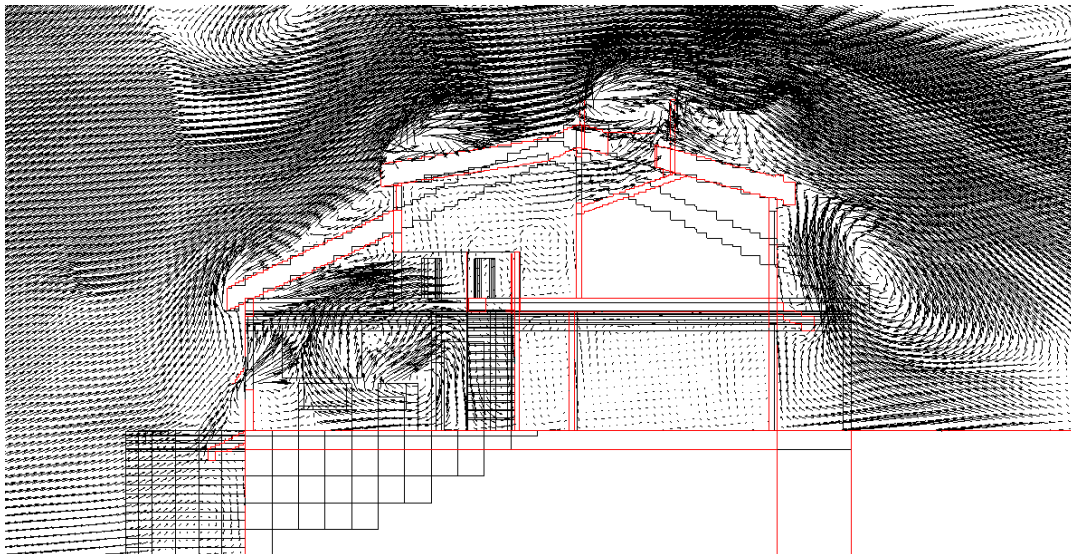


**Figure 41: CFD representation of air flow through the house in a cross section showing the increased air flows at the inlet and outlet with low air speeds in most areas of the house.**

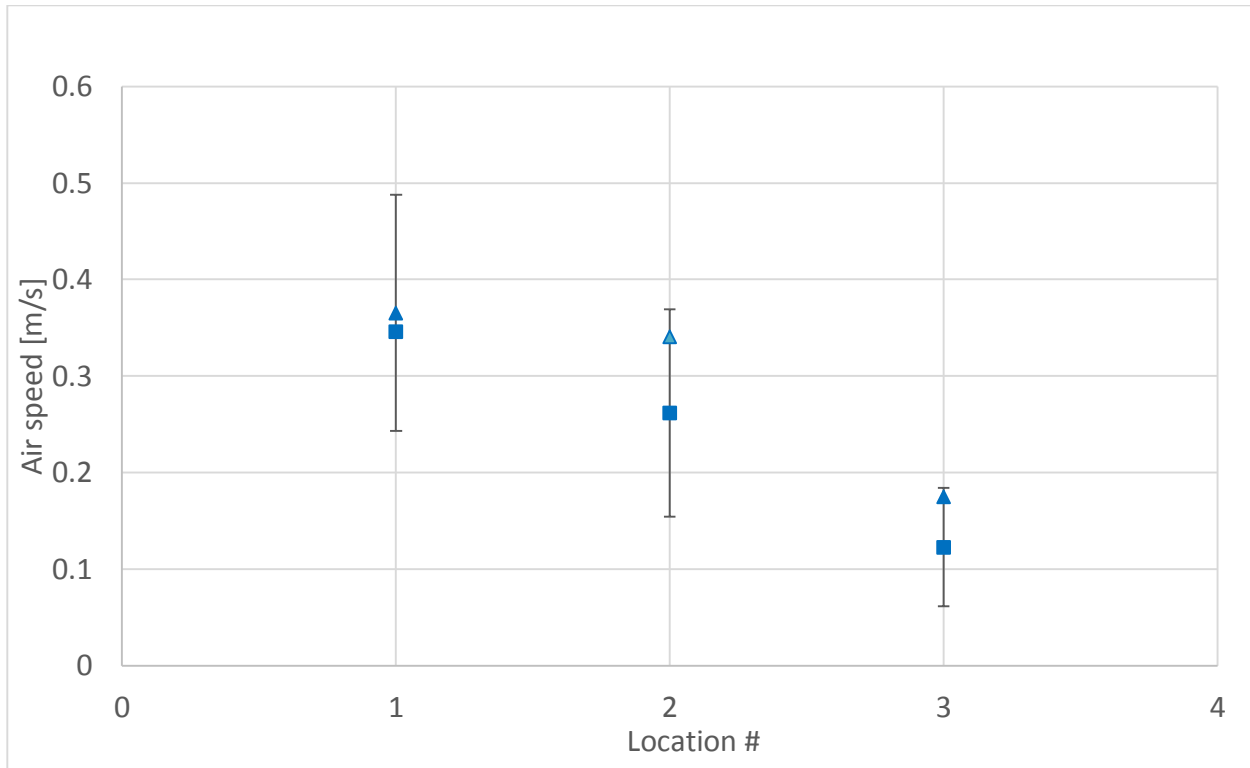


**Figure 42: Comparison of simulated (triangle) and measured air speeds (square) near the skylights, location 1 (Figure 20, sensor a), beam, location 2 (Figure 20, sensor b), and central area, location 3 (Figure 20, sensor c). Error bars represent one standard deviation from the mean.**

The air flow rates in the CFD model were determined by integrating across entire the area of the lower window inlets and the skylight outlets in the CFD model (Figure 43). For the outlets, two values were measured, one at the inlet to the chimney and one at the outlet, to ensure they were equal and to confirm the mass was conserved. Comparing these with hourly averages calculated by the dynamic model for representative days shows that CFD typically predicted values higher than those by the dynamic model. This may be explained by the CFD software’s inability to properly model infiltration, whereas the dynamic model included infiltration. Unfortunately, due to the complexity of measuring air flow rates in the house, which extends to problems relating to lack of control and equipment to passively measure, these simulated values cannot be directly compared to the rates experienced in the house and simulation is the only

possible evaluation. The results of the air flow rates through the inlets and outlets can be seen in Table 15.

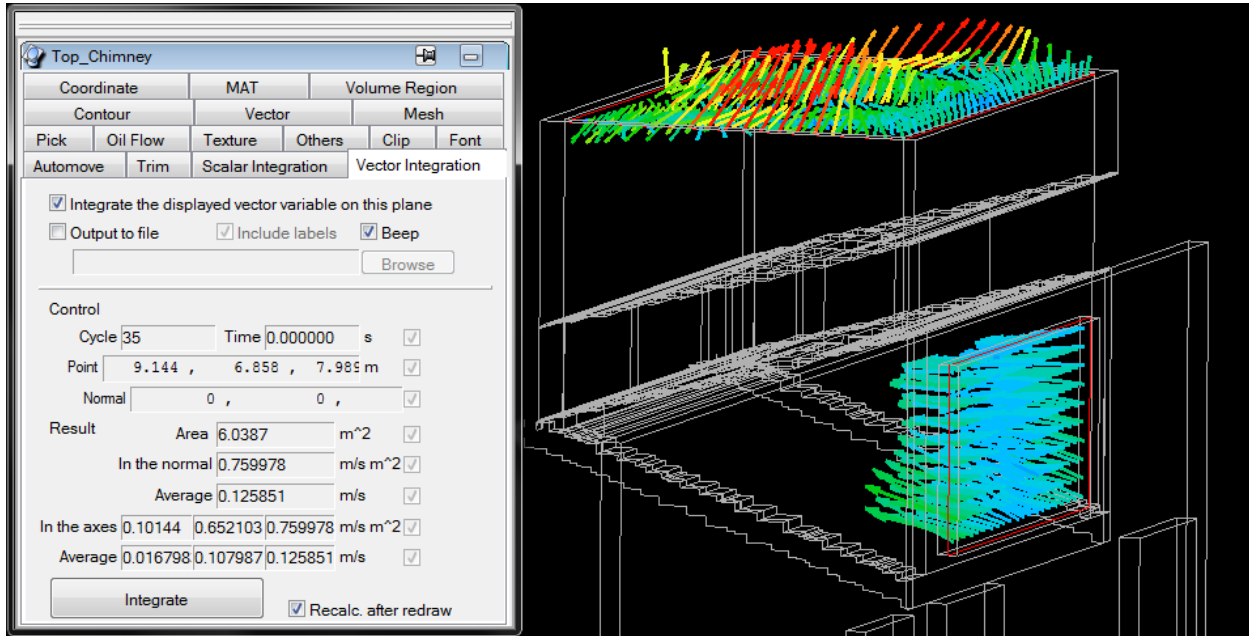


Figure 43: Integrating the air velocity across the openings results in the volumetric air flow.

Table 15: Volumetric Air flow [ $m^3/s$ ] results compared for 1 m/s wind on a typical day.

Location	CFD [ $m^3/s$ ]	Dynamic-Thermal [ $m^3/s$ ]
Skylight Outlet	0.760	0.617
Lower Window West	0.373	0.281
Lower Window East	0.364	0.281
Lower Windows Total	0.738	0.563

## 6.7. Assessment of adaptive thermal comfort

The prevailing mean outdoor temperature was calculated using Equation Eq. 30, resulting in a single value for each day measured. Plotting the corresponding indoor operative temperatures on the first floor as a function of these prevailing mean outdoor temperatures resulted in a comfort chart that provided a good judgement of adaptive comfort throughout the summer for the most commonly occupied area. Figure 44 shows the house performed very well and the vast majority of data points fell within the zones in which 80% of occupants feel

comfortable according to ASHRAE Standard 55. There was a moderate number of points that fell outside of this threshold, particularly in the regions where occupants would be expected to feel cold; however, based on the surveys provided to the occupants, no discomfort was felt at any time throughout the investigated timeframe. These points are also explained by the fact that the heating system was never used throughout the summer, resulting in cooler temperatures, especially overnight.

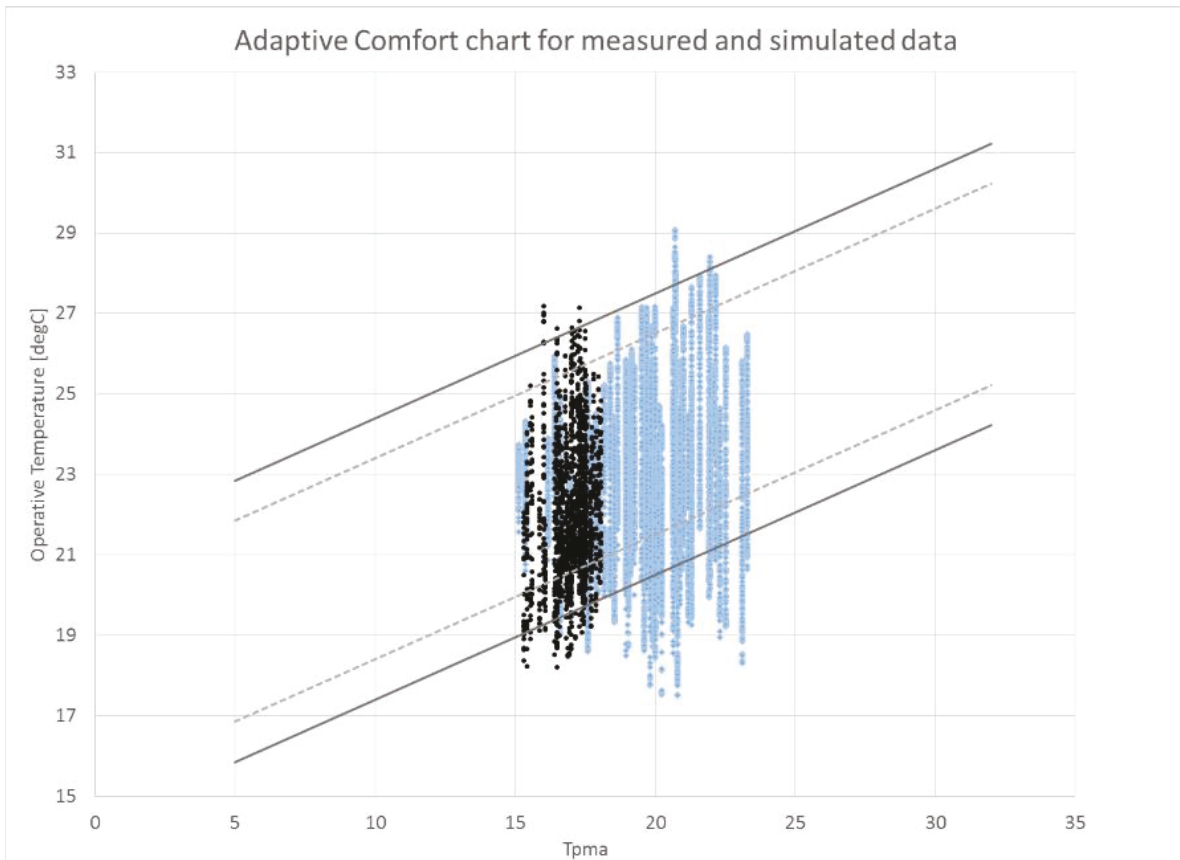


**Figure 44: The operative temperatures of the first floor for each measurement's respective prevailing mean outdoor temperature. Recorded data shown in blue, dynamic thermal model results are shown in black.**

The same method applied to the dynamic thermal model showed similar results, as most data points fell within the 80% comfortable threshold. The most notable difference was the lack of variation in prevailing mean outdoor average temperature, as it only ranged between roughly

15°C and 18°C. The real data had a much larger and higher range. This is likely explained by the unusually warm summer experienced in 2014, whereas the weather file is representative of a typical year. This said, the operative temperatures of both data sets at overlapping prevailing mean outdoor temperatures do match well and there is very good agreement between the two sets of data.

Because the vast majority of points of recorded data do fall within ASHRAE Standard 55 comfort zones, it can be concluded that the house is performing exceptionally, as expected. Data points that do fall outside of this range carry less significance as the occupants reported zero times at which they felt uncomfortable during the months recorded, and chose not to close any windows to warm the house up.

## **6.8. Evaluation of chimney-cap technologies**

To consider the scenario had the Aerocap or a similar venturi-shaped cap been installed on the chimney of the house, a test case was examined as well. Using results from van Hooff et al. (2011), the wind pressure coefficients on the roof of the house were changed at the location of the chimney to values varying between  $-1.21$  and  $-1.35$  depending on the orientation of the wind. The venturi-shaped cap was optimized in shape to maximize the pressure differential across the inside and outside of the chimney; whereas, the design of the Aerocap was not engineered and was based on basic fundamentals of physics and thus its effects can be expected to be less than that of the model tested in the work by van Hooff et al. For comparison with results of a previous simulation, the simulation was run under an unaltered weather file as with the simulation for the comfort analysis such that natural operation of the house could be

predicted. The results showed insignificant difference between the two simulations and temperatures dropped an average 0.50 °C over the range of dates simulated (Figure 45).

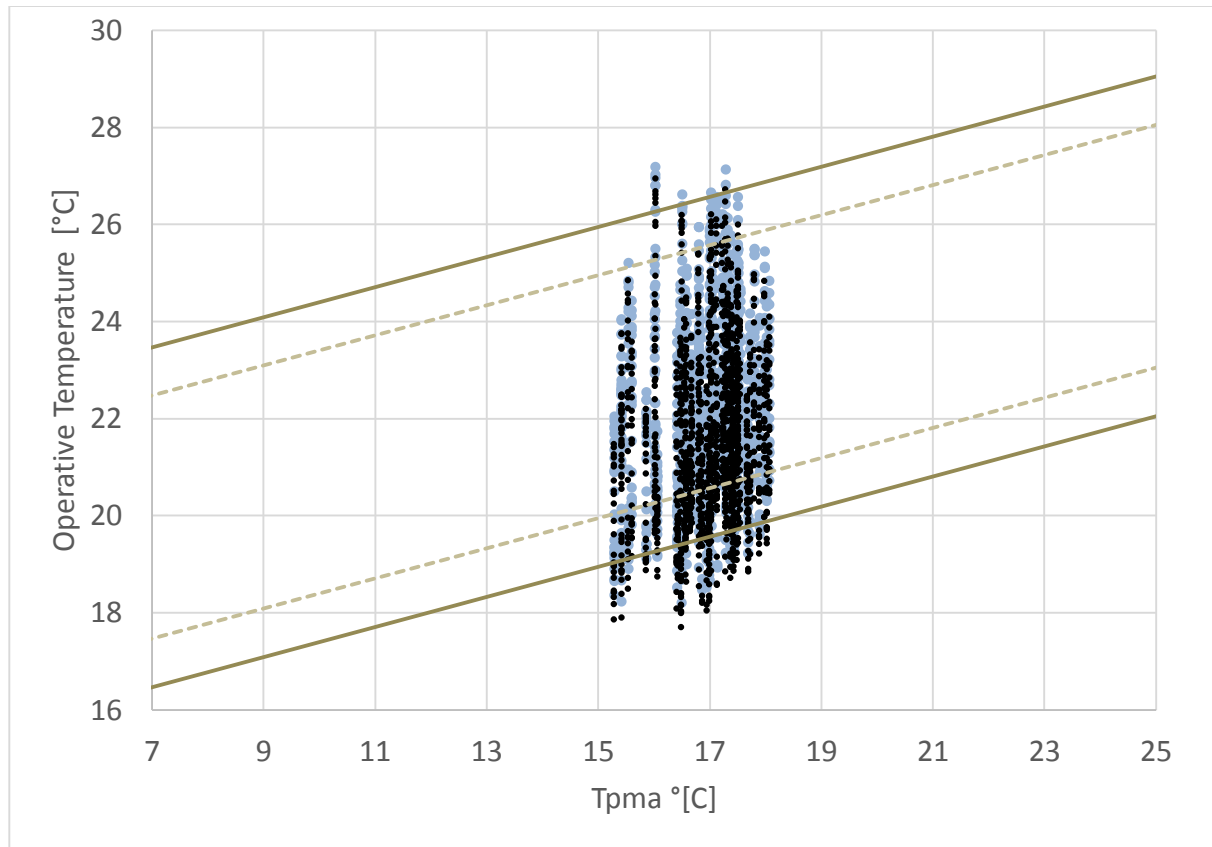


**Figure 45:** A comfort chart of operative temperatures under typical conditions (blue) and with a venture-shaped cap on the chimney (black).

While venturi shapes installed on roofs has been shown to work in industrial applications, it is not necessary in this case study and the decision to not install any cap on the chimney was justified. As the chimney cap only increases air flow while wind is blowing, this increased air flow accounts for very little in temperature reduction. Wind speeds are considerably lower at the lower altitudes of houses as opposed to atop tall buildings. Furthermore, the effects of a chimney cap may come at the cost of potentially reduced solar

gains in the chimney which could reduce the effect of thermal buoyancy, as well as cause poor aesthetics.

## **6.9. Comfort conditions in the bedroom**

This research focused on the comfort in the main living areas of the house; however, the comfort in the bedrooms is equally important as it is where the occupants spend the entire night as well as perhaps some other hours of the day. While the occupants never expressed any dissatisfaction with the interior conditions, it can be seen in

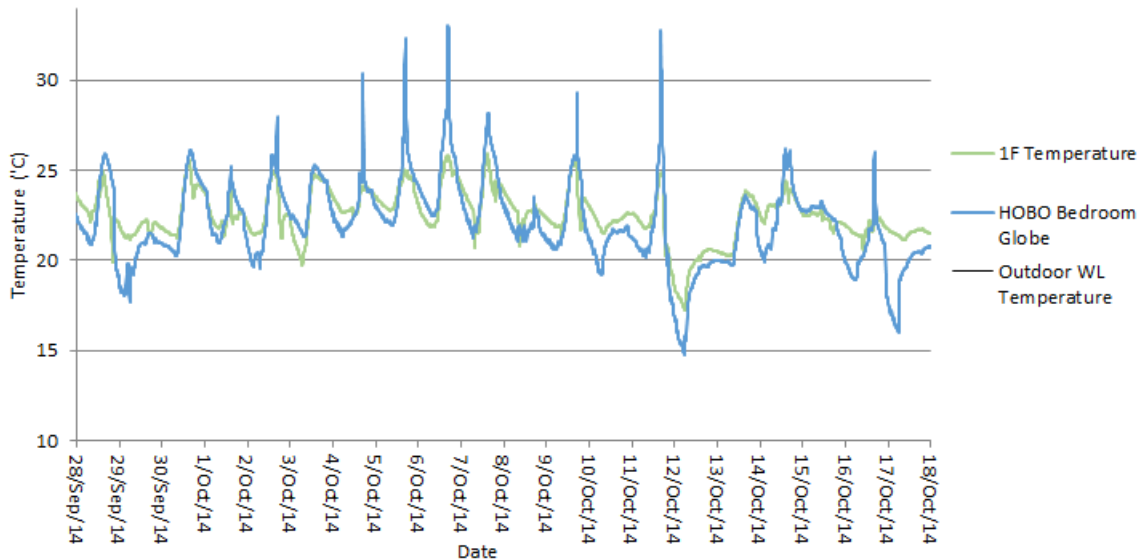
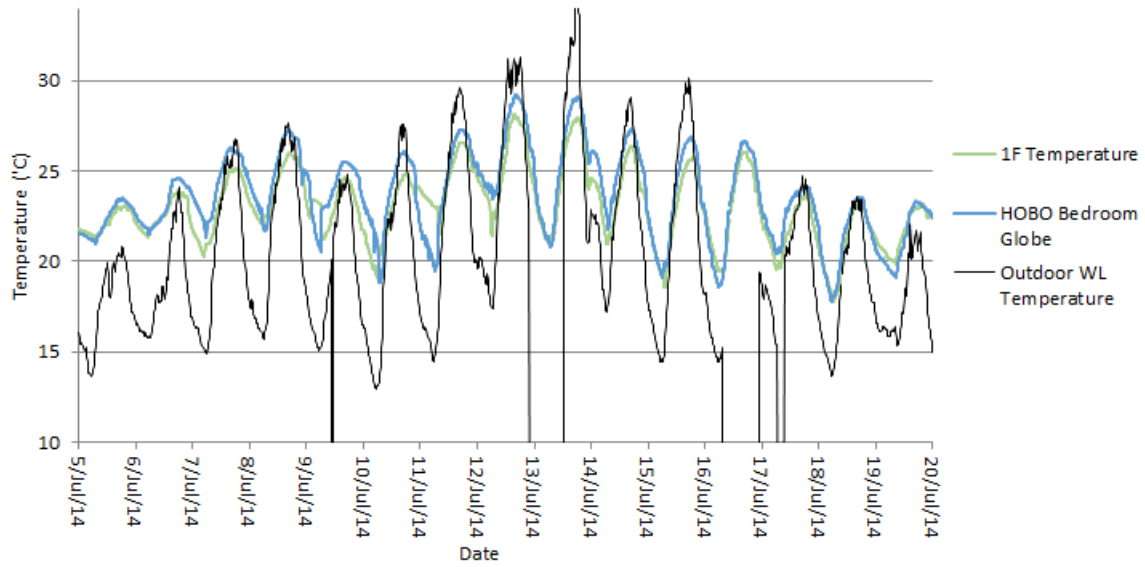
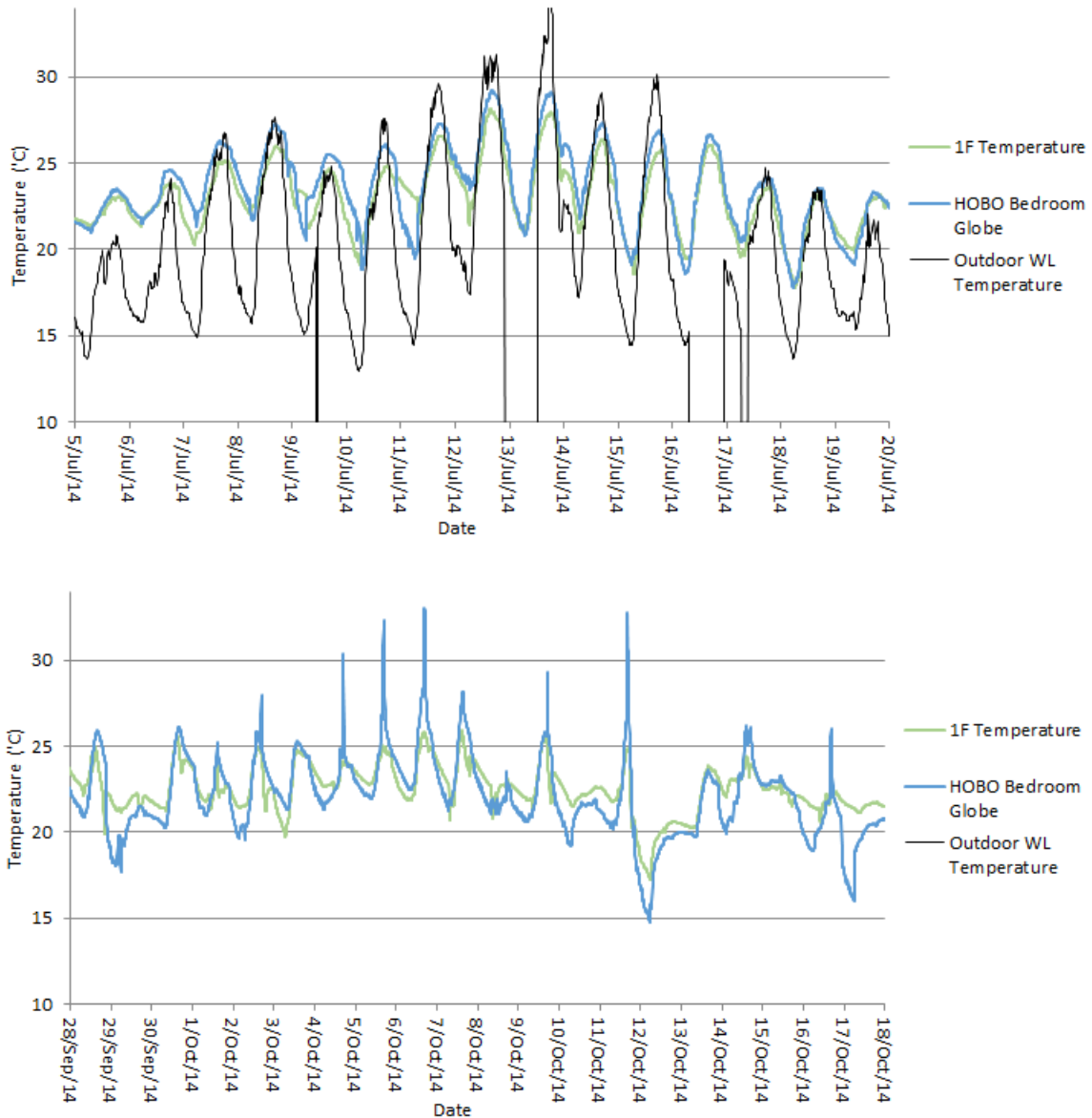
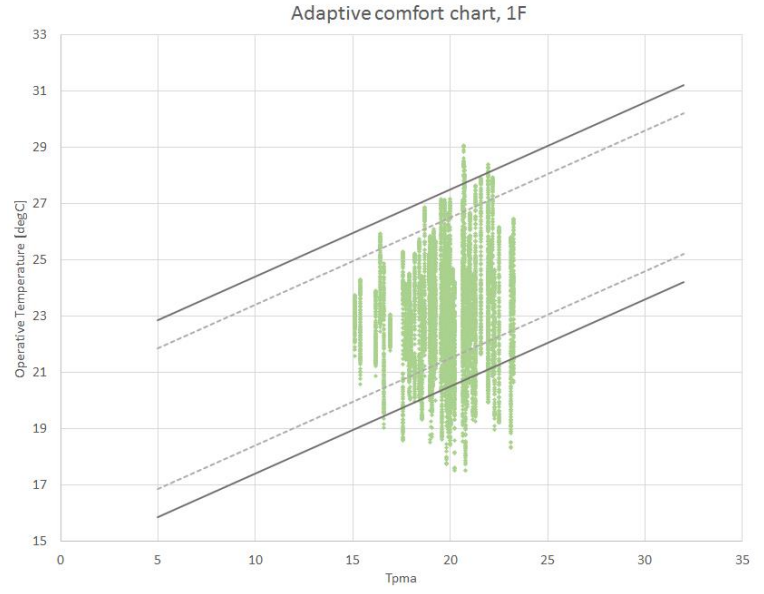
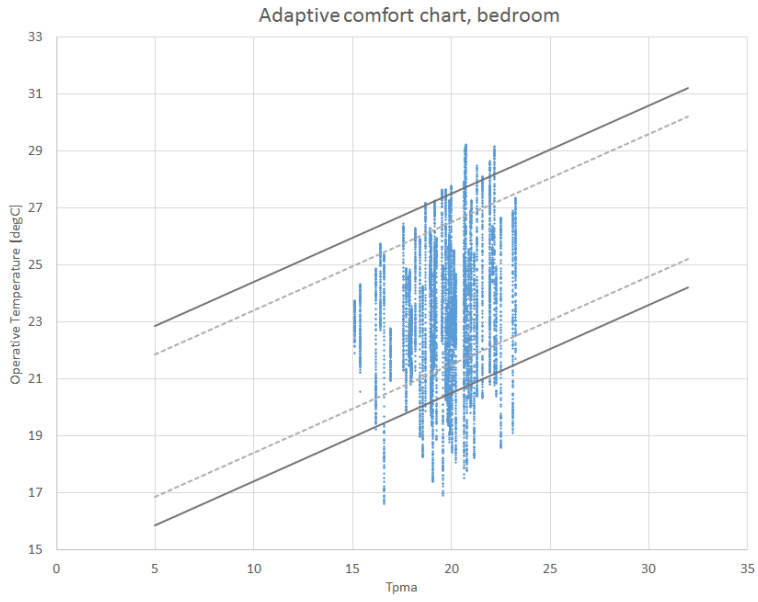


Figure 46a that the operative temperature in the bedroom remained relatively similar to the conditions seen at the living areas of the atrium. While this was true for most of the period recorded, later in the year the bedroom was shown to overheat as well as get quite cold overnight (Figure 46b). This could be due to some windows left open as the occupants were away, as even in this time the occupants expressed no discomfort.



**Figure 46: Operative temperatures of the bedroom (top, a) and the first floor of the atrium (bottom, b). Note that there is no data for the outdoor temperature in the graph on the bottom.**

The adaptive thermal comfort of the bedroom showed generally comparable conditions as the atrium (Figure 47); however, there are some other areas outside of the adaptive thermal comfort zones. Again, these can be explained as times when the occupants were comfortable despite these cooler and warmer conditions, or they are times when the house or bedroom was unoccupied.



**Figure 47: Adaptive thermal comfort of the bedroom (left, a) and the first floor of the atrium (right, b).**

## 7. CONCLUSIONS

This thesis has presented a systematic study on the Harmony House and its characteristics and construction that allow it to sustain exceptional thermal comfort without any mechanical cooling, despite uncomfortable outdoor conditions. The extent of this research was focused on the moderate climate of the Pacific Northwest during late spring to early fall. As made clearly evident in the introduction, there is a great need to reduce global energy consumption as the vast majority of energy is generated from sources that produce much carbon dioxide. The movement towards greener sources of energy is necessary amongst all industries, including in the building sector and residential housing.

To help achieve the net-zero energy goal targeted by the Harmony House, it was designed to be passively cooled exclusively by natural ventilation during the summer months and shoulder seasons, while using minimal energy for heating in the winter. The conditions throughout the summer and fall were monitored, providing data to assess the indoor temperature and air speeds. The data was further used to construct the whole-building and CFD models to assess the ventilation and cooling capability possible by the house.

The monitoring of the house revealed the architect's design was highly successful in maintaining comfortable indoor temperatures without mechanical cooling during the timeframe that was recorded, especially during typical summer conditions when the outdoor temperature was not excessively hot. The goal was achieved through a combination of good architectural design principles and strategies, including the integrated approach using thermal mass and natural ventilation to keep interior temperatures comfortable. Temperature readings in the living areas rarely fell outside acceptable comfort conditions defined for adaptive thermal comfort. Despite times when the temperature was outside these boundaries, the occupants never reported

discomfort at any time. Had they felt discomfort, they could have certainly taken action to increase the temperature during these times. The air speeds measured suggested there was good air movement and ventilation, as they were placed along a direct air flow path between the main inlets and outlets. Air speeds also remained low and rarely surpassed  $0.2\text{ m/s}$  in occupied areas. Only measurements at the outlet occasionally measured at values as high as  $0.6\text{ m/s}$ ; however, these points were of no concern as the area cannot be said to ever be occupied. One of the greatest accomplishments of the house was the induced formation of thermal stratification within the main atrium. This was an excellent design choice by the architect as it allowed warm air to rise, carrying much of the thermal energy out of the house. The induced pressure differential at the lower levels of the atrium caused cool air to come in through the lower windows, which was the main source of cooling in the house.

To visualize and assess the mechanisms of natural ventilation in the house, computer simulations can help considerably. A detailed model requires large amounts of accurate inputs, so in the models developed, the more significant inputs were given a greater focus. Many inputs were obtained during the literature review as previous work has provided evidence that energy modeling software and CFD has accurately predicted conditions in many other different, though comparable, scenarios. One focus that required greater investigation was on the windows that most facilitated the ventilation into and out of the house, as there have been few studies on the discharge coefficient for awning windows or angled large skylights. The coefficients for these particular windows were determined using CFD supplemented with what previous work was available, though not applicable to use directly. CFD was used in place of planned physical models and experiments for reasons out of the researcher's control. The results of these simulations were definite values of the discharge coefficients of the windows for varying

opening angles and configurations. Obtaining these for use in the whole-building energy model allowed more accurate representations of flow rates and induced cooling.

The energy modeling was able to accurately represent the conditions recorded on site, which allowed the extrapolation of how the house would perform under other scenarios and with the use of more natural-ventilation-promoting strategies. Using the modeling software, it was demonstrated that the planned use of the Aerocap to enhance air flow driven by wind was not necessary and the decision to omit it from the construction was sound. The conditions directly compared were the air and operative temperatures at various locations and heights in the house, and the air speeds at strategically determined locations, given the limited available resources. Temperature stratification was most accurate during the peaks of the days while some deviations were observed during the night. This was likely due to the difficulty in determining the effect of thermal mass in the house. Air speeds were generally comparable though the CFD analysis was steady-state and the recorded conditions fluctuated rapidly, as expected with variable wind conditions. Still, the wind speeds in the CFD model were in good agreement with the average wind speeds recorded. This was the case for all scenarios tested, which included a range of common summer temperatures in the local climate as well as a variation of the most common wind speeds.

## 8. LIMITATIONS AND FURTHER WORK

The research uncovered many limitations inherent of on-site measurements needed for the validation of the dynamic thermal and CFD models. A further developed methodology to address these limitations will allow better assessment of a house designed to incorporate natural ventilation. Further work is recommended in the following areas:

- The study focused on the living areas of the house, mainly in the main atrium; however, maintaining thermal comfort in the bedrooms at night is equally important. Data was collected over the same period of time, in the master bedroom. Data recorded includes air temperature, operative temperature, and relative humidity. The analysis of the data, in conjunction with the atrium data could be used to investigate the comfort in the bedroom at all times. Suffice to say that from the questionnaires, the owners always expressed thermal satisfaction while sleeping.
- The characterizations of air flow through the openings was modeled using CFD. A small indoor test structure was planned to recreate air flows through the openings and validate CFD component models. A window and a skylight has already been supplied by the companies which supplied those installed in the Harmony House. These may be used to validate the CFD findings once the test shed is approved for construction.
- Coefficients of pressure ( $C_p$ ) on ventilation-enhancing technologies were obtained from literature. CFD models may be built and calibrated to obtain these coefficients when situated on the structure they are meant to be considered for. Inputting these

- coefficients into the dynamic thermal models may allow for higher accuracy of results. Small-scale tests may validate the CFD models. Once validated the technologies can be further optimized according to their placement and surroundings.
- Improved methods need to be investigated to harmonize the coupling between the unrepeatable on-site measurements, thermal models, and CFD models. This may include direct inputs from weather data into the models and more accurate scheduling applied to windows and doors.
  - To improve the reliability of natural ventilation designs, methods need to be investigated to address the uncertainty inherent to the wind and thermal forces driving natural ventilation.
  - Only two additional ventilation strategies, the Aerocap and the venturi-shaped cap, were tested using the dynamic thermal energy simulation. The testing of other technologies or shaped-caps could further be investigated for their cooling potentials.
  - Methods of measurement should be improved to include more sensors while remaining invisible to the building occupants. This is necessary because there were many assumptions that had to be made in describing the characteristics of the air flow and the environment in the house. Increased reliability is also important to reduce the amount of missing data from on-site recordings allowing this data to entirely replace weather files, creating more accurate simulations.
  - As some weather data obtained on site proved to be unreliable, it could be beneficial to include the data obtained from other weather stations or local airport data.

- While the house was highly successful at keeping the relative humidity in the house around 50%-60%, there is no data to analyze how the comfort in the house is affected at excessively low or high humidities.
- Thermal mass can be difficult to predict in a constructed house, even if documentation of materials used is available. The thermal mass in a house can potentially change air flows and temperatures inside drastically, and thus, as much knowledge as possible should be known, to help assess the conditions within house by both monitoring, and modeling.

## REFERENCES

- Agilent Technologies. (2012). Agilent 34970A Data Acquisition/Switch Unit Family.
- Allard, F., Bienfait, D., Haghghat, F., Liebecq, G., van der Maas, K., Pelletret, R., . . . Walker, R. (1992). *Air flow through large openings in buildings*. International Energy Agency, Annex 20: Air Flow Patterns within Buildings.
- Allocca, C., Chen, Q., & Glicksman, L. R. (2003). Design analysis of single-sided natural ventilation. *Energy and Buildings* 35, 785-795.
- ASHRAE. (2009). Climatic Design Information. In *ASHRAE -- Fundamentals*.
- ASHRAE. (2013). *Standard 90.1: Energy Standard for Buildings Except Low-Rise Residential Buildings*. Atlanta, GA: ASHRAE.
- ASHRAE. (n.d.). *ANSI/ASHRAE Standard 55-2013: Thermal Environmental Conditions for Human Occupancy*. Atlanta, GA: American Society for Heating, Refriger., and Air Conditioning Eng. Inc.
- Awbi, H. (2003). *Ventilation of Buildings, Second Edition*. New York City: Spon Press.
- Aynsley, R. (2007). *Natural Ventilation in Passive Design*. BEDP Environmental Design Guide.
- Balaras, C. (1996). The role of thermal mass on the cooling load of buildings. An overview of computational methods. *Energy and Buildings* 24, 1-10.
- Bansal, N. K., Mathur, R., & Bhandari, M. S. (1994). A Study of Solar Chimney Assisted Wind Tower System for Natural Ventilation in Buildings. *Building and Environment* 29.4, 495-500.
- Bassiouny, R., & Koura, N. S. (2008). An analytical and numerical study of solar chimney use for room natural ventilation. *Energy and Buildings* 40, 865-873.
- Brager, G., & de Dear, R. (2000). A Standard for Natural Ventilation. *ASHRAE Journal*.
- Cable, M. (2009). *An Evaluation of Turbulence Models for the Numerical Study of Forced and Natural Convective Flow in Atria*. Kingston, Ontario.
- Campbell Scientific, Inc. (2015). BlackGlobe Temperature Sensor for Heat Stress.
- Canada Mortgage and Housing Corporation. (n.d.). *Harmony House*. Retrieved 10 14, 2015, from <https://www.cmhc-schl.gc.ca/en/inpr/su/eqho/haho/index.cfm>

- Chen, Q. (1995). Comparison of Different k-e Models for Indoor Air Flow Computations. *Numerical Heat Transfer, Part B: Fundamentals: An International Journal of Computation and Methodology*, 353-369.
- Chen, Q. (2004). Using computational tools to factor wind into architectural environment design. *Energy and Buildings* 36, 1197-1209.
- Chen, Q. (2009). Ventilation performance prediction for buildings: A method overview and recent applications. *Building and Environment* 44, 848-858.
- Cheng-Hu, H., Kurabuchi, T., & Ohba, M. (2005). Numerical Study of Cross-Ventilation Using Two-Equation RANS Turbulence Models. *International Journal of Ventilation* 4.2, 123-132.
- Coley, D. A. (2008). Representing Top-hung Windows in Thermal Models. *International Journal of Ventilation* 7.2, 151-158.
- Cook, M. J., Ji, Y., & Hunt, G. R. (2003). CFD Modelling of Natural Ventilation: Combined Wind and Buoyancy Forces. *International Journal of Ventilation* 1.3, 167-179.
- Cooper, P., & Linden, P. F. (1992). Multiple Sources of Buoyancy in a Naturally Ventilated Enclosure. *11th Australasian Fluid Mechanics Conference*, (pp. 351-354). Hobart, Australia.
- CRADLE-CFD. (n.d.). *Products and Services, scSTREAM*. Retrieved 01 12, 2016, from Software Cradle Co. Ltd.: <http://www.cradle-cfd.com/products/scstream/index.html>
- de Dear, R. J., & Brager, G. S. (1998). Developing an Adaptive Model of Thermal Comfort and Preference. *ASHRAE Transactions Vol 104 Part 1*.
- de Dear, R., & Brager, G. (2002). Thermal comfort in naturally ventilated buildings: revisions to ASHRAE Standard 55. *ASHRAE Journal*.
- DesignBuilder Software Ltd. (2015). DesignBuilder EnergyPlus Simulation Documentation for DesignBuilder v4.5.
- Ding, W., Hasemi, Y., & Yamada, T. (2005). Natural ventilation performance of a double-skin facade with a solar chimney. *Energy and Buildings* 37, 411-418.
- Dwyer. (2015). Series MS Magnesense Differential Pressure Transmitter.
- Emmerich, S. J. (2001). Validation of Multizone IAQ Modeling of Residential-Scale Buildings: A Review. *Transactions - ASHRAE* 107(2), 619-628.

- Environment Canada. (2015). Canadian Climate Normals 1981-2010. Environment Canada. Retrieved November 2015, from [http://climate.weather.gc.ca/climate\\_normals/index\\_e.html](http://climate.weather.gc.ca/climate_normals/index_e.html)
- Ernest, D. R., Bauman, F. S., & Arens, E. A. (1991). The prediction of indoor air motion for occupant cooling in naturally ventilated buildings. *ASHRAE Transactions* 97, 539-552.
- European Committee for Standardization. (n.d.). *EN 15251*.
- Evola, G., & Popov, V. (2006). Computational analysis of wind driven natural ventilation in buildings. *Energy and Buildings* 38, 491-501.
- Fabi, V., Andersen, R. V., Corgnati, S., & Olesen, B. W. (2012). Occupants' window opening behaviour: A literature review of factors influencing occupant behaviour and models. *Building and Environment* 58, 188-198.
- Fanger, P. O. (1970). *Thermal comfort. Analysis and applications in environmental engineering*. McGraw-Hill Inc.
- Flourentzou, F., Van der Maas, J., & Roulet, C. A. (1998). Natural ventilation for passive cooling: measurement of discharge coefficients. *Energy and Buildings* 27, 283-292.
- Gagliano, A., Patania, F., Nocera, F., & Signorello, C. (2014). Assessment of the dynamic thermal performance of massive buildings. *Energy and Buildings* 72, 361-370.
- Gan, G. (2010). Interaction Between Wind and Buoyancy Effects in Natural Ventilation of Buildings. *The Open Construction and Building Technology Journal*, 134-145.
- Gregory, K., Moghtaderi, B., Sugo, H., & Page, A. (2007). Effect of thermal mass on the thermal performance of various Australian residential construction systems. *Energy and Buildings* 40, 459-465.
- Grosso, M. (1991). Wind pressure distribution around buildings: a parametrical model. *Energy and Buildings* 18, 101-131.
- Hassan, A. S., & Ramli, M. (2010). Natural Ventilation of Indoor Air Temperature: A Case Study of the Traditional Malay House in Penang. *American Journal of Engineering and Applied Sciences* 3.3, 521-528.
- Heiselberg, P. (2002). *Principles of hybrid ventilation, Hybrid ventilation center, Annex 35 IEA ECB BCS Hybrid ventilation*.
- Heiselberg, P., Bjorn, E., & Nielsen, P. V. (2002). Impact of Open Windows on Room Air Flow and Thermal Comfort. *International Journal of Ventilation*, 91-100.

- Heiselberg, P., Svidt, K., & Nielsen, P. V. (2001). Characteristics of airflow from open windows. *Building and Environment* 36, 859-869.
- Hooff, T., Blocken, B., Aanen, L., & Bronsema, B. (2011). A venturi-shaped roof for wind-induced natural ventilation of buildings: Wind tunnel and CFD evaluation of different design configurations. *Building and Environment* 46, 1797-1807.
- Hult, E. L., Iaccarino, G., & Fischer, M. (2012). Using CFD Simulations to Improve the Modeling of Window Discharge Coefficients. *SimBuild, Madison*.
- Humphreys, M. (1977). The optimum diameter for a globe thermometer for use indoors. *Annals of Occupational Hygiene* 20.2, 135-140.
- Humphreys, M., Nicol, F., & Roaf, S. (2015). *Adaptive Thermal Comfort: Foundations and Analysis*. Routledge .
- Hunt, G. R., & Linden, P. F. (1999). The fluid mechanics of natural ventilation - displacement ventilation by buoyancy-driven flows assisted by wind. *Building and Environment* 34, 707-720.
- Iba, C., Hokoi, S., Ogura, D., & Ito, S. (2013). Thermal environment in detached houses with atrium: Towards proper utilization of atrium space in traditional dwellings "Kyo-machiya". *2nd Central European Symposium on Building Physics*. Vienna, Austria.
- Integrated Environmental Solutions Limited. (2007). MacroFlo Calculation Methods <Virtual Environment> 6.0.
- International Energy Agency; Energy Conservation in Buildings and Community Systems. (2002). *Impact of the uncertainties on wind pressures on the prediction of thermal comfort performances*. Brussels: IEA ECBCS Annex 35.
- IPCC, Intergovernmental Panel on Climate Change. (2013). *The physical science basis report 2013*. Working Group I Contribution to the Fifth Assessment Report of the Intergovernmental Panel on Climate Change.
- Iqbal, A., Afshari, A., Wigo, H., & Heiselberg, P. (2015). Discharge coefficient of centre-pivot roof windows. *Building and Environment* 92, 635-643.
- Iqbal, A., Nielsen, P. V., Afshari, A., & Heiselberg, P. (2012). Numerical predictions of the discharge coefficient of a window with moveable flap. *Healthy Buildings 2012*.
- Jiang, Y., & Chen, Q. (2002). Effect of fluctuating wind direction on cross natural ventilation in buildings from large eddy simulations. *Building and the Environment*, 37, 379-386.

- Karava, P. (2008). *Airflow Prediction in Buildings for Natural Ventilation Design: Wind Tunnel Measurements and Simulation*. Montreal.
- Karava, P., Stathopoulos, T., & Athientis, A. K. (2004). Wind Driven Flow through Openings - A Review of Discharge Coefficients. *International Journal of Ventilation*, 255-266.
- Katayama, T., Tsutsumi, J., & Ishii, A. (1992). Full-scale measurements and wind tunnel tests on cross-ventilation. *Journal of Wind Engineering and Industrial Aerodynamics*, 2553-2562.
- Kato, S., Murakami, S., Mochida, A., Akabayashi, S.-i., & Tominaga, Y. (1992). Velocity-pressure field of cross ventilation with open window analyzed by wind tunnel and numerical simulation. *Journal of Wind Engineering and Industrial Aerodynamics* 41-44, 2575-2586.
- Khan, N., Su, Y., & Riffat, S. B. (2008). A review on wind driven ventilation technologies. *Energy and Buildings* 40, 1586-1604.
- Khanal, R., & Lei, C. (2011). Solar Chimney - A passive strategy for natural ventilation. *Energy and Buildings* 43, 1811-1819.
- Kim, J., & de Dear, R. (2012). Impact of different building modes on occupant expectaitons of the main IEQ factors. *Building and Environment*.
- Klock, R., & Mullock, J. (2001). *The weather of British Columbia, Graphic area forecast 31 pacific region*. NAC Canada.
- Kobayashi, T., Sandberg, M., Kotani, H., & Claesson, L. (2010). Experimental investigation and CFD analysis of cross-ventilated flow through single room detached house model. *Buildings and Environment* 45, 2723-2734.
- Kollmuss, A., & Agyeman, J. (2002). Mind the Gap: why do people act environmentally and what are the barriers to pro-environmental behaviour? *Environmental Education Research, Vol. 8, No. 3*.
- Kosny, J., Petrie, T., Gawin, D., Childs, P., Desjarlais, A., & Christian, J. (2001). Energy Benefits of Application of Massive Walls in Residential Buildings. *Thermal Envelopes VIII*.
- Li, Y., & Delsante, A. (2001). Natural ventilation by combined wind and thermal forces. *Building and Environment* 36, 59-71.
- Linden, P. F. (1999). The Fluid Mechanics of Natural Ventilation. *Annu. Rev. Fluid Mech.*, 201-238.

- Lo, J., & Novoselac, A. (2011). CFD Simulation of Cross-Ventilation Using Fluctuating Pressure Boundary Conditions. *ASHRAE Transactions 117.1*.
- Loonen, P., Hoes, P., & Hensen, J. (2014). Performance prediction of buildings with responsive building elements: challenges and solutions. *IBPSA-England conference on Building Simulation and Optimization*. London: BSO14.
- Ma, P., & Lin-Shu, W. (2012). Effective Heat Capacity of Interior Planar Thermal Mass (iPTM). *Energy and Buildings 47*, 44-52.
- Mathur, J., & Mathur, S. (2006). Experimental investigation on four different types of solar chimneys. *Advances in Energy Research 12*, 151-156.
- Menchaca Brandan, M. A. (2012). *Study of Airflow and Thermal Stratification in Naturally Ventilated Rooms*. Cambridge, MA: Massachusetts Institute of Technology.
- Nicol, F., & Humphreys, M. (2010). Derivation of the adaptive equations for thermal comfort in free-running buildings in European standard EN15251. *Buildings and Environment 45*, 11-17.
- Nicol, F., Humphreys, M., & Roaf, S. (2012). *Adaptive Thermal Comfort: Principles and Practice*. Abingdon, UK: Routledge.
- Nielsen, P. V. (2004). Computational fluid dynamics and room air movement. *Indoor Air 14*.
- Nitatwichit, C., Khunatorn, Y., & Tippyawong, N. (2008). Investigation and characterization of cross ventilating flows through openings in a school classroom. *Journal of the Chinese Institute of Engineers, Vol. 31*, 587-603.
- Oke, T. (1988). Street design and urban canopy layer climate. *Energy and Buildings 11*, 103-113.
- Olsen, E. L., & Chen, Q. (2003). Energy consumption and comfort analysis for different low-energy cooling systems in a mild climate. *Energy and Buildings 35*, 560-571.
- onset HOBO Data Loggers. (2013). TMCx-HD Water/Soil Temperature Sensor.
- onset HOBO Data Loggers. (2015). HOBO U12 Logger, Multi-channel energy & environmental monitoring.
- onset HOBO Data Loggers. (2015). HOBO UX90 Loggers.
- Perez-Lombard, L., Ortiz, J., & Pout, C. (2008). A review on buildings energy consumption information. *Energy and Buildings 40*, 394-398.

- Pimentel, D., Rodrigues, G., Wang, T., Abrams, R., Goldberg, K., Staecker, H., . . . Boerke, S. (1994). Renewable Energy: Economic and Environmental Issues. *Bioscience, Vol. 44*, 536-547.
- Posner, J. D., Buchanan, C. R., & Dunn-Rankin, D. (2003). Measurement and Prediction of Indoor Air in a Model Room. *Energy and Buildings 35*, 515-526.
- Prestandard prEN 15242. (2005). Ventilation for buildings - Calculation methods for the determination of air flow rates in buildings including infiltration.
- Retrotec. (2015). Blower Door Operation Manual.
- Roetzel, A., Tsangrassoulis, A., Dietrich, U., & Busching, S. (2010). A review of occupant control on natural ventilation. *Renewable and Sustainable Energy Reviews 14*, 1001-1013.
- Russell, M., Sherman, M., & Rudd, A. (2005). Review of Residential Ventilation Technologies. *HVAC&R Research*.
- Saito, T., Kuno, S., Ota, S., & Mimura, M. (2014). The effect of natural ventilation on physiological and psychological responses to the indoor thermal environment of Japanese housing. *The 13th International Conference on Indoor Air Quality and Climate*. Hong Kong.
- Sandberg, M. (2004). An Alternate View on the Theory of Cross-Ventilation. *International Journal of Ventilation Volume 2 No 4*, 409-418.
- Santamouris, M. (2007). *Advances in Passive Cooling*. London, UK: Routledge.
- Santamouris, M. (2013). *Energy and climate in the urban built environment*. Routledge.
- Sawachi, T., Narita, K.-i., Kiyota, N., Seto, H., Nishizawa, S., & Ishikawa, Y. (2004). Wind Pressure and Air Flow in a Full-Scale Building Model under Cross Ventilation. *International Journal of Ventilation Volume 2 No. 4*, 343-357.
- Seifert, J., Li, Y., & Axley, J. (2006). Calculation of wind-driven cross ventilation in buildings with large openings. *Journal of Wind Engineering and Industrial Aerodynamics 94.12*, 925-947.
- Sherman, M. H., & Matson, N. E. (2002). Air tightness of new U.S. houses: A preliminary report. *Lawrence Berkeley National Laboratory, LBNL-48671*.
- Spencer, J., & Zhai, Z. (2007). Fast Evaluation of Sustainable Heating and Cooling Strategies for Solar Homes with Integrated Energy and CFD Modeling. *Building Simulation 2007*, (pp. 1677-1683).

- Spengler, J. D., & Chen, Q. (2000). Indoor Air Quality Factors in Designing a Healthy Building. *Review of Energy and the Environment* 25, 567-600.
- Stern, F., Wilson, R. V., Coleman, H. W., & Paterson, E. G. (1999). *Verification and Validation of CFD Simulations*. Iowa Institute of Hydraulic Research, Huntsville.
- Straw, M., Baker, C., & Robertson, A. (2000). Experimental measurements and computations of the wind-induced ventilation of a cubic structure. *Journal of Wind Engineering and Industrial Aerodynamics* 88, 213-230.
- Sustainability Television. (n.d.). Harmony House Series: Episode 12, Natural Ventilation. Retrieved 01 15, 2016, from <https://www.sustainabilitytelevision.com/video-series/harmony-house-series>
- Takizawa, M., Kurabuchi, T., & Ohba, M. (2014). Research of the Ventilation Performance Prediction of a House. *Indoor Air*.
- Tan, G., & Glicksman, L. R. (2005). Application of integrating multi-zone model with CFD simulation to natural ventilation prediction. *Energy and Buildings* 37, 1049-1057.
- Tantasavasdi, C., Srebric, J., & Chen, Q. (2001). Natural ventilation design for houses in Thailand. *Energy and Buildings* 33, 815-824.
- Tantasavasdi, C., Srebric, J., & Chen, Q. (2001). Natural ventilation design for houses in Thailand. *Energy and Buildings* 33, 815-824.
- Teclé, A., Bitsuamlak, G. T., & Teshome, J. E. (2013). Wind-driven natural ventilation in a low-rise building: A Boundary Layer Wind Tunnel Study. *Building and Environment* 59, 275-289.
- The Department of the Environment, Transport, and the Regions. (1998). *Natural ventilation in non-domestic buildings*. London.
- Tominaga, Y., Mochida, A., Murakami, S., & Sawaki, S. (2008). Comparison of various k-ε models and LES applied to flow around a high-rise building model with 1:1:2 shape placed within the surface boundary layer. *Journal of Wind Engineering and Industrial Aerodynamics* 96, 389-411.
- True, J. J., Sandberg, M., Heiselberg, P., & Nielsen, P. V. (2003). Cross Ventilation Analysed as a Wind Catchment Phenomena.
- TSI Inc. (2012). Air Velocity Transducers Models 8455, 8465, AND 8475.
- Tzikopoulos, A., Karatza, M., & Paravantis, J. (2005). Modeling energy efficiency of bioclimatic buildings. *Emergy and Buildings* 37, 529-544.

- U.S. Energy Information Administration. (2015). *Annual Energy Outlook 2015 with projections to 2040*. Washington: Office of Integrated and International Energy Analysis, U.S. Department of Energy.
- V.Geros, M.Santamouris, N.Papanikolaou, & G.Guarracino. (2001). Night ventilation in urban environment. *22nd Annual AIVC Conference, Market Opportunities for Advanced Ventilation Technology*. Bath, UK.
- van den Engel, P., Kemperman, R., & Doolaard, H. (2012). Natural and hybrid ventilation principles based on buoyancy, sun and wind. *HVAC Journal*.
- van Hooff, T., Blocken, B., Aanen, L., & Bronsema, B. (2011). A venturi-shaped roof for wind-induced natural ventilation of buildings: Wind tunnel and CFD evaluation of different design configurations. *Buildings and Environment* 46, 1797-1807.
- Wang, L., & Chen, Q. (2007). Theoretical and Numerical Studies of Coupling Multizone and CFD Models for Building Air Distribution Simulations. *Indoor Air* 17, 348-361.
- Wang, L., & Chen, Q. (2007). Validation of a Coupled Multizone-CFD Program for Building Airflow and Contaminant Transport Simulations. *HVAC&R Research Vol. 13, No. 2*.
- Wang, L., & Chen, Q. (2008). Evaluation of some assumptions used in multizone airflow network models. *Building and Environment* 43, 1671-1677.
- Yam, J., Li, Y., & Zheng, Z. (2003). Nonlinear coupling between thermal mass and natural ventilation in buildings. *International Journal of Heat and Mass Transfer* 46, 1251-1264.
- Yang, C., Shi, H., Yang, X., & Zhao, B. (2010). Research on Flow Resistance Characteristics with Different Window/Door Opening Angles. *HVAC&R Research*.
- Zhai, Z., Zhang, Z., Zhang, W., & Chen, Q. (2007). Evaluation of Various Turbulence Models in Predicting Airflow and Turbulence in Enclosed Environments by CFD: Part-1: Summary of Prevalent Turbulence Models. *HVAC&R Research*, 13.6.

## APPENDIX A – Floor plan and sensor location

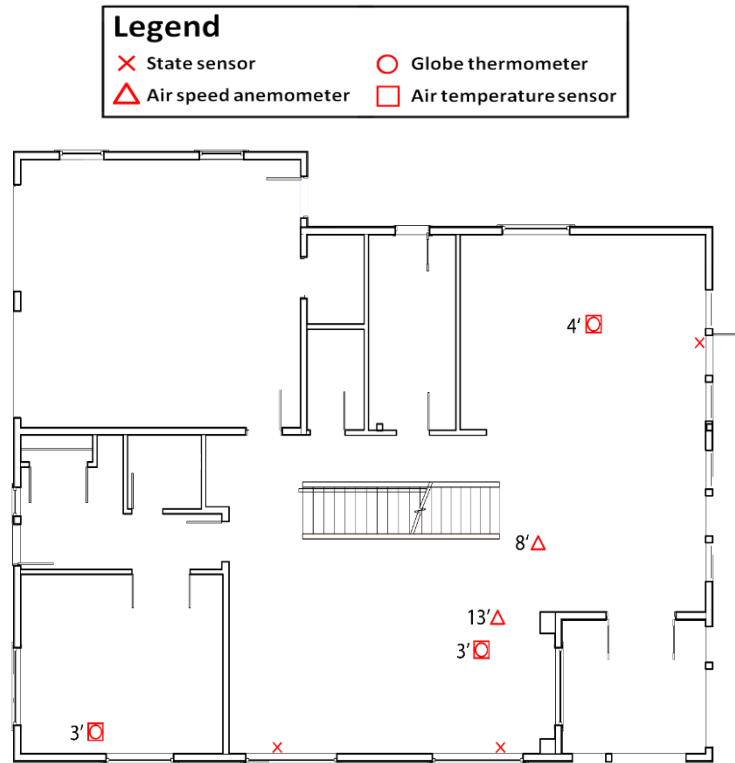


**Figure 48: Main floor of the Harmony House. This area consists of six temperature sensors, two air-speed sensors, and three state sensors. Numbers beside sensor symbols indicate their approximate height, in feet, above the floor level.**

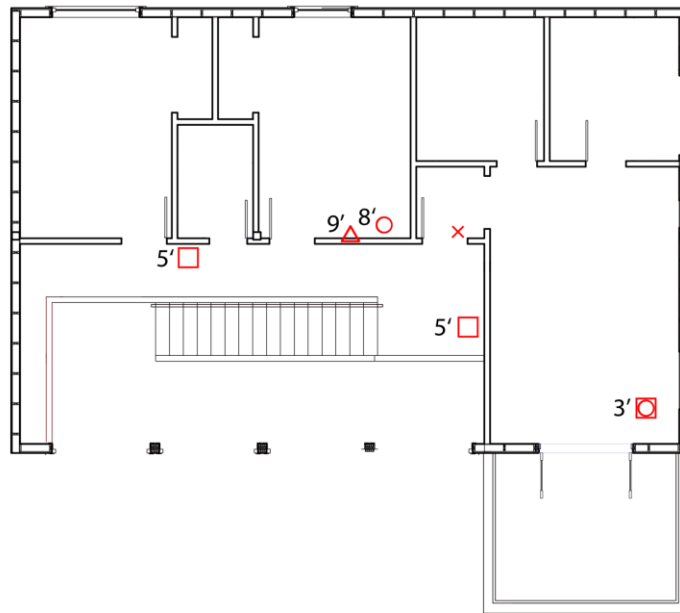


**Figure 49: Upper floor of the Harmony House. This area consists of five temperature sensors, one air-speed sensor, and one state sensor.**

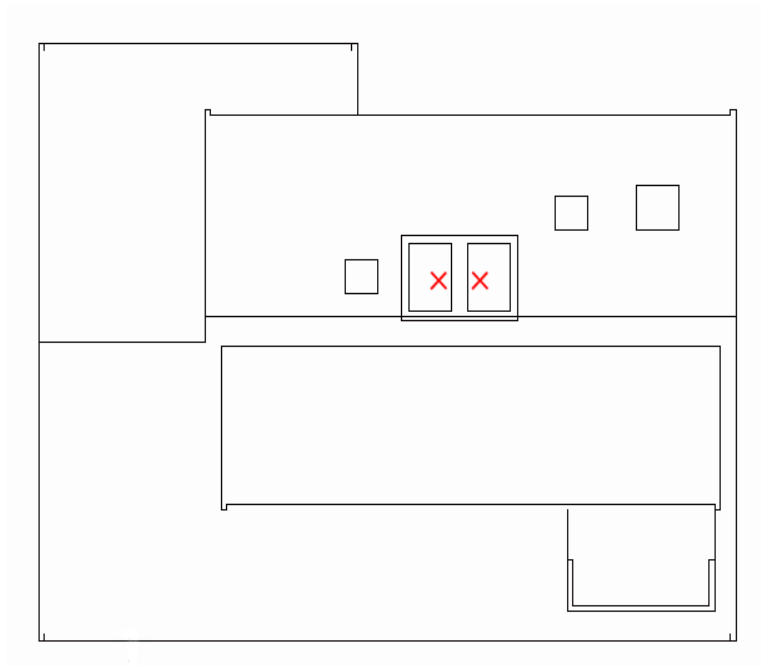
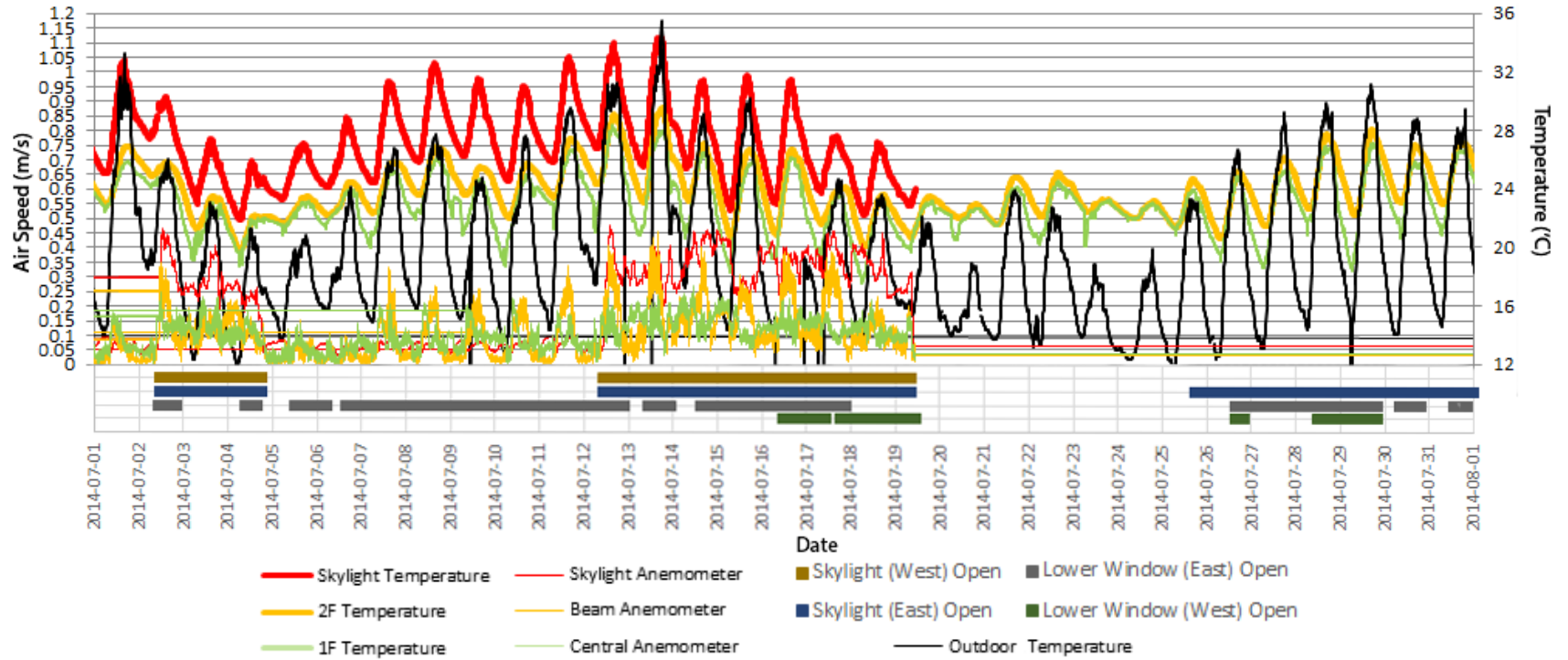


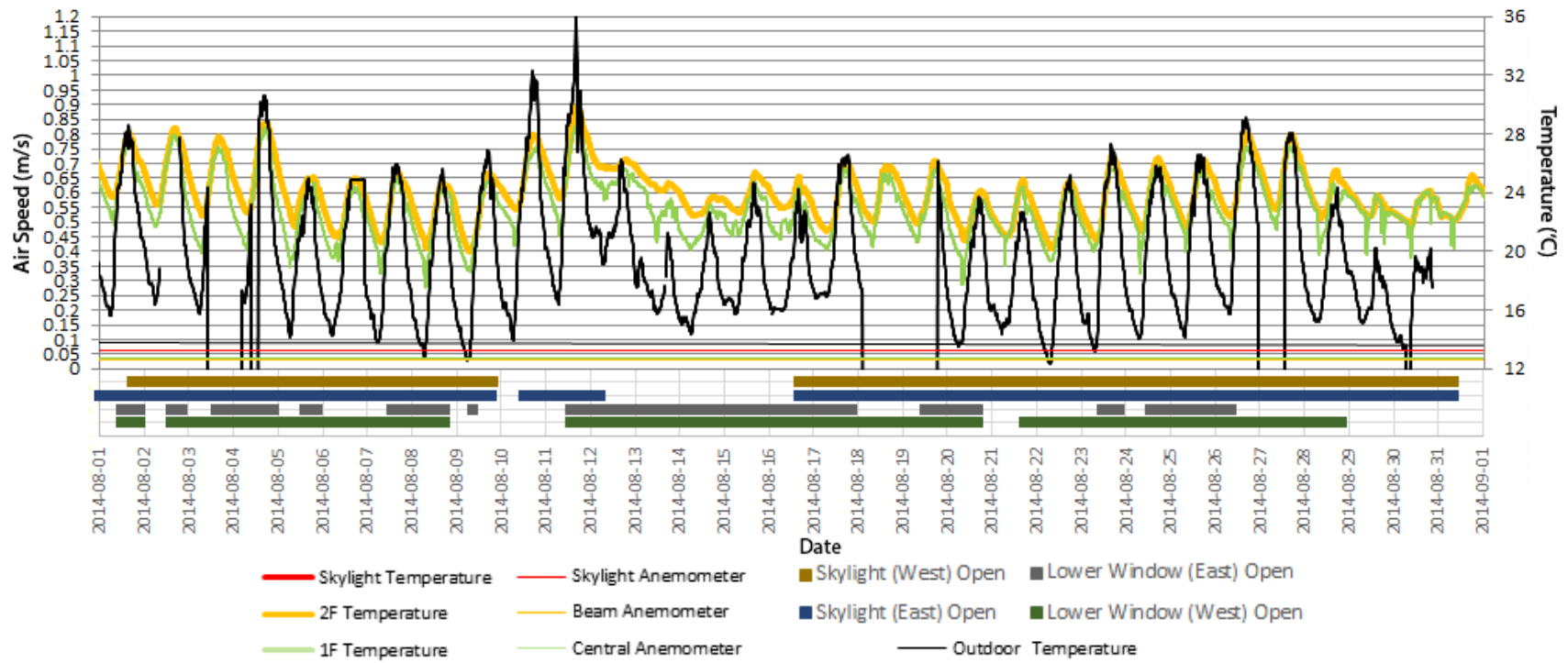
**Figure 50: Roof of the Harmony House. This area consists of two state sensors, one on each skylight.**

# APPENDIX B – Compiled data

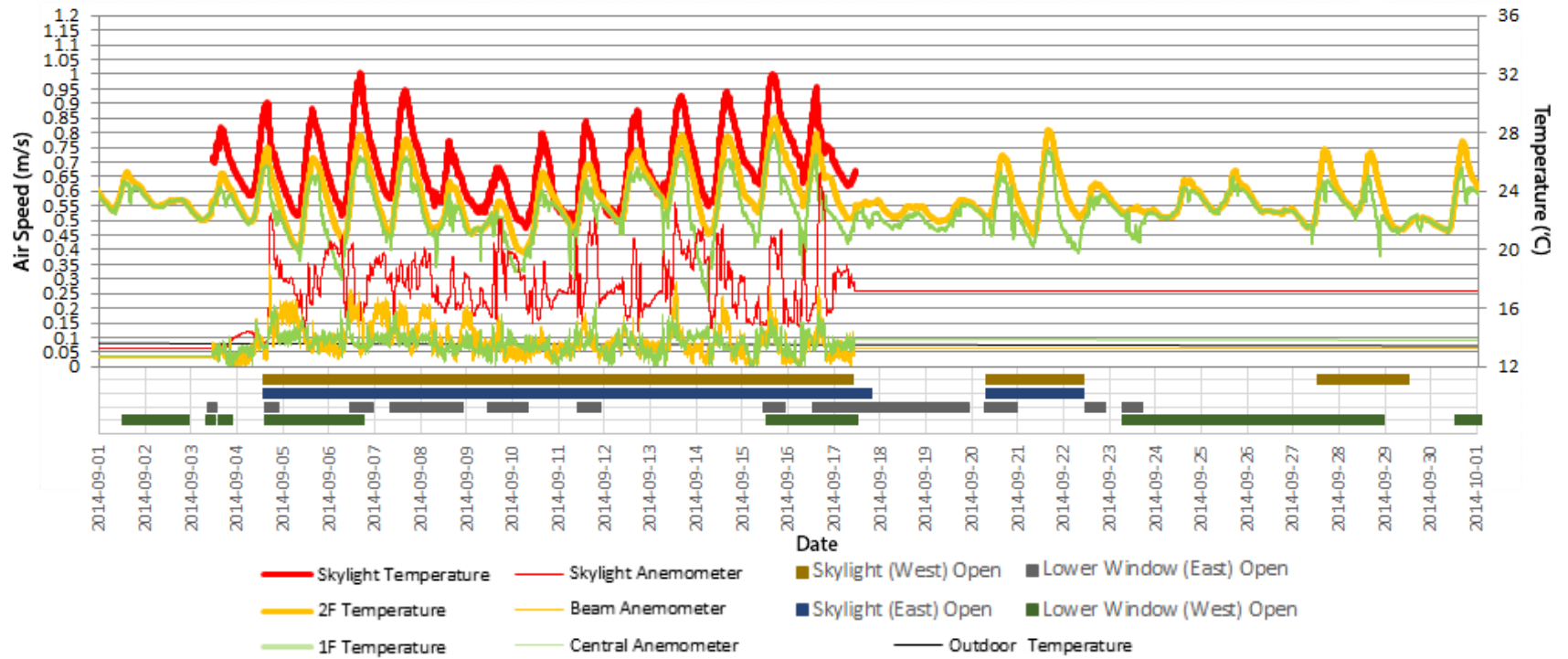
July



### August

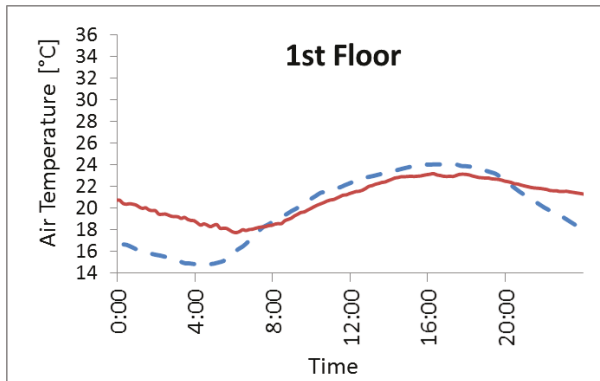


## September

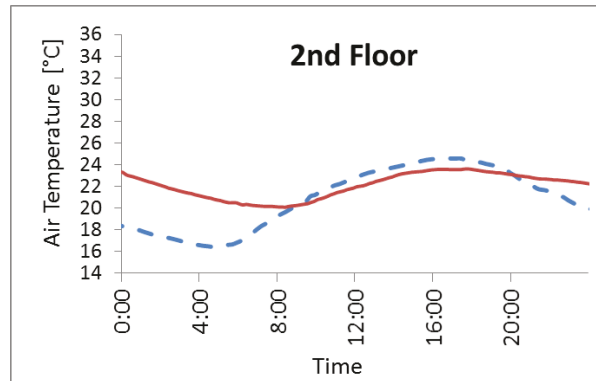


## APPENDIX C – Results from the validation of the dynamic thermal model

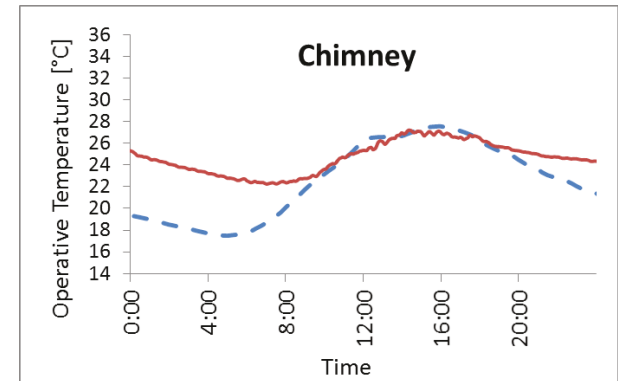
0 m/s, Cool day



Simulated: 24.1°C  
Measured: 23.2°C

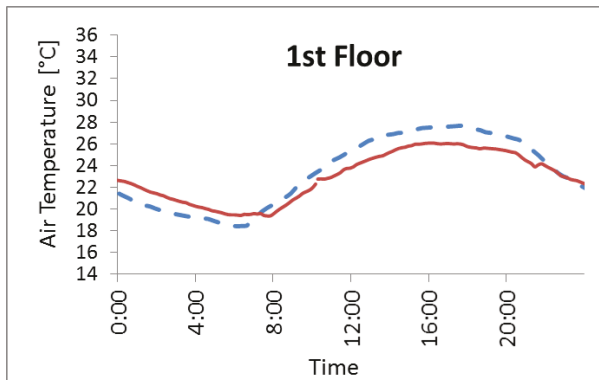


Simulated: 24.6°C  
Measured: 23.6°C

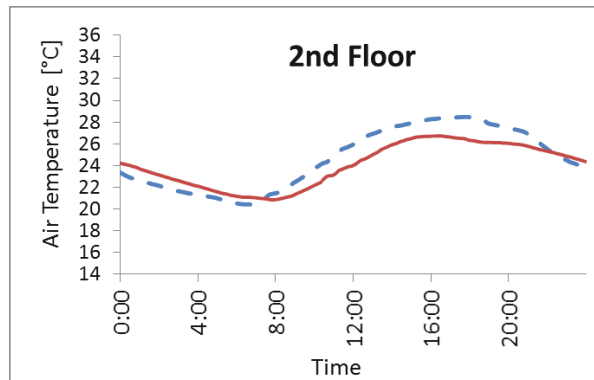


Simulated: 27.0°C  
Measured: 26.9°C

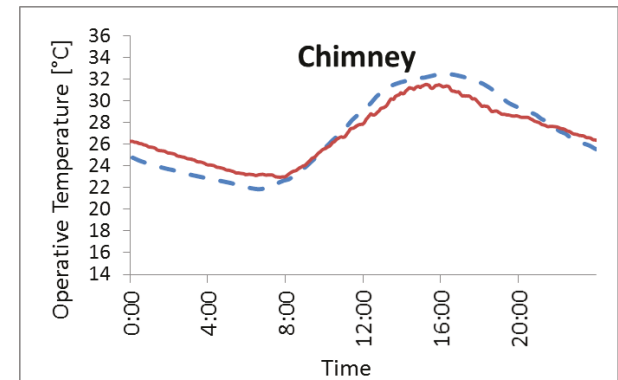
0 m/s, Typical day



Simulated: 27.5°C  
Measured: 26.0°C

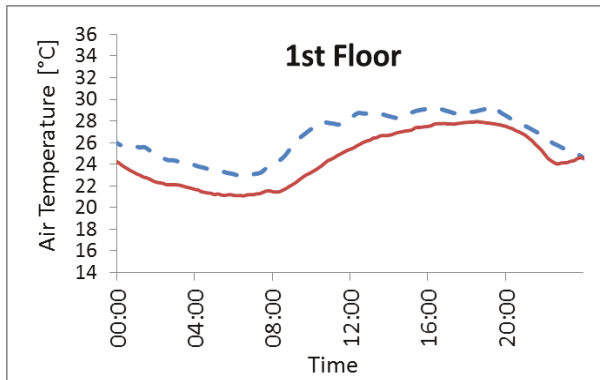


Simulated: 28.3°C  
Measured: 26.7°C

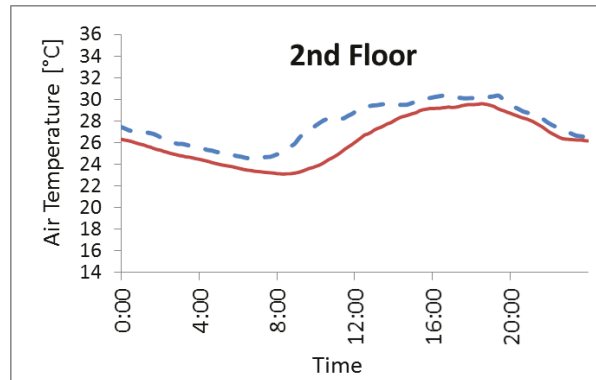


Simulated: 32.2°C  
Measured: 31.2°C

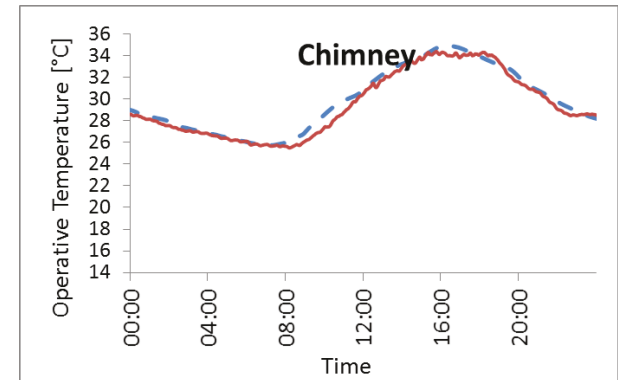
0 m/s, Warm day



Simulated: 29.1°C  
Measured: 27.9°C

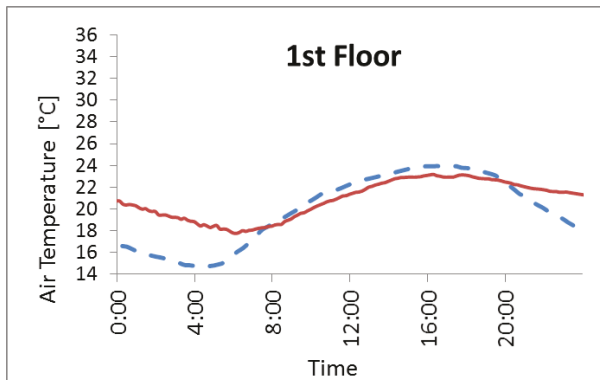


Simulated: 30.2°C  
Measured: 29.5°C

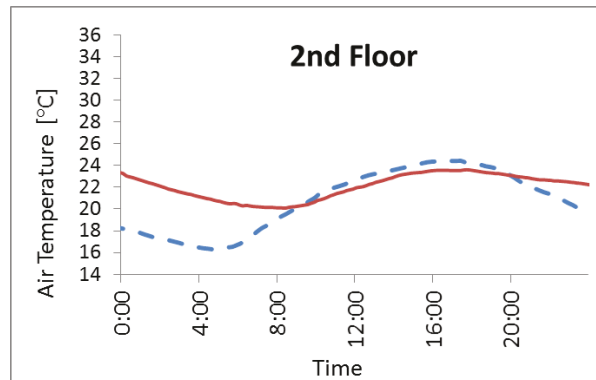


Simulated: 34.3°C  
Measured: 34.1°C

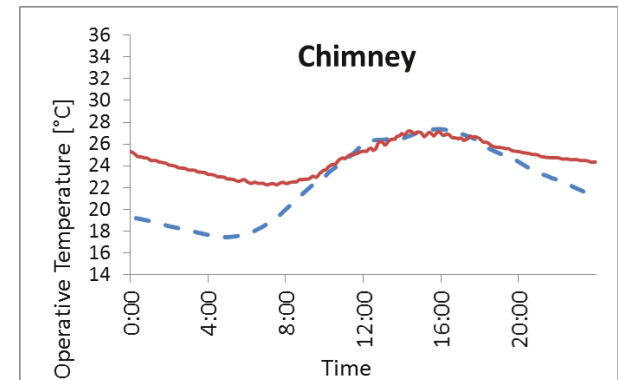
1 m/s, Cool day



Simulated: 24.0°C  
Measured: 23.1°C

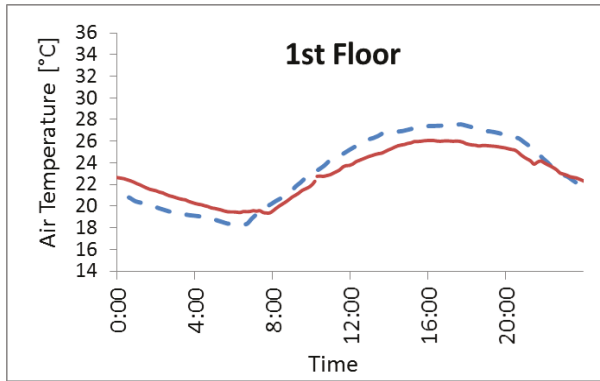


Simulated: 24.3°C  
Measured: 23.6°C

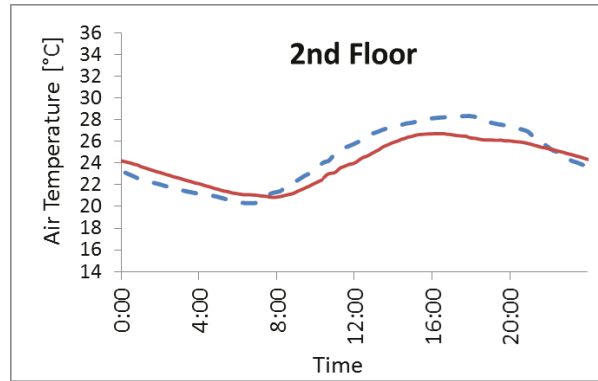


Simulated: 27.1°C  
Measured: 27.1°C

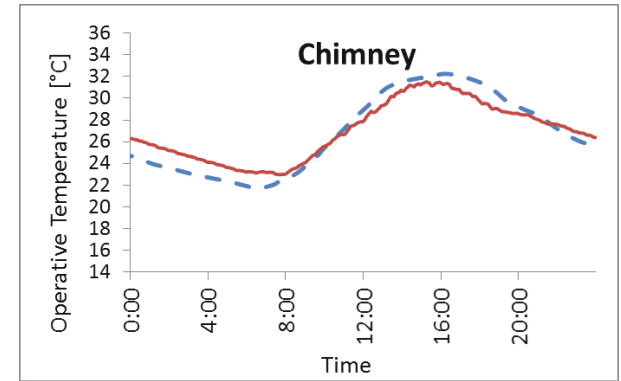
1 m/s, Typical day



Simulated: 27.4°C  
Measured: 26.0°C

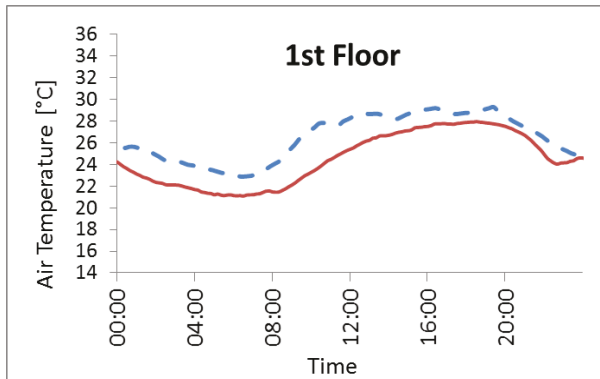


Simulated: 28.2°C  
Measured: 26.7°C

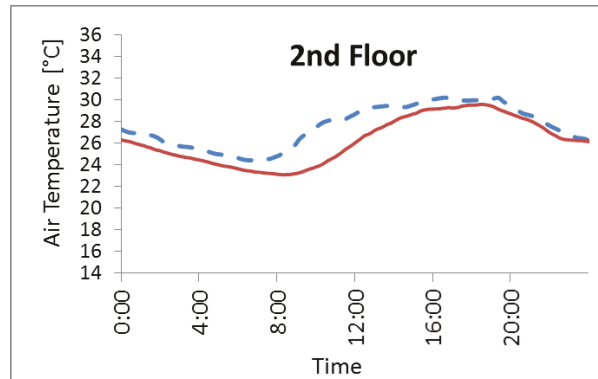


Simulated: 31.5°C  
Measured: 31.2°C

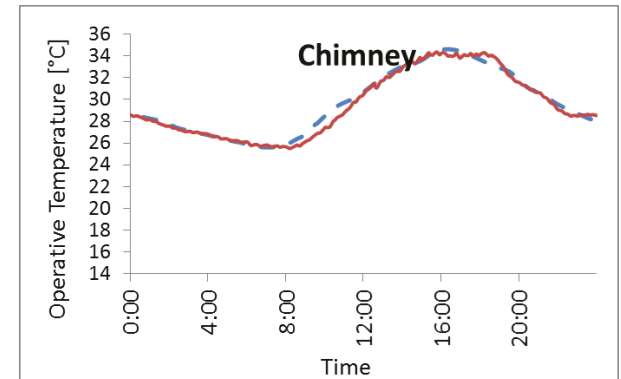
1 m/s, Warm day



Simulated: 28.7°C  
Measured: 27.7°C

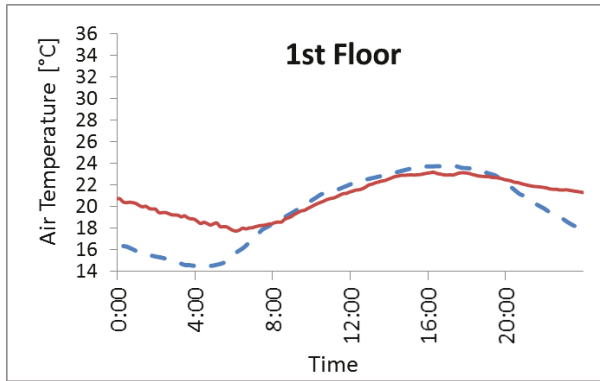


Simulated: 30.2°C  
Measured: 29.6°C

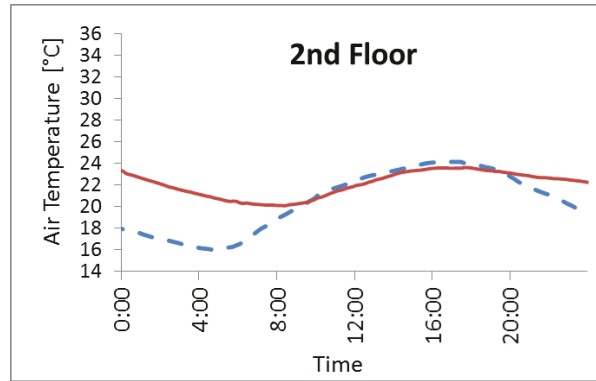


Simulated: 34.0°C  
Measured: 33.9°C

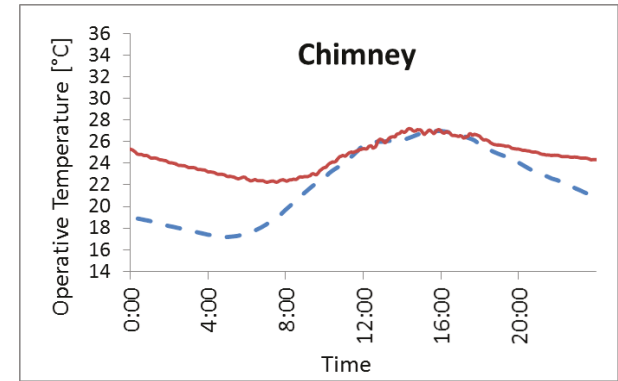
2 m/s, Cool day



Simulated: 23.7°C  
Measured: 23.1°C

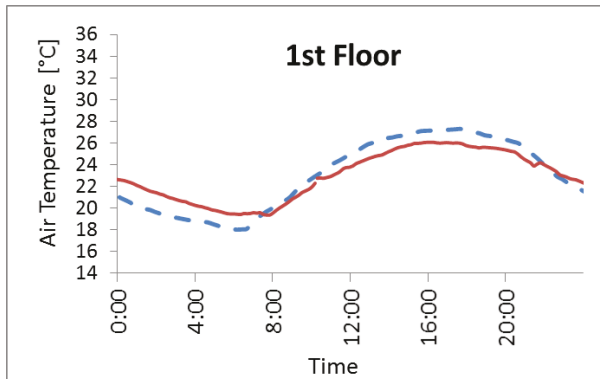


Simulated: 24.0°C  
Measured: 23.6°C

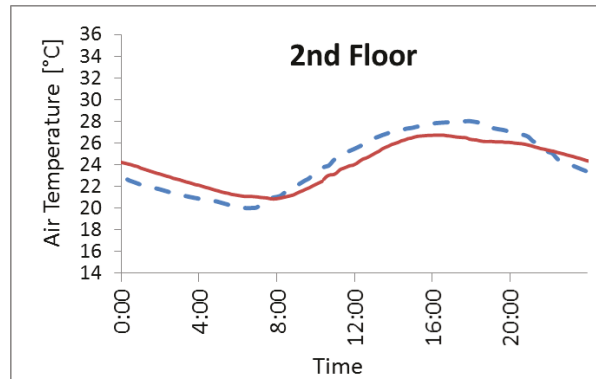


Simulated: 26.7°C  
Measured: 26.8°C

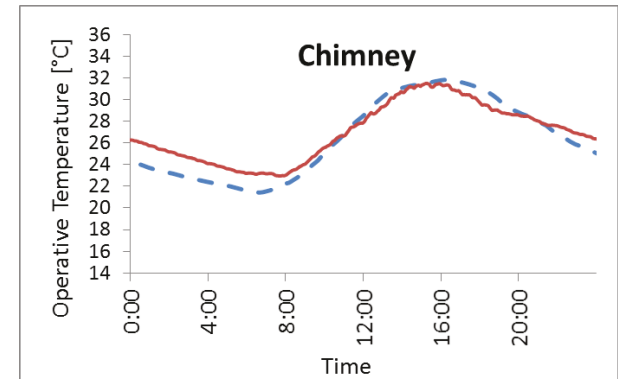
2 m/s, Typical day



Simulated: 27.1°C  
Measured: 26.0°C

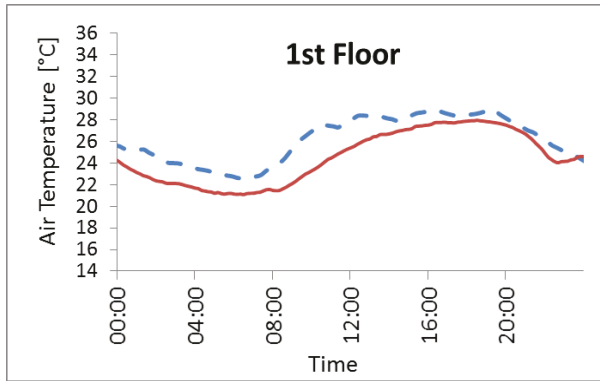


Simulated: 27.9°C  
Measured: 26.7°C

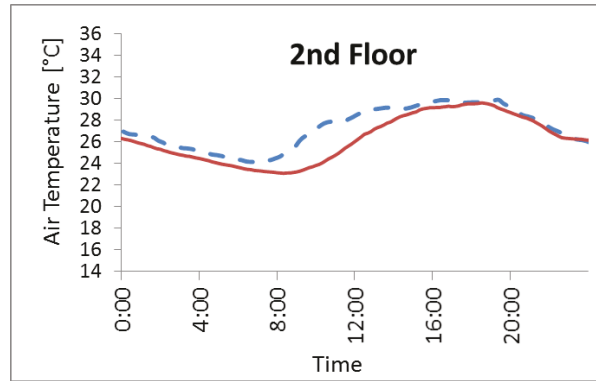


Simulated: 31.5°C  
Measured: 31.4°C

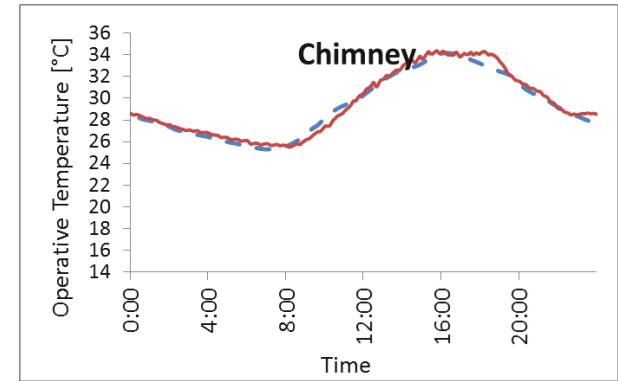
2 m/s, Warm day



Simulated: 27.9°C  
Measured: 27.5°C



Simulated: 29.5°C  
Measured: 29.4°C

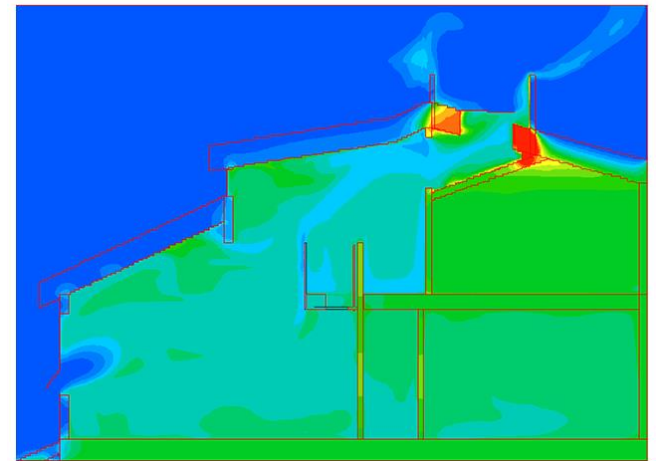
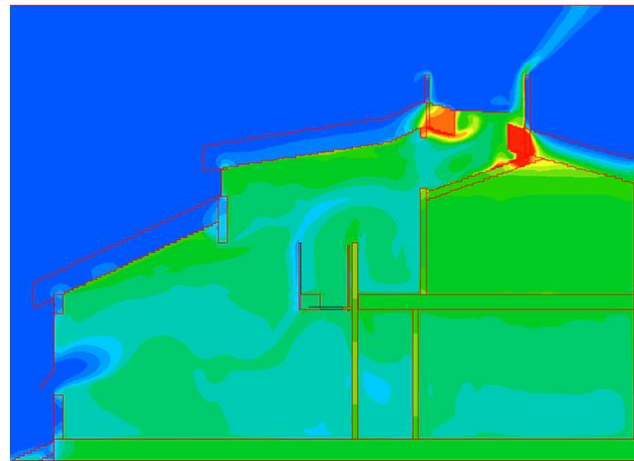
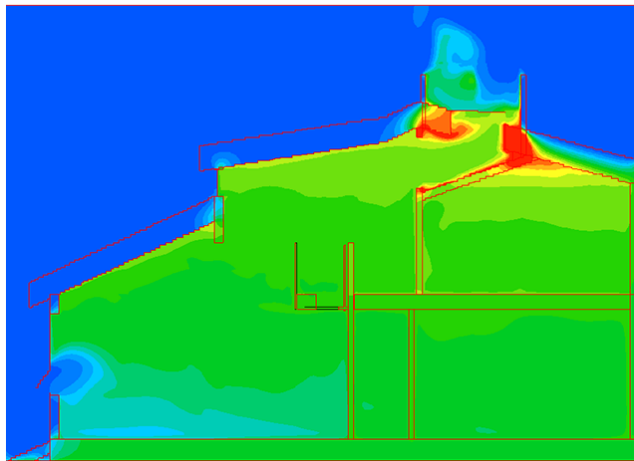


Simulated: 34.1°C  
Measured: 34.2°C

## APPENDIX D – Results of the CFD model

Cool Day

Temperature [C]



Air speed: 0 m/s

Air speed: 1 m/s

Air speed: 2 m/s

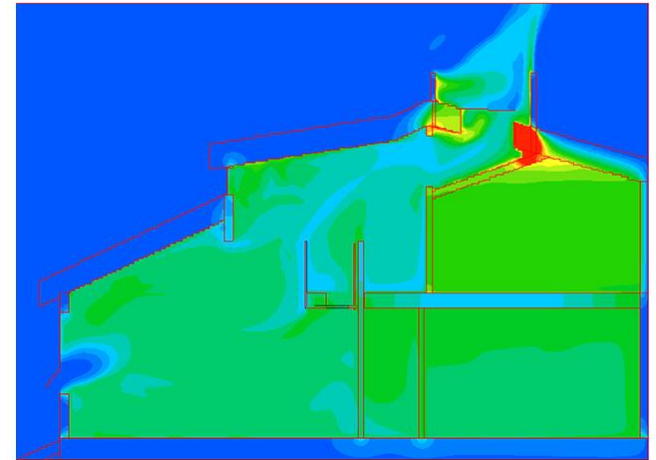
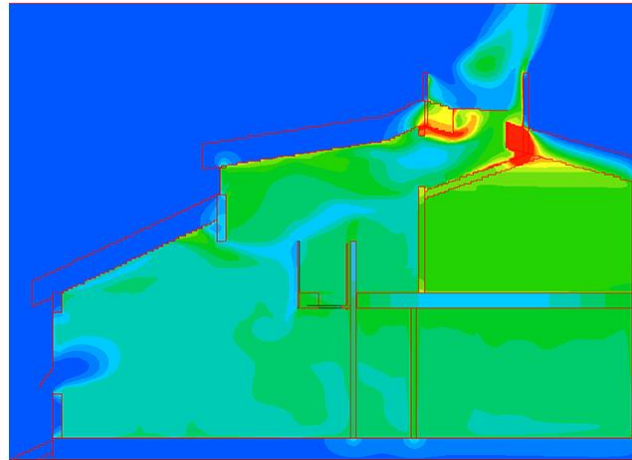
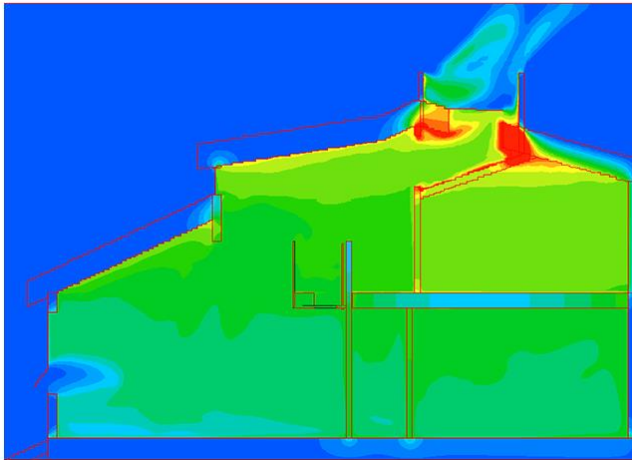
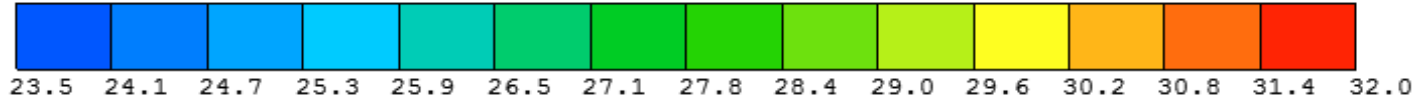
1F wall temperature: 24.5°C  
 2F wall temperature: 25.5°C  
 Skylight wall temperature: 31.5°C  
 Cycle of convergence: 184

1F wall temperature: 24.5°C  
 2F wall temperature: 25.5°C  
 Skylight wall temperature: 31.5°C  
 Cycle of convergence: 167

1F wall temperature: 24.5°C  
 2F wall temperature: 25.5°C  
 Skylight wall temperature: 31.5°C  
 Cycle of convergence: 174

Typical Day

Temperature [C]



Air speed: 0 m/s

1F wall temperature: 28°C  
 2F wall temperature: 30°C  
 Skylight wall temperature: 38°C  
 Cycle of convergence: 116

Air speed: 1 m/s

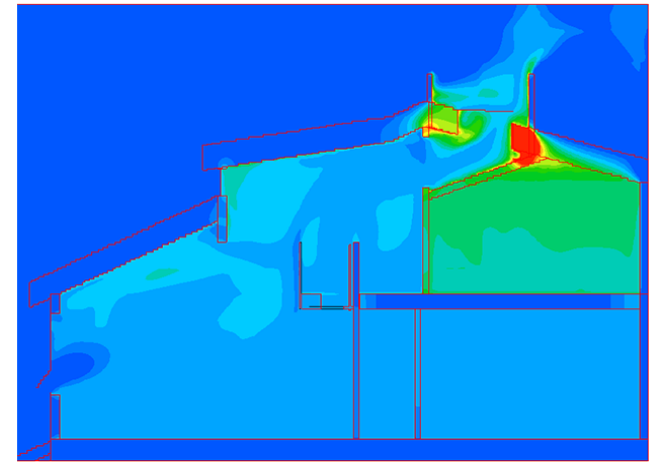
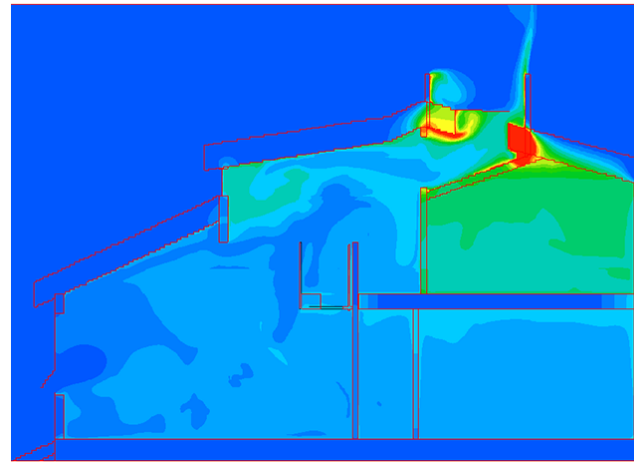
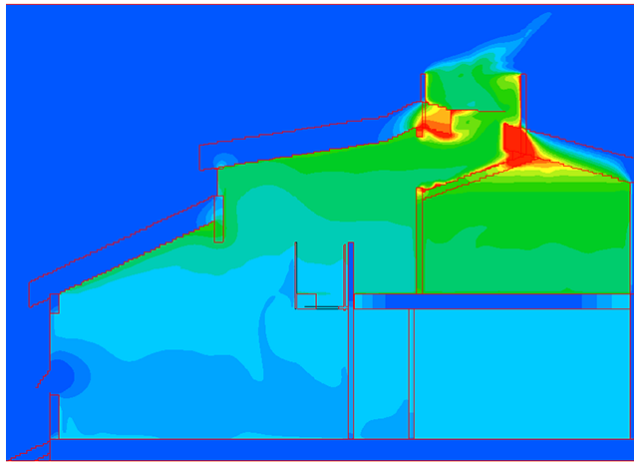
1F wall temperature: 28°C  
 2F wall temperature: 30°C  
 Skylight wall temperature: 38°C  
 Cycle of convergence: 128

Air speed: 2 m/s

1F wall temperature: 28°C  
 2F wall temperature: 30°C  
 Skylight wall temperature: 38°C  
 Cycle of convergence: 129

**Warm Day**

Temperature [C]



Air speed: 0 m/s

1F wall temperature: 30°C  
 2F wall temperature: 32°C  
 Skylight wall temperature: 41°C  
 Cycle of convergence: 292

Air speed: 1 m/s

1F wall temperature: 30°C  
 2F wall temperature: 32°C  
 Skylight wall temperature: 41°C  
 Cycle of convergence: 95

Air speed: 2 m/s

1F wall temperature: 30°C  
 2F wall temperature: 32°C  
 Skylight wall temperature: 41°C  
 Cycle of convergence: 130

# APPENDIX E – Results of questionnaire

## Harmony House Occupants Comfort Questionnaire

We are conducting an evaluation of your home to assess how well it performs for those who occupy it. This information will be used as part of our study. Thank you for filling out this questionnaire.

Name: LES MONCRIEFF

### Schedule

- Where would you most likely be and how much time is spent in the following locations on a typical week day? Please checkmark (☑) where applicable.

	Early Morning	Morning	Midday	Afternoon	Evening	Night	Hours spent
Bedroom	☑					☑	7
Living Room				☑	☑	☑	2
Kitchen					☑		1
Solarium		☑					1
Office		☑					2
Other		☑					
Not at home				☑			6

- Where would you most likely be and how much time is spent in the following locations on a typical weekend day? Please checkmark (☑) where applicable.

	Early Morning	Morning	Midday	Afternoon	Evening	Night	Hours spent
Bedroom	☑					☑	7
Living Room				☑	☑	☑	3
Kitchen	☑		☑		☑		2
Solarium	☑	☑					1
Office			☑		☑		4
Other							
Not at home							5

## Comfort

For each of the following spaces in your home (bedroom, living room, solarium, kitchen area, office), please rate your experience on a typical warm day of the year and on a typical cold day of the year. Please circle where appropriate.

### Bedroom

- Temperature (1-too cool, 4-adequate, 7-too hot)

Warm day	Too cold	1	2	3	4	5	6	7	Too warm
Cold day		1	2	3	4	5	6	7	

- Temperature uniformity (1-uniform, 2-small variations, 3-large variations)

Warm day	Uniform	1	2	3	Large variations
Cold day		1	2	3	

- Air movement (1-not enough, 4-adequate, 7-too drafty)

Warm day	Not enough	1	2	3	4	5	6	7	Too drafty
Cold day		1	2	3	4	5	6	7	

- Air freshness (1-fresh, 2-acceptable, 3-stale)

Warm day	Fresh	1	2	3	Stale
Cold day		1	2	3	

- Humidity (1-too dry, 3-adequate, 5-too humid)

Warm day	Too dry	1	2	3	4	5	Too damp
Cold day		1	2	3	4	5	

- Smell (1-no smell, 2-acceptable, 3-smelly)

Warm day	No smell	1	2	3	Smelly
Cold day		1	2	3	

**Living room**

- Temperature (1-too cool, 4-adequate, 7-too hot)

Warm day Cold day	Too cold	1	2	3	4	5	6	7	Too warm
		1	2	3	4	5	6	7	

- Temperature uniformity (1-uniform, 2-small variations, 3-large variations)

Warm day Cold day	Uniform	1	2	3	Large variations
		1	2	3	

- Air movement (1-not enough, 4-adequate, 7-too drafty)

Warm day Cold day	Not enough	1	2	3	4	5	6	7	Too drafty
		1	2	3	4	5	6	7	

- Air freshness (1-fresh, 2-acceptable, 3-stale)

Warm day Cold day	Fresh	1	2	3	Stale
		1	2	3	

- Humidity (1-too dry, 3-adequate, 5-too humid)

Warm day Cold day	Too dry	1	2	3	4	5	Too damp
		1	2	3	4	5	

- Smell (1-no smell, 2-acceptable, 3-smelly)

Warm day Cold day	No smell	1	2	3	Smelly
		1	2	3	

**Solarium**

- Temperature (1-too cool, 4-adequate, 7-too hot)

Warm day Cold day	Too cold	1	2	3	4	5	6	7	Too warm
		1	2	3	4	5	6	7	

- Temperature uniformity (1-uniform, 2-small variations, 3-large variations)

Warm day Cold day	Uniform	1	2	3	Large variations
		1	2	3	

- Air movement (1-not enough, 4-adequate, 7-too drafty)

Warm day Cold day	Not enough	1	2	3	4	5	6	7	Too drafty
		1	2	3	4	5	6	7	

- Air freshness (1-fresh, 2-acceptable, 3-stale)

Warm day Cold day	Fresh	1	2	3	Stale
		1	2	3	

- Humidity (1-too dry, 3-adequate, 5-too humid)

Warm day Cold day	Too dry	1	2	3	4	5	Too damp
		1	2	3	4	5	

- Smell (1-no smell, 2-acceptable, 3-smelly)

Warm day Cold day	No smell	1	2	3	Smelly
		1	2	3	

**Kitchen area**

- Temperature (1-too cool, 4-adequate, 7-too hot)

Warm day	Too cold	1	2	3	4	5	6	7	Too warm
Cold day		1	2	3	4	5	6	7	

- Temperature uniformity (1-uniform, 2-small variations, 3-large variations)

Warm day	Uniform	1	2	3	Large variations
Cold day		1	2	3	

- Air movement (1-not enough, 4-adequate, 7-too drafty)

Warm day	Not enough	1	2	3	4	5	6	7	Too drafty
Cold day		1	2	3	4	5	6	7	

- Air freshness (1-fresh, 2-acceptable, 3-stale)

Warm day	Fresh	1	2	3	Stale
Cold day		1	2	3	

- Humidity (1-too dry, 3-adequate, 5-too humid)

Warm day	Too dry	1	2	3	4	5	Too damp
Cold day		1	2	3	4	5	

- Smell (1-no smell, 2-acceptable, 3-smelly)

Warm day	No smell	1	2	3	Smelly
Cold day		1	2	3	

**Office**

- Temperature (1-too cool, 4-adequate, 7-too hot)

Warm day	Too cold	1	2	3	4	5	6	7	Too warm
Cold day		1	2	3	4	5	6	7	

- Temperature uniformity (1-uniform, 2-small variations, 3-large variations)

Warm day	Uniform	1	2	3	Large variations
Cold day		1	2	3	

- Air movement (1-not enough, 4-adequate, 7-too drafty)

Warm day	Not enough	1	2	3	4	5	6	7	Too drafty
Cold day		1	2	3	4	5	6	7	

- Air freshness (1-fresh, 2-acceptable, 3-stale)

Warm day	Fresh	1	2	3	Stale
Cold day		1	2	3	

- Humidity (1-too dry, 3-adequate, 5-too humid)

Warm day	Too dry	1	2	3	4	5	Too damp
Cold day		1	2	3	4	5	

- Smell (1-no smell, 2-acceptable, 3-smelly)

Warm day	No smell	1	2	3	Smelly
Cold day		1	2	3	

### Controls

How often (1-never, 2-seldom, 3-sometimes, 4-regularly, 5-often) do you use the following controls and when (M-morning, N-noon, A-afternoon, E-evening, N-night)? Please circle all that apply.

- House thermostat

Warm day	Never	1	2	3	4	5	Often	M	N	A	E	N
Cold day		1	2	3	4	5		M	N	A	E	N

- Main skylight

Warm day	Never	1	2	3	4	5	Often	M	N	A	E	N
Cold day		1	2	3	4	5		M	N	A	E	N

- Bedroom skylight

Warm day	Never	1	2	3	4	5	Often	M	N	A	E	N
Cold day		1	2	3	4	5		M	N	A	E	N

- Windows living room

Warm day	Never	1	2	3	4	5	Often	M	N	A	E	N
Cold day		1	2	3	4	5		M	N	A	E	N

- Windows bedroom

Warm day	Never	1	2	3	4	5	Often	M	N	A	E	N
Cold day		1	2	3	4	5		M	N	A	E	N

- Windows office

Warm day	Never	1	2	3	4	5	Often	M	N	A	E	N
Cold day		1	2	3	4	5		M	N	A	E	N

7

- Windows solarium

*NO WINDOWS*

Warm day	Never	1	2	3	4	5	Often	M	N	A	E	N
Cold day		1	2	3	4	5		M	N	A	E	N

- Door solarium

Warm day	Never	1	2	3	4	5	Often	M	N	A	E	N
Cold day		1	2	3	4	5		M	N	A	E	N

- Front door

Warm day	Never	1	2	3	4	5	Often	M	N	A	E	N
Cold day		1	2	3	4	5		M	N	A	E	N

- Bedroom door (to the exterior)

Warm day	Never	1	2	3	4	5	Often	M	N	A	E	N
Cold day		1	2	3	4	5		M	N	A	E	N

- Kitchen door (to the exterior)

Warm day	Never	1	2	3	4	5	Often	M	N	A	E	N
Cold day		1	2	3	4	5		M	N	A	E	N

- Blinds living room

Warm day	Never	1	2	3	4	5	Often	M	N	A	E	N
Cold day		1	2	3	4	5		M	N	A	E	N

- Blinds bedroom

Warm day	Never	1	2	3	4	5	Often	M	N	A	E	N
Cold day		1	2	3	4	5		M	N	A	E	N

8

- Blinds kitchen

Warm day	Never	1	2	3	4	5	Often	M	N	A	E	N
Cold day		1	2	3	4	5		M	N	A	E	N

- Blinds office

Warm day	Never	1	2	3	4	5	Often	M	N	A	E	N
Cold day		1	2	3	4	5		M	N	A	E	N

- Please provide the thermostat heating and cooling set points:

- Heating set point = 22 °C FALL, WINTER, SPRING
- Cooling set point = \_\_\_ °C ~ NEVER USED

### Miscellaneous

- Please checkmark (☑) what best describes your typical clothing on a typical warm day of the year and on a typical cold day of the year.

	Warm day	Cold day
Short sleeve shirt	☑	
Long sleeve shirt		☑
Pants/Long skirt		☑
Shorts/Short skirt	☑	
Dress		
Tights		
Sweater		
Jacket		
Long socks		
Short socks		☑
Shoes	NEVER	
Other (please specify)		

9

- If you ever feel discomfort, please specify where in your home (kitchen, bedroom, living room, solarium, office, other), at what time of the day (early morning, morning, midday, afternoon, evening, night), and how you would best describe the source of this discomfort. Please draw lines to connect all entries that apply.

Where:	When:	Source:
<input type="checkbox"/> Bedroom	<input type="checkbox"/> Early Morning	<input type="checkbox"/> Air is too cold
<input type="checkbox"/> Living room	<input type="checkbox"/> Morning	<input type="checkbox"/> Air is too hot
<input type="checkbox"/> Solarium	<input type="checkbox"/> Midday	<input type="checkbox"/> Walls are too cold
<input type="checkbox"/> Kitchen	<input type="checkbox"/> Afternoon	<input type="checkbox"/> Walls are too hot
<input type="checkbox"/> Office	<input type="checkbox"/> Evening	<input type="checkbox"/> Windows are too cold
<input type="checkbox"/> Other (please specify)	<input type="checkbox"/> Night	<input type="checkbox"/> Windows are too hot
		<input type="checkbox"/> Floors are too cold
		<input type="checkbox"/> Floors are too hot
		<input type="checkbox"/> Too much solar heat
		<input type="checkbox"/> Static hair, flaky skin, dry eyes, nose etc.
		<input type="checkbox"/> Skin feels sticky, air is oppressive
		<input type="checkbox"/> Big temperature difference between ankle and head
		<input type="checkbox"/> Air movement too low
		<input type="checkbox"/> Air movement too high
		<input type="checkbox"/> Drafts from windows
		<input type="checkbox"/> Drafts from vents

- AIR TEMP. IS CONSTANT THROUGHOUT.
- USING WINDOWS AND BLINDS, WE CAN EASILY CONTROL TEMP. AND AIRFLOW DURING HOT SUMMER DAYS.
- SUMMER MONTHS THE THERMOSTAT IS OFF
- DURING SPRING, FALL AND WINTER WE SET THE THERMOSTAT AT 21-22°
- THE TEMP. IN HOT SUMMER MONTHS IS CONTROLLED BY USING THE SKYLIGHTS WINDOWS AND BLINDS.

10

## Harmony House Occupants Comfort Questionnaire

We are conducting an evaluation of your home to assess how well it performs for those who occupy it. This information will be used as part of our study. Thank you for filling out this questionnaire.

Name: LINDA MONCRIEFF

### Schedule

- Where would you most likely be and how much time is spent in the following locations on a typical week day? Please checkmark (☑) where applicable.

	Early Morning	Morning	Midday	Afternoon	Evening	Night	Hours spent
Bedroom	☑					☑	8
Living Room				☑			3
Kitchen		☑	☑		☑		3
Solarium		☑					1
Office							0
Other							
Not at home				☑			6

- Where would you most likely be and how much time is spent in the following locations on a typical weekend day? Please checkmark (☑) where applicable.

	Early Morning	Morning	Midday	Afternoon	Evening	Night	Hours spent
Bedroom						☑	8
Living Room			☑	☑		☑	4
Kitchen	☑	☑		☑	☑		3
Solarium							
Office							
Other							
Not at home							4

1

### Comfort

For each of the following spaces in your home (bedroom, living room, solarium, kitchen area, office), please rate your experience on a typical warm day of the year and on a typical cold day of the year. Please circle where appropriate.

#### Bedroom

- Temperature (1-too cool, 4-adequate, 7-too hot)

Warm day Cold day	Too cold	1	2	3	4	5	6	7	Too warm
		1	2	3	4	5	6	7	

- Temperature uniformity (1-uniform, 2-small variations, 3-large variations)

Warm day Cold day	Uniform	1	2	3	Large variations
		1	2	3	

- Air movement (1-not enough, 4-adequate, 7-too drafty)

Warm day Cold day	Not enough	1	2	3	4	5	6	7	Too drafty
		1	2	3	4	5	6	7	

- Air freshness (1-fresh, 2-acceptable, 3-stale)

Warm day Cold day	Fresh	1	2	3	Stale
		1	2	3	

- Humidity (1-too dry, 3-adequate, 5-too humid)

Warm day Cold day	Too dry	1	2	3	4	5	Too damp
		1	2	3	4	5	

- Smell (1-no smell, 2-acceptable, 3-smelly)

Warm day Cold day	No smell	1	2	3	Smelly
		1	2	3	

2

**Living room**

- Temperature (1-too cool, 4-adequate, 7-too hot)

Warm day	Too cold	1	2	3	4	5	6	7	Too warm
Cold day		1	2	3	4	5	6	7	

- Temperature uniformity (1-uniform, 2-small variations, 3-large variations)

Warm day	Uniform	1	2	3	Large variations
Cold day		1	2	3	

- Air movement (1-not enough, 4-adequate, 7-too drafty)

Warm day	Not enough	1	2	3	4	5	6	7	Too drafty
Cold day		1	2	3	4	5	6	7	

- Air freshness (1-fresh, 2-acceptable, 3-stale)

Warm day	Fresh	1	2	3	Stale
Cold day		1	2	3	

- Humidity (1-too dry, 3-adequate, 5-too humid)

Warm day	Too dry	1	2	3	4	5	Too damp
Cold day		1	2	3	4	5	

- Smell (1-no smell, 2-acceptable, 3-smelly)

Warm day	No smell	1	2	3	Smelly
Cold day		1	2	3	

**Solarium**

- Temperature (1-too cool, 4-adequate, 7-too hot)

Warm day	Too cold	1	2	3	4	5	6	7	Too warm
Cold day		1	2	3	4	5	6	7	

- Temperature uniformity (1-uniform, 2-small variations, 3-large variations)

Warm day	Uniform	1	2	3	Large variations
Cold day		1	2	3	

- Air movement (1-not enough, 4-adequate, 7-too drafty)

Warm day	Not enough	1	2	3	4	5	6	7	Too drafty
Cold day		1	2	3	4	5	6	7	

- Air freshness (1-fresh, 2-acceptable, 3-stale)

Warm day	Fresh	1	2	3	Stale
Cold day		1	2	3	

- Humidity (1-too dry, 3-adequate, 5-too humid)

Warm day	Too dry	1	2	3	4	5	Too damp
Cold day		1	2	3	4	5	

- Smell (1-no smell, 2-acceptable, 3-smelly)

Warm day	No smell	1	2	3	Smelly
Cold day		1	2	3	

**Kitchen area**

- Temperature (1-too cool, 4-adequate, 7-too hot)

Warm day	Too cold	1	2	3	4	5	6	7	Too warm
Cold day		1	2	3	4	5	6	7	

- Temperature uniformity (1-uniform, 2-small variations, 3-large variations)

Warm day	Uniform	1	2	3	Large variations
Cold day		1	2	3	

- Air movement (1-not enough, 4-adequate, 7-too drafty)

Warm day	Not enough	1	2	3	4	5	6	7	Too drafty
Cold day		1	2	3	4	5	6	7	

- Air freshness (1-fresh, 2-acceptable, 3-stale)

Warm day	Fresh	1	2	3	Stale
Cold day		1	2	3	

- Humidity (1-too dry, 3-adequate, 5-too humid)

Warm day	Too dry	1	2	3	4	5	Too damp
Cold day		1	2	3	4	5	

- Smell (1-no smell, 2-acceptable, 3-smelly)

Warm day	No smell	1	2	3	Smelly
Cold day		1	2	3	

**Office**

- Temperature (1-too cool, 4-adequate, 7-too hot)

Warm day	Too cold	1	2	3	4	5	6	7	Too warm
Cold day		1	2	3	4	5	6	7	

- Temperature uniformity (1-uniform, 2-small variations, 3-large variations)

Warm day	Uniform	1	2	3	Large variations
Cold day		1	2	3	

- Air movement (1-not enough, 4-adequate, 7-too drafty)

Warm day	Not enough	1	2	3	4	5	6	7	Too drafty
Cold day		1	2	3	4	5	6	7	

- Air freshness (1-fresh, 2-acceptable, 3-stale)

Warm day	Fresh	1	2	3	Stale
Cold day		1	2	3	

- Humidity (1-too dry, 3-adequate, 5-too humid)

Warm day	Too dry	1	2	3	4	5	Too damp
Cold day		1	2	3	4	5	

- Smell (1-no smell, 2-acceptable, 3-smelly)

Warm day	No smell	1	2	3	Smelly
Cold day		1	2	3	

### Controls

How often (1-never, 2-seldom, 3-sometimes, 4-regularly, 5-often) do you use the following controls and when (M-morning, N-noon, A-afternoon, E-evening, N-night)? Please circle all that apply.

- House thermostat

Warm day	Never	1	2	3	4	5	Often	M	N	A	E	N
Cold day		1	2	3	4	5		M	N	A	E	N

- Main skylight

Warm day	Never	1	2	3	4	5	Often	M	N	A	E	N
Cold day		1	2	3	4	5		M	N	A	E	N

- Bedroom skylight

Warm day	Never	1	2	3	4	5	Often	M	N	A	E	N
Cold day		1	2	3	4	5		M	N	A	E	N

- Windows living room

Warm day	Never	1	2	3	4	5	Often	M	N	A	E	N
Cold day		1	2	3	4	5		M	N	A	E	N

- Windows bedroom

Warm day	Never	1	2	3	4	5	Often	M	N	A	E	N
Cold day		1	2	3	4	5		M	N	A	E	N

- Windows office

Warm day	Never	1	2	3	4	5	Often	M	N	A	E	N
Cold day		1	2	3	4	5		M	N	A	E	N

7

- Windows solarium

*ONLY DOORS*

Warm day	Never	1	2	3	4	5	Often	M	N	A	E	N
Cold day		1	2	3	4	5		M	N	A	E	N

- Door solarium

Warm day	Never	1	2	3	4	5	Often	M	N	A	E	N
Cold day		1	2	3	4	5		M	N	A	E	N

- Front door

Warm day	Never	1	2	3	4	5	Often	M	N	A	E	N
Cold day		1	2	3	4	5		M	N	A	E	N

- Bedroom door (to the exterior)

Warm day	Never	1	2	3	4	5	Often	M	N	A	E	N
Cold day		1	2	3	4	5		M	N	A	E	N

- Kitchen door (to the exterior)

Warm day	Never	1	2	3	4	5	Often	M	N	A	E	N
Cold day		1	2	3	4	5		M	N	A	E	N

- Blinds living room

Warm day	Never	1	2	3	4	5	Often	M	N	A	E	N
Cold day		1	2	3	4	5		M	N	A	E	N

- Blinds bedroom

Warm day	Never	1	2	3	4	5	Often	M	N	A	E	N
Cold day		1	2	3	4	5		M	N	A	E	N

8

- Blinds kitchen

Warm day	Never	1	2	3	4	5	Often	M	N	A	E	N
Cold day		1	2	3	4	5		M	N	A	E	N

- Blinds office

Warm day	Never	1	2	3	4	5	Often	M	N	A	E	N
Cold day		1	2	3	4	5		M	N	A	E	N

- Please provide the thermostat heating and cooling set points:

- Heating set point = 22 °C *FALL, SUMMER, WINTER*
- Cooling set point =      °C *NEVER USED*

### Miscellaneous

- Please checkmark (☐) what best describes your typical clothing on a typical warm day of the year and on a typical cold day of the year.

	Warm day	Cold day
Short sleeve shirt	✓	
Long sleeve shirt		
Pants/Long skirt	✓	
Shorts/Short skirt	✓	
Dress		
Tights		
Sweater		
Jacket		
Long socks		
Short socks		
Shoes	<i>NEVER</i>	
Other (please specify)		

9

- If you ever feel discomfort, please specify where in your home (kitchen, bedroom, living room, solarium, office, other), at what time of the day (early morning, morning, midday, afternoon, evening, night), and how you would best describe the source of this discomfort. Please draw lines to connect all entries that apply.

Where:	When:	Source:
<input type="checkbox"/> Bedroom	<input type="checkbox"/> Early Morning	<input type="checkbox"/> Air is too cold
<input type="checkbox"/> Living room	<input type="checkbox"/> Morning	<input type="checkbox"/> Air is too hot
<input type="checkbox"/> Solarium	<input type="checkbox"/> Midday	<input type="checkbox"/> Walls are too cold
<input type="checkbox"/> Kitchen	<input type="checkbox"/> Afternoon	<input type="checkbox"/> Walls are too hot
<input type="checkbox"/> Office	<input type="checkbox"/> Evening	<input type="checkbox"/> Windows are too cold
<input type="checkbox"/> Other (please specify)	<input type="checkbox"/> Night	<input type="checkbox"/> Windows are too hot
		<input type="checkbox"/> Floors are too cold
		<input type="checkbox"/> Floors are too hot
		<input type="checkbox"/> Too much solar heat
		<input type="checkbox"/> Static hair, flaky skin, dry eyes, nose etc.
		<input type="checkbox"/> Skin feels sticky, air is oppressive
		<input type="checkbox"/> Big temperature difference between ankle and head
		<input type="checkbox"/> Air movement too low
		<input type="checkbox"/> Air movement too high
		<input type="checkbox"/> Drafts from windows
		<input type="checkbox"/> Drafts from vents

10